Coloured generalised Young diagrams for affine Weyl-Coxeter groups

R.C. King and T.A. Welsh

School of Mathematics, The University of Southampton,
Highfield, Hampshire SO17 1BJ, U.K.
rck@maths.soton.ac.uk taw@maths.soton.ac.uk

Submitted: Sep 24, 2006; Accepted: Jan 9, 2007; Published: Jan 17, 2007
Mathematics Subject Classifications: 20F55, 17B67, 05A17, 05E99

Abstract

Coloured generalised Young diagrams $T(w)$ are introduced that are in bijective correspondence with the elements w of the Weyl-Coxeter group W of $\mathbf{g}$, where $\mathbf{g}$ is any one of the classical affine Lie algebras $\mathbf{g} = A_\ell^{(1)}$, $B_\ell^{(1)}$, $C_\ell^{(1)}$, $D_\ell^{(1)}$, $A_{2\ell}^{(2)}$, $A_{2\ell-1}^{(2)}$ or $D_{\ell+1}^{(2)}$. These diagrams are coloured by means of periodic coloured grids, one for each $\mathbf{g}$, which enable $T(w)$ to be constructed from any expression $w = s_{i_1} s_{i_2} \cdots s_{i_t}$ in terms of generators s_k of W, and any (reduced) expression for w to be obtained from $T(w)$. The diagram $T(w)$ is especially useful because $w(\Lambda) - \Lambda$ may be readily obtained from $T(w)$ for all Λ in the weight space of $\mathbf{g}$.

With $\overline{\mathbf{g}}$ a certain maximal finite dimensional simple Lie subalgebra of $\mathbf{g}$, we examine the set W_s of minimal right coset representatives of $\overline{W}$ in W, where $\overline{W}$ is the Weyl-Coxeter group of $\overline{\mathbf{g}}$. For $w \in W_s$, we show that $T(w)$ has the shape of a partition (or a slight variation thereof) whose r-core takes a particularly simple form, where r or $r/2$ is the dual Coxeter number of $\mathbf{g}$. Indeed, it is shown that W_s is in bijection with such partitions.

1 Prologue

1.1 Introduction

In this paper, we introduce a novel means of depicting elements, w, of the Weyl-Coxeter groups, W, of the classical affine Lie algebras $\mathbf{g} = A_\ell^{(1)}$, $B_\ell^{(1)}$, $C_\ell^{(1)}$, $D_\ell^{(1)}$, $A_{2\ell}^{(2)}$, $A_{2\ell+1}^{(2)}$, $D_{\ell+1}^{(2)}$. In this scheme, every Weyl-Coxeter group element w corresponds to a generalised Young diagram which is *coloured* according to the entries of an underlying $\mathbf{g}$-dependent periodic grid. The resulting object is denoted $T(w)$ and we refer to it as a *coloured diagram*. A typical $T(w)$ is given in Fig. 1.

$$T(w) = \begin{array}{|c|c|c|c|c|c|c|c|c|c|c|c|c|c|}
\hline
0_{\frac{1}{2}} & 2_1 & 3_1 & 4_1 & 4_1 & 3_1 & 2_1 & 1_{\frac{3}{2}} & 0_{\frac{3}{2}} & 2_2 & 3_2 & 4_2 & 4_2 & 3_2 \\
\hline
1_{\frac{1}{2}} & 0_{\frac{1}{2}} & 2_1 & 3_1 & 4_1 & 4_1 & 3_1 & 2_1 & 0_{\frac{3}{2}} \\
\cline{1-9}
2_0 & 1_{\frac{1}{2}} & 0_{\frac{1}{2}} & 2_1 & 3_1 & 4_1 & 4_1 \\
\cline{1-7}
3_0 & 2_0 & 1_{\frac{1}{2}} & 0_{\frac{1}{2}} \\
\cline{1-4}
\end{array}$$

Figure 1: Typical coloured diagram in the case $\mathbf{g} = A_7^{(2)}$

One way to arrive at $T(w)$ is to evaluate $w(\rho) - \rho$ where ρ is the Weyl vector of $\mathbf{g}$. In fact, $T(w)$ serves to encode $w(\rho) - \rho$ by means of its shape, which is specified by means of a *generalised partition* $\lambda(w)$, and certain depth parameters referred to as *charges*. More generally, $T(w)$ encodes $w(\Lambda) - \Lambda$ in an equally simple way by means of its coloured entries and associated depth charges for all $\Lambda \in \mathbf{h}^*$, where $\mathbf{h}^*$ is the dual of the Cartan subalgebra $\mathbf{h}$ of $\mathbf{g}$.

We characterise the set $\{T(w) \,|\, w \in W\}$ and show that the correspondence between w and $T(w)$ is a bijection. In addition, we provide algorithms for passing from w to $T(w)$ and *vice versa*. These owe their origin to the fact that $T(ws_k)$ can be readily obtained from $T(w)$, where s_k is any one of the Coxeter generators of W. This property enables $T(w)$ itself to be constructed using only an expression $w = s_{i_1} s_{i_2} \cdots s_{i_t}$ for w in terms of the generators of W. Moreover, by comparing $T(w)$ and $T(ws_k)$, it can be easily ascertained whether $\ell(ws_k) = \ell(w) + 1$ or $\ell(ws_k) = \ell(w) - 1$, where $\ell : W \to \mathbb{Z}_{\geq 0}$ is the length function on W. Given $T(w)$, this enables the generation of one or more expressions $w = s_{i_1} s_{i_2} \cdots s_{i_t}$ for w that are *reduced* in that $t = \ell(w)$.

In this paper, we are especially concerned with the relationship between $\mathbf{g}$ and a natural maximal simple Lie subalgebra $\overline{\mathbf{g}}$. Consequently, we view the Weyl-Coxeter group $\overline{W}$ of $\overline{\mathbf{g}}$ as a subgroup of W, and we study the set W_s of minimal length (right) coset representatives of W with respect to $\overline{W}$. In this context, the use of coloured generalised Young diagrams is convenient in that, given $T(w)$, it may be immediately decided whether or not $w \in W_s$. In this paper we characterise the set $\{T(w) \,|\, w \in W_s\}$ in terms of partitions having certain cores. This characterisation is useful in applications to the character theory of $\mathbf{g}$.

1.2 Overview

This paper is an outgrowth of material presented in Chapter 5 of Hussin's thesis [8]. In fact, for the $\mathbf{g} = A_\ell^{(1)}$ case, some of the results presented here were first proved in [8] using different methods. These results were then used to provide a method for determining branching rules $A_\ell^{(1)} \downarrow A_\ell$ through the calculation of $w(\Lambda) - \Lambda$ and $w(\rho) - \rho$, where $\Lambda \in \mathbf{h}^*$ [8, 9]. Hussin [8] also made progress in obtaining periodic grids that he conjectured would be appropriate to each of the other classical affine Lie algebras except $D_\ell^{(1)}$. The core parts of these grids were then used in [16] to provide a method for determining branching rules $\mathbf{g} \downarrow \overline{\mathbf{g}}$, where $\overline{\mathbf{g}}$ is a certain maximal finite dimensional Lie subalgebra of $\mathbf{g}$. In Section

2.2, we introduce periodic grids which are a refinement of the grids of [8], and introduce factors that account for the *depth* component. These grids can now be employed in the context of [16] to improve and complete the program begun there.

Doubly periodic versions of the $A_\ell^{(1)}$ grids described in Section 2.2 (up to a trivial renumbering) appear in the study of the representation theory of the symmetric group, particularly with regard to modular representations (see [10] and references therein). In [4], these doubly periodic grids were also shown to have a relevance in the representation theory of $A_\ell^{(1)}$. They soon became a cornerstone of the crystal basis theory of $A_\ell^{(1)}$ [21, 11].

More recently, realisations of the crystal graphs of the other classical affine Lie algebras have been given in terms of 'Young Walls' [14, 6]. These objects are based on grids that bear similarities to those that we give in Section 2.2. In fact, it is also possible to define realisations of the crystal graphs based on our grids, and these realisations are not obviously equivalent to those of [14, 6]. We will give details of this construction elsewhere. Here we confine our attention to singly periodic coloured grids.

In [18], elements of the affine Coxeter group $\tilde{A}_\ell$ are realised as permutations of $\mathbb{Z}$ that commute with a translation. This idea was extended to the other classical affine Coxeter groups $\tilde{B}_\ell$, $\tilde{C}_\ell$ and $\tilde{D}_\ell$ in [5], where these groups are realised as permutations of $\mathbb{Z}$ that commute with certain rigid transformations of $\mathbb{Z}$. The Weyl-Coxeter groups of $A_\ell^{(1)}$, $B_\ell^{(1)}$, $C_\ell^{(1)}$, $D_\ell^{(1)}$, $A_{2\ell}^{(2)}$, $A_{2\ell-1}^{(2)}$ and $D_{\ell+1}^{(2)}$ are isomorphic to $\tilde{A}_\ell$, $\tilde{B}_\ell$, $\tilde{C}_\ell$, $\tilde{D}_\ell$, $\tilde{C}_\ell$, $\tilde{B}_\ell$ and $\tilde{C}_\ell$ respectively. For the Weyl-Coxeter group W, the characterisation of $\{\lambda(w) : w \in W\}$ given in Section 2.7 is then seen to correspond to the above realisation of [18, 5]. The bijective map from each $\mathcal{P}(\mathbf{g})$ of Section 2.7 to the corresponding realisation of [18, 5] may then be easily constructed.

This paper is organised in such a way that all our key results are presented and copiously exemplified in Section 2. In Section 3, we gather together the definitions and results from the theories of affine Lie algebras, simple Lie algebras and Coxeter groups that are required in our proofs. The proofs themselves are given in Sections 4 and 5.

1.3 Bases of $\mathbf{h}^*$

Before discussing the construction of $T(w)$, we deviate briefly to mention the three useful bases of $\mathbf{h}^*$, each of which plays a role in what follows. These bases will be properly defined in Section 3 and the relationship between them expounded. Let $\mathbf{g}$ have rank ℓ (each of the seven affine algebras pinpointed above has rank ℓ) and let $I = \{0, 1, 2, \ldots, \ell\}$. In addition set $n = \ell$, apart from the case $\mathbf{g} = A_\ell^{(1)}$ for which we set $n = \ell + 1$, and let $N = \{1, 2, \ldots, n\}$. Then $\mathbf{h}^*$ has the three convenient bases:

- The root basis $\{\Lambda_0, \alpha_j \,|\, j \in I\}$. The α_j are the *simple roots* of $\mathbf{g}$.
- The weight basis $\{\delta, \Lambda_j \,|\, j \in I\}$. The Λ_j are the *fundamental weights* of $\mathbf{g}$, and δ is the *null root*.
- The natural basis $\{\Lambda_0, \delta, \epsilon_j \,|\, j \in N\}$. The ϵ_j are *Euclidean unit vectors* orthogonal to Λ_0 and δ.

In the weight basis, the Weyl vector $\rho \in P^+$ is defined by $\rho = \sum_{j\in I} \Lambda_j$. In the natural basis, let $\overline{\mathbf{h}}^* = \mathrm{span}\{\epsilon_1, \epsilon_2, \ldots, \epsilon_n\}$, with the usual constraint $\epsilon_1 + \epsilon_2 + \cdots + \epsilon_n = 0$ in the case $\mathbf{g} = A^{(1)}_{n-1}$. Then for all $\mathbf{g}$ and all $\lambda \in \mathbf{h}^*$, we can write:

$$\lambda = \overline{\lambda} + \tilde{L}(\lambda)\Lambda_0 - D(\lambda)\delta, \tag{1.1}$$

where $\overline{\lambda} \in \overline{\mathbf{h}}^*$ is the restriction of λ from $\mathbf{h}^*$ to $\overline{\mathbf{h}}^*$, $D(\lambda)$ is the *depth* of λ, and

$$\tilde{L}(\lambda) = \begin{cases} L(\lambda) & \text{if } \mathbf{g} \neq A^{(2)}_{2\ell}; \\ \frac{1}{2}L(\lambda) & \text{if } \mathbf{g} = A^{(2)}_{2\ell}, \end{cases} \tag{1.2}$$

where $L(\lambda)$ is the *level* of λ.

1.4 Method of attack

In recursively calculating $w(\rho) - \rho$ using an expression $w = s_i s_j \cdots s_k$ in terms of the generators of W, and setting $w = w' s_k$, we are led to consider:

$$w(\rho) - \rho = w'(\rho) - \rho - w'(\alpha_k). \tag{1.3}$$

The difference between $w(\rho) - \rho$ and $w'(\rho) - \rho$, namely $w'(\alpha_k)$, when expressed in the natural basis, represents the difference between the generalised partitions $\lambda(w)$ and $\lambda(w')$. This latter difference defines a set of nodes, which when coloured k, constitutes the difference between $T(w)$ and $T(w')$.

For an arbitrary weight $\Lambda = \sum_{j=0}^{\ell} m_j(\Lambda)\Lambda_j$ in the weight basis, we find similarly:

$$w(\Lambda) - \Lambda = w'(\Lambda) - \Lambda - m_k(\Lambda) w'(\alpha_k). \tag{1.4}$$

The difference between $w(\Lambda) - \Lambda$ and $w'(\Lambda) - \Lambda$ is then obtained by taking the contribution from the nodes coloured k above and multiplying it by $m_k(\Lambda)$.

If we do indeed proceed recursively, $w'(\alpha_k)$ itself can be calculated from the previously constructed $T(w')$ applied to $\Lambda = \alpha_k$, after noting that $m_j(\alpha_k)$ is nothing other than the element A_{jk} of the generalised Cartan matrix of $\mathbf{g}$.

The result is that for general $\Lambda = \sum_{j=0}^{\ell} m_j(\Lambda)\Lambda_j$, the value of $w(\Lambda) - \Lambda$ is obtained by stretching *each* node coloured k in $T(w)$ by a factor $m_k(\Lambda)$ for each $k \in I$.

Remarkably, for a given $\mathbf{g}$ and any particular $k \in I$, nodes coloured k are positioned consistently, whatever w, and independently of the expression for w in terms of the generators. This fact enables us to define coloured grids upon which we base our combinatorial constructions.

2 Main results

2.1 Generalised partitions

There are two different ways to construct $T(w)$. The first, more direct way, requires an independent means of calculating $w(\rho) - \rho$ in the natural basis. In the second construction,

$T(w)$ is built recursively using an expression for w in terms of the Coxeter generators of W, and $w(\rho) - \rho$ is calculated as a byproduct. Later, in Section 4, we show that these two constructions are consistent in that they lead from a given w to the same $T(w)$. In Sections 2.7 and 2.10, we characterise the set of all $T(w)$ as w runs through the sets W and W_s.

For the moment, we shall concentrate on the first means of constructing $T(w)$: so let $\lambda = w(\rho) - \rho$. Quite generally, the level is invariant under the Weyl-Coxeter group action. In particular, $L(w(\rho)) = L(\rho)$ for all $w \in W$, and thus $L(\lambda) = 0$. Thereupon, (1.1) leads to:

$$\lambda = w(\rho) - \rho = \overline{\lambda} - D(w(\rho) - \rho)\delta. \tag{2.1}$$

Since $\overline{\lambda} \in \overline{\mathbf{h}}^*$, we can write:

$$\overline{\lambda} = \sum_{i=1}^{n} \lambda_i(w)\epsilon_i, \tag{2.2}$$

where $\sum_{i=1}^{n} \lambda_i(w) = 0$ in the $\mathbf{g} = A_\ell^{(1)}$ case. This allows us to define the *generalised partition* $\lambda(w) = (\lambda(w)_1, \lambda(w)_2, \ldots, \lambda(w)_n)$.

It should be noted that the parts $\lambda(w)_i$ of $\lambda(w)$, although integers, are not necessarily positive nor weakly decreasing. This generalised partition serves to specify a corresponding generalised Young diagram or Ferrers diagram $F(w) = F^{\lambda(w)}$, where the numbers of boxes in the rows of $F(w)$ are given by the parts of $\lambda(w)$, extending to the right or left of a vertical axis according to whether the parts are positive or negative, respectively.

We can then obtain $T(w)$ by superposing $F(w)$ on a certain $\mathbf{g}$-dependent periodic coloured grid which we describe below in Section 2.2. $T(w)$ is then a coloured generalised Young diagram. Hereafter, we refer to such diagrams as *coloured diagrams*. It might be noted that although the depth factor $D(w(\rho) - \rho) \neq 0$ in general, it is not required in the construction of $T(w)$. In fact, as will be seen in Section 2.5, $D(w(\rho) - \rho)$ can itself be readily obtained using $T(w)$.

2.2 Coloured grids

The grid associated with the classical affine Lie algebra $\mathbf{g}$ of rank ℓ, has n rows where, as above, $n = \ell$ apart from the case $\mathbf{g} = A_\ell^{(1)}$ for which $n = \ell+1$. The grid is of infinite extent in both horizontal directions. Each node of the grid is then *coloured* with an element of the index set I. To be precise, let $h^\vee$ be the *dual Coxeter number* of $\mathbf{g}$, and define:

$$\tilde{h}^\vee = \begin{cases} h^\vee & \text{if } \mathbf{g} \neq C_\ell^{(1)}, \\ 2h^\vee & \text{if } \mathbf{g} = C_\ell^{(1)}. \end{cases} \tag{2.3}$$

If $C_{ij} = (i - j) \bmod \tilde{h}^\vee$, the colour $\eta_{ij} \in I$ of the node in the ith row and jth column of each grid is specified in the following table:

$$
\begin{array}{llll}
A_\ell^{(1)}: & \tilde{h}^\vee = \ell+1; & \eta_{ij} = C_{ij}; & \\
B_\ell^{(1)}: & \tilde{h}^\vee = 2\ell-1; & \eta_{ij} = \begin{cases} C_{ij} & \text{if } C_{ij} \leq l, \\ 2l - C_{ij} & \text{if } C_{ij} \geq l; \end{cases} \\
C_\ell^{(1)}: & \tilde{h}^\vee = 2\ell+2; & \eta_{ij} = \begin{cases} C_{ij} & \text{if } C_{ij} \leq l, \\ 2l + 1 - C_{ij} & \text{if } C_{ij} > l; \end{cases} \\
D_\ell^{(1)}: & \tilde{h}^\vee = 2\ell-2; & \eta_{ij} = \begin{cases} C_{ij} & \text{if } C_{ij} \leq l, \\ 2l - 1 - C_{ij} & \text{if } C_{ij} > l; \end{cases} \\
A_{2\ell}^{(2)}: & \tilde{h}^\vee = 2\ell+1; & \eta_{ij} = \begin{cases} C_{ij} & \text{if } C_{ij} \leq l, \\ 2l - C_{ij} & \text{if } C_{ij} \geq l; \end{cases} \\
A_{2\ell-1}^{(2)}: & \tilde{h}^\vee = 2\ell; & \eta_{ij} = \begin{cases} C_{ij} & \text{if } C_{ij} \leq l, \\ 2l + 1 - C_{ij} & \text{if } C_{ij} > l; \end{cases} \\
D_{\ell+1}^{(2)}: & \tilde{h}^\vee = 2\ell; & \eta_{ij} = \begin{cases} C_{ij} & \text{if } C_{ij} \leq l, \\ 2l - C_{ij} & \text{if } C_{ij} \geq l; \end{cases}
\end{array}
\tag{2.4}
$$

The grids extend both to the right ($j > 0$) and to the left ($j \leq 0$) of a fixed vertical axis. For the $\ell = 4$ case of each of the seven sequences of **g**, we show the first 15 columns of the grid to the right of the vertical axis and the first five columns to the left.

$$
A_4^{(1)}: \quad \tilde{h}^\vee = 5; \quad
\begin{array}{r|l}
0\;\;4\;\;3\;\;2\;\;1 & 0\;\;4\;\;3\;\;2\;\;1\;\;0\;\;4\;\;3\;\;2\;\;1\;\;0\;\;4\;\;3\;\;2\;\;1 \\
1\;\;0\;\;4\;\;3\;\;2 & 1\;\;0\;\;4\;\;3\;\;2\;\;1\;\;0\;\;4\;\;3\;\;2\;\;1\;\;0\;\;4\;\;3\;\;2 \\
2\;\;1\;\;0\;\;4\;\;3 & 2\;\;1\;\;0\;\;4\;\;3\;\;2\;\;1\;\;0\;\;4\;\;3\;\;2\;\;1\;\;0\;\;4\;\;3 \\
3\;\;2\;\;1\;\;0\;\;4 & 3\;\;2\;\;1\;\;0\;\;4\;\;3\;\;2\;\;1\;\;0\;\;4\;\;3\;\;2\;\;1\;\;0\;\;4 \\
4\;\;3\;\;2\;\;1\;\;0 & 4\;\;3\;\;2\;\;1\;\;0\;\;4\;\;3\;\;2\;\;1\;\;0\;\;4\;\;3\;\;2\;\;1\;\;0
\end{array}
$$

$$
B_4^{(1)}: \quad \tilde{h}^\vee = 7; \quad
\begin{array}{r|l}
3\;\;4\;\;3\;\;2\;\;1 & 0\;\;2\;\;3\;\;4\;\;3\;\;2\;\;1{\sim}0\;\;2\;\;3\;\;4\;\;3\;\;2\;\;1{\sim}0 \\
2\;\;3\;\;4\;\;3\;\;2 & 1{\sim}0\;\;2\;\;3\;\;4\;\;3\;\;2\;\;1{\sim}0\;\;2\;\;3\;\;4\;\;3\;\;2\;\;1{\sim} \\
{\sim}0\;\;2\;\;3\;\;4\;\;3 & 2\;\;1{\sim}0\;\;2\;\;3\;\;4\;\;3\;\;2\;\;1{\sim}0\;\;2\;\;3\;\;4\;\;3\;\;2 \\
1{\sim}0\;\;2\;\;3\;\;4 & 3\;\;2\;\;1{\sim}0\;\;2\;\;3\;\;4\;\;3\;\;2\;\;1{\sim}0\;\;2\;\;3\;\;4\;\;3
\end{array}
$$

$$
C_4^{(1)}: \quad \tilde{h}^\vee = 10; \quad
\begin{array}{r|l}
4{-}4\;\;3\;\;2\;\;1 & 0{-}0\;\;1\;\;2\;\;3\;\;4{-}4\;\;3\;\;2\;\;1\;\;0{-}0\;\;1\;\;2\;\;3 \\
3\;\;4{-}4\;\;3\;\;2 & 1\;\;0{-}0\;\;1\;\;2\;\;3\;\;4{-}4\;\;3\;\;2\;\;1\;\;0{-}0\;\;1\;\;2 \\
2\;\;3\;\;4{-}4\;\;3 & 2\;\;1\;\;0{-}0\;\;1\;\;2\;\;3\;\;4{-}4\;\;3\;\;2\;\;1\;\;0{-}0\;\;1 \\
1\;\;2\;\;3\;\;4{-}4 & 3\;\;2\;\;1\;\;0{-}0\;\;1\;\;2\;\;3\;\;4{-}4\;\;3\;\;2\;\;1\;\;0{-}0
\end{array}
$$

$$
D_4^{(1)}: \quad \tilde{h}^\vee = 6; \quad
\begin{array}{r|l}
2\;\;4{\sim}3\;\;2\;\;1 & 0\;\;2\;\;4{\sim}3\;\;2\;\;1{\sim}0\;\;2\;\;4{\sim}3\;\;2\;\;1{\sim}0\;\;2\;\;4{\sim} \\
{\sim}0\;\;2\;\;4{\sim}3\;\;2 & 1{\sim}0\;\;2\;\;4{\sim}3\;\;2\;\;1{\sim}0\;\;2\;\;4{\sim}3\;\;2\;\;1{\sim}0\;\;2 \\
1{\sim}0\;\;2\;\;4{\sim}3 & 2\;\;1{\sim}0\;\;2\;\;4{\sim}3\;\;2\;\;1{\sim}0\;\;2\;\;4{\sim}3\;\;2\;\;1{\sim}0 \\
2\;\;1{\sim}0\;\;2\;\;4 & 3\;\;2\;\;1{\sim}0\;\;2\;\;4{\sim}3\;\;2\;\;1{\sim}0\;\;2\;\;4{\sim}3\;\;2\;\;1{\sim}
\end{array}
$$

$$A_8^{(2)}: \quad \tilde{h}^\vee = 9; \quad \begin{array}{r|l} 3\ \ 4\ \ 3\ \ 2\ \ 1 & 0{-}0\ \ 1\ \ 2\ \ 3\ \ 4\ \ 3\ \ 2\ \ 1\ \ 0{-}0\ \ 1\ \ 2\ \ 3\ \ 4 \\ 2\ \ 3\ \ 4\ \ 3\ \ 2 & 1\ \ 0{-}0\ \ 1\ \ 2\ \ 3\ \ 4\ \ 3\ \ 2\ \ 1\ \ 0{-}0\ \ 1\ \ 2\ \ 3 \\ 1\ \ 2\ \ 3\ \ 4\ \ 3 & 2\ \ 1\ \ 0{-}0\ \ 1\ \ 2\ \ 3\ \ 4\ \ 3\ \ 2\ \ 1\ \ 0{-}0\ \ 1\ \ 2 \\ {-}0\ \ 1\ \ 2\ \ 3\ \ 4 & 3\ \ 2\ \ 1\ \ 0{-}0\ \ 1\ \ 2\ \ 3\ \ 4\ \ 3\ \ 2\ \ 1\ \ 0{-}0\ \ 1 \end{array}$$

$$A_7^{(2)}: \quad \tilde{h}^\vee = 8; \quad \begin{array}{r|l} 4{-}4\ \ 3\ \ 2\ \ 1 & 0\ \ 2\ \ 3\ \ 4{-}4\ \ 3\ \ 2\ \ 1{\sim}0\ \ 2\ \ 3\ \ 4{-}4\ \ 3\ \ 2 \\ 3\ \ 4{-}4\ \ 3\ \ 2 & 1{\sim}0\ \ 2\ \ 3\ \ 4{-}4\ \ 3\ \ 2\ \ 1{\sim}0\ \ 2\ \ 3\ \ 4{-}4\ \ 3 \\ 2\ \ 3\ \ 4{-}4\ \ 3 & 2\ \ 1{\sim}0\ \ 2\ \ 3\ \ 4{-}4\ \ 3\ \ 2\ \ 1{\sim}0\ \ 2\ \ 3\ \ 4{-}4 \\ {\sim}0\ \ 2\ \ 3\ \ 4{-}4 & 3\ \ 2\ \ 1{\sim}0\ \ 2\ \ 3\ \ 4{-}4\ \ 3\ \ 2\ \ 1{\sim}0\ \ 2\ \ 3\ \ 4{-} \end{array}$$

$$D_5^{(2)}: \quad \tilde{h}^\vee = 8; \quad \begin{array}{r|l} 3\ \ 4\ \ 3\ \ 2\ \ 1 & 0\ \ 1\ \ 2\ \ 3\ \ 4\ \ 3\ \ 2\ \ 1\ \ 0\ \ 1\ \ 2\ \ 3\ \ 4\ \ 3\ \ 2 \\ 2\ \ 3\ \ 4\ \ 3\ \ 2 & 1\ \ 0\ \ 1\ \ 2\ \ 3\ \ 4\ \ 3\ \ 2\ \ 1\ \ 0\ \ 1\ \ 2\ \ 3\ \ 4\ \ 3 \\ 1\ \ 2\ \ 3\ \ 4\ \ 3 & 2\ \ 1\ \ 0\ \ 1\ \ 2\ \ 3\ \ 4\ \ 3\ \ 2\ \ 1\ \ 0\ \ 1\ \ 2\ \ 3\ \ 4 \\ 0\ \ 1\ \ 2\ \ 3\ \ 4 & 3\ \ 2\ \ 1\ \ 0\ \ 1\ \ 2\ \ 3\ \ 4\ \ 3\ \ 2\ \ 1\ \ 0\ \ 1\ \ 2\ \ 3 \end{array}$$

For each $\mathbf{g}$, the colouring of the nodes of the grid is directly related to the structure of the Dynkin diagram of $\mathbf{g}$ shown in Table 1. In fact, the colour k of a node in a grid is nothing other than the label $k \in \{0, 1, \ldots \ell\}$ of the vertex in the Dynkin diagram that corresponds to the simple root α_k of $\mathbf{g}$.

In each grid, the vertical axis separates two columns of nodes. The nodes of the column $j = 1$ to its immediate right are coloured $0, 1, \ldots, n-1$ from top to bottom. The sequence of colours reading from left to right across each row must then accord with reading the labels of the vertices of the corresponding Dynkin diagram either clockwise for $A_\ell^{(1)}$ or to and fro across the diagram with a reflection of the sequence at either end for each of the other classical affine Lie algebras, $\mathbf{g}$. If a node coloured k is associated with a long root α_k corresponding to a vertex at the end of a Dynkin diagram (in that it is linked to only one other vertex) then each node coloured k in the grid is doubled to give a tied pair $k - k$. The grids also feature unordered pairs $i \sim j$ when the corresponding ith and jth vertices of the Dynkin diagram of $\mathbf{g}$ occur at a branched end, with both linked to the same vertex by a single edge. It will be convenient to refer to such values i and j as associated. The values 1 and 0 are associated for each $\mathbf{g} = B_\ell^{(1)}$, $D_\ell^{(1)}$ and $A_{2\ell-1}^{(2)}$, and the values ℓ and $\ell - 1$ are associated for $\mathbf{g} = D_\ell^{(1)}$. We also refer to a neighbouring pair of nodes in the grid with associated colours as an associated pair. Whenever an associated pair in the grid doesn't straddle the vertical axis, the pair is unordered and denoted $i \sim j$. However, if an associated pair straddles the vertical axis, the pair is always ordered as indicated in the above grids.

In each of the above grids, the colourings are periodic across each row with period $\tilde{h}^\vee$. Moreover, within each period each colour k appears precisely $\tilde{c}_k^\vee$ times where,

$$\tilde{c}_k^\vee = \begin{cases} c_k^\vee & \text{if } \mathbf{g} \neq C_\ell^{(1)}; \\ 2c_k^\vee & \text{if } \mathbf{g} = C_\ell^{(1)}, \end{cases} \tag{2.5}$$

Algebra	Dynkin diagram	Range
$A_1^{(1)}$	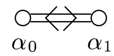	$\ell = 1$
$A_\ell^{(1)}$	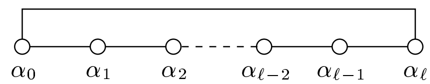	$\ell \geq 2$
$B_\ell^{(1)}$	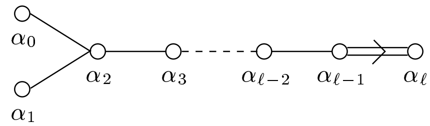	$\ell \geq 3$
$C_\ell^{(1)}$	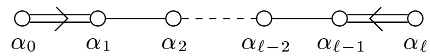	$\ell \geq 2$
$D_\ell^{(1)}$	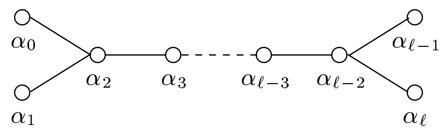	$\ell \geq 4$
$A_2^{(2)}$	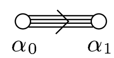	$\ell = 1$
$A_{2\ell}^{(2)}$	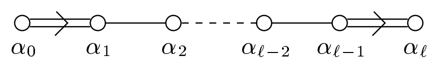	$\ell \geq 2$
$A_{2\ell-1}^{(2)}$	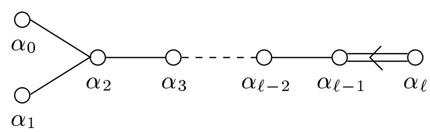	$\ell \geq 3$
$D_{\ell+1}^{(2)}$	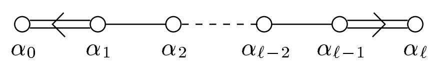	$\ell \geq 2$

Table 1: Dynkin diagrams of classical affine Lie algebras

and $c_k^\vee$ is the kth *comark* of $\mathbf{g}$ for $k \in I$. In addition, if we define the *diagonal* of the node in the ith row and jth column of each grid to be the value $i - j$, then two nodes whose diagonals differ by a multiple of $\tilde{h}^\vee$ are of the same colour. Moreover, the sequence of colours obtained from reading a $\tilde{h}^\vee$-ribbon (a contiguous sequence of $\tilde{h}^\vee$ nodes for which the difference between the diagonals of one node and the next is precisely -1) is a cyclic permutation of the sequence of colours associated with the basic horizontal period.

As will be seen later, the structure of the coloured grid for each $\mathbf{g}$ can be traced to the properties of the generalised Cartan matrix $A = (A_{ij})_{i,j \in I}$ of $\mathbf{g}$, and the relationship between the simple root basis and the natural basis.

A node in any one of the above grids that has colour k is simply referred to as a k-node. In what follows, a tied pair of nodes $k - k$ cannot be bisected. On the other hand, the constituent i-node and j-node of an unordered pair of nodes $i \sim j$ may be interchanged in certain circumstances, and they may be bisected.

2.3 Definition of the coloured diagram

The coloured diagram $T(w)$ is now obtained by superposing the generalised Young diagram $F(w)$ on the coloured grid of $\mathbf{g}$. The superposition must be such that the n rows of $F(w)$ coincide with the n rows of the coloured grid, and the vertical axis of $F(w)$ must also coincide with that of the coloured grid. $T(w)$ then consists of that part of the coloured grid overlapped by $F(w)$, modified if necessary by interchanging the colours of some, but not necessarily all, unordered pairs $i \sim j$ if one of the pair of nodes lies within $F(w)$ and the other does not. In addition, if $\lambda(w)_i = 0$ and the values i and j are associated, then in some instances $T(w)$ is augmented by the pair of boxes $\boxed{i}\boxed{j}$ in the ith row of $T(w)$.

Example 2.3.1 *For $A_4^{(1)}$ and $w = s_0 s_3 s_4 s_3 s_1 s_0$, we obtain $\lambda(w) = (3, 2, -3, 0, -2)$. There are neither tied pairs nor unordered pairs in the coloured grid and the passage from $F(w)$ to $T(w)$ by way of superposition on the coloured grid is as follows:*

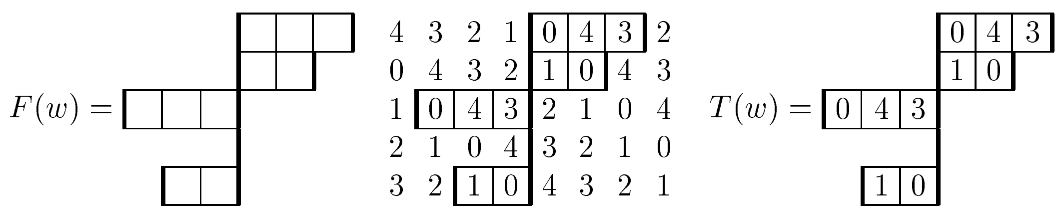

In the above example, we have marked with lines of double thickness both the reference vertical axis and the vertical edges in each row of $F(w)$ and $T(w)$ that are furthest from the vertical axis. The *profiles* of $F(w)$ and $T(w)$ are defined to be this latter set of vertical edges. Of course, the profile of $T(w)$ is identical to that of $F(w)$.

In this example it can be seen that $T(w)$ is not only *weight-balanced*, in the sense that there are equal numbers of boxes to the left and to the right of the vertical axis, but also *colour-balanced* in that for any colour k there as many k-nodes to the left of the vertical axis as there are to the right. In fact, these properties always hold in the $A_\ell^{(1)}$ case, but are peculiar to that case.

When for given $\lambda(w)$, the profile of $F(w)$ bisects an unordered pair $i \sim j$, the order of the pair is then fixed, with one or other of the i-node and the j-node being included in $T(w)$. This situation arises in the following $D_4^{(1)}$ example.

Example 2.3.2 *For $\mathbf{g} = D_4^{(1)}$ and $w = s_0 s_2 s_1 s_4 s_2 s_3 s_0$, we find that $\lambda(w) = (4, 4, 3, -3)$. The superposition of $F(w)$ on the coloured grid then gives:*

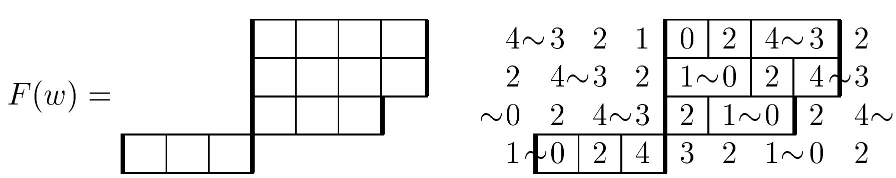

However, the profile of $F(w)$ bisects two unordered pairs, $4 \sim 3$ in the second row and $1 \sim 0$ in the fourth. The corresponding coloured diagram in this case is given by:

$T(w) =$ 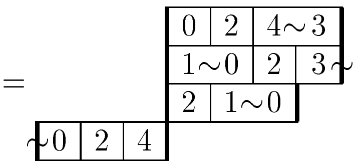

where we see that the bisected unordered pair $4 \sim 3$ in the second row has been reordered to give $3 \sim 4$ with the 3-node included in $T(w)$ and the 4-node excluded. All other entries of $T(w)$ appear as in the $D_4^{(1)}$ grid.

In the above example, the apparently arbitrary choice as to which bisected unordered pairs are to be reordered is in fact dictated by the general requirement that $T(w)$ is *even-handed*, where we say that a coloured diagram T is even-handed if the numbers of i-nodes and j-nodes in T are both even for all associated pairs i and j.

We must also consider the special case where $\lambda(w)_i = 0$ and the reference vertical axis is straddled by an associated i-node and j-node. If the numbers of i-nodes and j-nodes in the superposition of $F(w)$ on the grid are both odd, then in passing from $F(w)$ to $T(w)$ the diagram is augmented by the inclusion of a pair $\boxed{i}\boxed{j}$ in the ith row. If these numbers of nodes are both even then no augmentation occurs.

These two situations are illustrated in the following two examples for which $\mathbf{g} = D_4^{(1)}$ and $i = 4$.

Example 2.3.3 *For $\mathbf{g} = D_4^{(1)}$ and $w = s_0s_3s_1s_4s_3s_2s_4s_3$, we obtain $\lambda(w) = (5,5,2,0)$ so that $\lambda(w)_4 = 0$. Superposition of $F(w)$ on the grid gives:*

$F(w) =$ 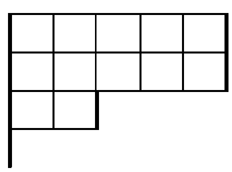 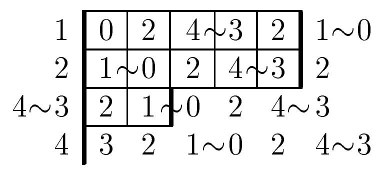

Here, the number of k-nodes inside the superposition of $F(w)$ on the grid is even for each $k \in \{0,1,3,4\}$. Therefore, on the one hand, it is unnecessary to reorder the pair $1 \sim 0$ bisected by the profile of $F(w)$ in the third row. On the other hand, it is not required to augment the fourth row of $T(w)$ by $\boxed{4}\boxed{3}$. Hence:

$T(w) =$ 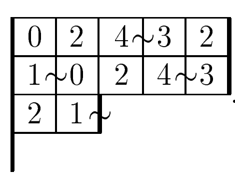.

Example 2.3.4 *For $\mathbf{g} = D_4^{(1)}$ and $w = s_0s_2s_4s_3s_2$, we obtain $\lambda(w) = (5,1,0,0)$. Once again $\lambda(w)_4 = 0$ and superposition of $F(w)$ on the grid gives:*

$F(w) =$ 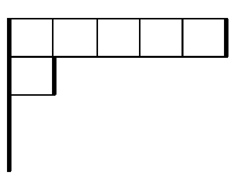 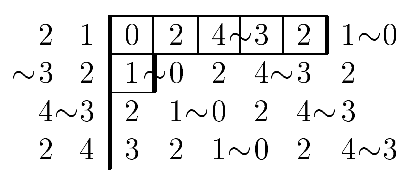

This time, the number of k-nodes inside the superposition of $F(\lambda)$ on the grid is odd for each $k \in \{0, 1, 3, 4\}$. It follows that the pair $1 \sim 0$ bisected by the profile in the second row must be reordered, and the fourth row augmented with $\boxed{4}\boxed{3}$ *to give:*

$$T(w) = \begin{array}{c|ccccc} & 0 & 2 & 4 \sim & 3 & 2 \\ & 0 \sim & & & & \\ & & & & & \\ 4 & 3 & & & & \end{array} .$$

Note that, even in this previous example, the profile of $T(w)$ coincides with that of $F(w)$.

In the case $w = 1$, we have $w(\rho) - \rho = 0$. Therefore, $\lambda(1) = (0, 0, \ldots, 0)$, and both $F(1)$ and $T(1)$ are trivial diagrams whose profiles coincide with the vertical axis.

2.4 Recursive generation of coloured diagrams

Let W be the Weyl-Coxeter group of $\mathbf{g}$ and let $w \in W$. The prescription of $T(w)$ given in Sections 2.1, 2.2 and 2.3 above relies on first being able to calculate $w(\rho) - \rho$. In this section, we show how the necessity of using this prescription can be obviated, and $T(w)$ constructed recursively using no more than an expression for w in terms of the generators $s_0, s_1, \ldots, s_\ell$ of W and the coloured grid pertaining to $\mathbf{g}$.

The construction owes its existence to the fact that for each $w' \in W$ and $k \in I$, the coloured diagram $T(w's_k)$ is readily obtained from $T(w')$ using the coloured grid pertaining to $\mathbf{g}$. To be precise we have the following algorithm:

Algorithm 2.4.1 *Let $T(1)$ be the trivial diagram with profile coinciding with the vertical axis of the coloured grid for $\mathbf{g}$. Let $w = s_{i_1} s_{i_2} \cdots s_{i_t}$ be any expression for $w \in W$ in terms of generators s_k of the Weyl-Coxeter group W of $\mathbf{g}$. Then $T(w)$ is constructed from $T(1)$ through the successive action of $s_{i_1}, s_{i_2}, \ldots, s_{i_t}$, where this action is defined as follows. For $w = w's_k$, the action of s_k on $T(w')$ gives $T(w)$ where $T(w)$ is obtained from $T(w')$ by appending or deleting as appropriate all those k-nodes that are adjacent to the profile of $T(w')$ when superposed on the coloured grid of $\mathbf{g}$. For this purpose, a k-node in the coloured grid of $\mathbf{g}$ is said to be adjacent to the profile of $T(w')$ if it is either:*

- *next to one of the vertical edges that define the profile; or*
- *one of a tied pair next to such an edge; or*
- *one of an associated pair next to such an edge.*

This procedure is illustrated in the following examples in which all nodes adjacent to the profile of $T(w')$ are identified in the diagram next to $T(w')$, whether or not they lie within $T(w')$ itself.

Example 2.4.2 *Consider the case* $\mathbf{g} = C_4^{(1)}$ *where, for* $w' = s_0s_1s_2s_3s_4s_0s_1s_0$ *the coloured diagram* $T(w')$ *takes the form:*

$$T(w') = \begin{array}{|c|c|c|c|c|c|c|}\hline 0 & 0 & 1 & 2 & 3 & 4 & 4 \\ \hline 1 & 0 & 0 & 1 \\ \cline{1-4} 2 & 1 & 0 & 0 \\ \cline{1-4} 3 \\ \cline{1-1} \end{array}\ , \qquad \begin{array}{|c|c|c|c|c|c|c|l}\hline 0 & 0 & 1 & 2 & 3 & 4 & 4 & 3 \\ \hline 1 & 0 & 0 & 1 & 2 \\ \cline{1-4} 2 & 1 & 0 & 0 & 1 \\ \cline{1-4} 3 & 2 \\ \cline{1-1} \end{array}\ .$$

In the diagram to the right here we have written $T(w')$ *together with all nodes from the underlying* $C_4^{(1)}$ *grid that are adjacent to its profile. We now form* $T(w's_k)$ *for* $k = 0$ *and* $k = 3$ *using Algorithm 2.4.1. For* $k = 0$ *we remove the tied pair* $0 - 0$ *adjacent to the profile, and for* $k = 3$ *we add the adjacent* 3*-node in the first row and remove the adjacent* 3*-node in the fourth row to give:*

$$T(w's_0) = \begin{array}{|c|c|c|c|c|c|c|}\hline 0 & 0 & 1 & 2 & 3 & 4 & 4 \\ \hline 1 & 0 & 0 & 1 \\ \cline{1-4} 2 & 1 \\ \cline{1-2} 3 \\ \cline{1-1} \end{array} \quad \textit{and} \quad T(w's_3) = \begin{array}{|c|c|c|c|c|c|c|c|}\hline 0 & 0 & 1 & 2 & 3 & 4 & 4 & 3 \\ \hline 1 & 0 & 0 & 1 \\ \cline{1-4} 2 & 1 & 0 & 0 \\ \cline{1-4} \\ \end{array}$$

respectively.

Example 2.4.3 *For* $\mathbf{g} = B_4^{(1)}$ *and* $w' = s_0s_2s_3s_4s_3s_2$*, we have:*

$$T(w') = \begin{array}{|c|c|c|c|c|c|}\hline 0 & 2 & 3 & 4 & 3 & 2 \\ \hline 0 \\ \cline{1-1} \\ \\ \end{array}\ , \qquad \begin{array}{r|c|c|c|c|c|c|l}\cline{2-7} & 0 & 2 & 3 & 4 & 3 & 2 & 1\sim 0 \\ \cline{2-7} & 0\sim 1 \\ \cline{2-2} 3 & 2 \\ 4 & 3 \end{array}\ .$$

We apply Algorithm 2.4.1 twice to obtain:

$$T(w's_1) = \begin{array}{|c|c|c|c|c|c|c|}\hline 0 & 2 & 3 & 4 & 3 & 2 & 1 \\ \hline \multicolumn{2}{|c|}{1\sim 0} \\ \cline{1-2} \\ \\ \end{array} \quad \textit{and} \quad T(w's_1s_0) = \begin{array}{|c|c|c|c|c|c|c|}\hline 0 & 2 & 3 & 4 & 3 & 2 & 1\sim 0 \\ \hline 1\sim \\ \cline{1-1} \\ \\ \end{array}\ .$$

Note that here in passing from $T(w')$ *to* $T(w's_1)$*, a* 1*-node has been appended to both the first and second rows (the pair* $1 \sim 0$ *in the second row is then unordered: we choose to display the* 1 *to the left of the* 0 *to accord with the coloured grids described previously).*

The above rule also applies to the special case in which $T(w')$ contains the augmented pair $\boxed{i}\boxed{j}$, after noting that here $\lambda(w')_i = 0$, and the profiles of $F(w')$ and $T(w')$ coincide with the vertical axis in the ith row. We use the case considered in Example 2.3.4 above to illustrate the application of the rule given above in Algorithm 2.4.1 in this instance.

Example 2.4.4 *Let* $\mathbf{g} = D_4^{(1)}$ *and* $w' = s_0 s_2 s_4 s_3 s_2$*, so that* $\lambda(w') = (5, 1, 0, 0)$ *and:*

$T(w') =$ 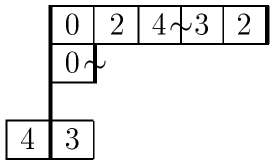 , 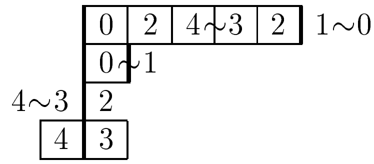 .

Here, the profile of $T(w')$ *in the 4th row is adjacent to nodes of colours 3 and 4 in* $T(w')$*. We thus obtain:*

$T(w's_3) =$ 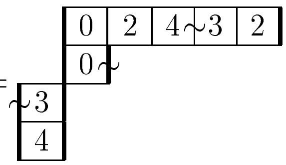 *and* $T(w's_4) =$ 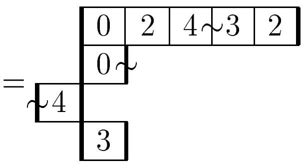 ,

with $\lambda(w's_3) = (5, 1, -1, -1)$ *and* $\lambda(w's_4) = (5, 1, -1, 1)$*. Note that the profiles of* $T(w's_3)$ *and* $T(w's_4)$ *in the 4th row lie one unit to the left and right respectively of the vertical axis.*

If the vertical axis bisects an associated pair, i and j, in the ith row, and $\lambda(w)_i = \pm 1$ then, by definition, the profile of $F(w)$ is adjacent to both an i-node and a j-node. However, only one of these two nodes is present in $T(w)$. This is the case for $i = 4$ in both $T(w's_3)$ and $T(w's_4)$ in Example 2.4.4 above. Assume that it is the i-node (resp. j-node) that is the single node present. Then that node is removed from the ith row to produce the ith row of $T(ws_i)$ (resp. $T(ws_j)$) which is now empty. On the other hand, $T(ws_j)$ (resp. $T(ws_i)$) is obtained by replacing the single node with the augmentation $\boxed{i}\boxed{j}$. Note that, in effect, a j-node (resp. i-node) has been added to the ith row of $T(w)$, but not immediately next to the profile. This is entirely in accordance with the rules described in Algorithm 2.4.1, together with the reordering necessary for consistency with the requirements that any associated pair straddling the vertical axis must take the particular order specified in the coloured grid. This latter case is illustrated by the passage from $T(w's_3)$ back to $T(w's_3s_3) = T(w')$ (resp. $T(w's_4)$ back to $T(w's_4s_4) = T(w')$) in the above Example 2.4.4 where $i = 4$ and $j = 3$. Note that $\lambda(ws_i)_i = \lambda(ws_j)_i = 0$ and that the profile in the ith row of both $T(ws_i)$ and $T(ws_j)$ coincides with that of the vertical axis.

Having illustrated the passage from $T(w')$ to $T(w's_k)$, we see, as stated in Algorithm 2.4.1, that given an expression $w = s_{i_1} s_{i_2} \cdots s_{i_t}$, we may start from the trivial coloured diagram $T(1)$ and construct $T(w)$ in a sequence of t steps starting first with $T(s_{i_1})$, then $T(s_{i_1} s_{i_2})$, and so on.

Example 2.4.5 *For* $\mathbf{g} = A_4^{(1)}$*, consider* $w = s_0 s_3 s_4 s_3 s_1 s_0$*. Then* $T(w)$ *is obtained from* $T(1)$ *via the following six steps:*

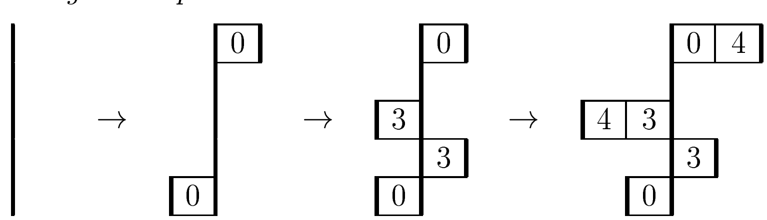

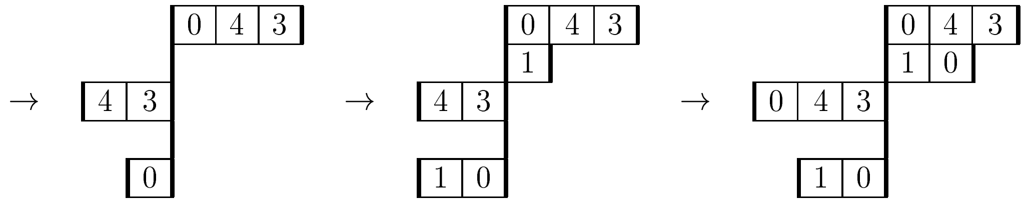

Note that the resulting $T(w)$ agrees with that given in Example 2.3.1, and that at every stage the coloured diagram is both weight-balanced and colour-balanced in that the same number of k-nodes lie on each side of the vertical axis for all $k \in \{0,1,2,3,4\}$.

Example 2.4.6 *For $\mathbf{g} = B_4^{(1)}$, consider $w = s_0 s_2 s_3 s_4 s_3 s_2 s_1$. Then $T(w)$ is obtained from $T(1)$ via the following seven steps:*

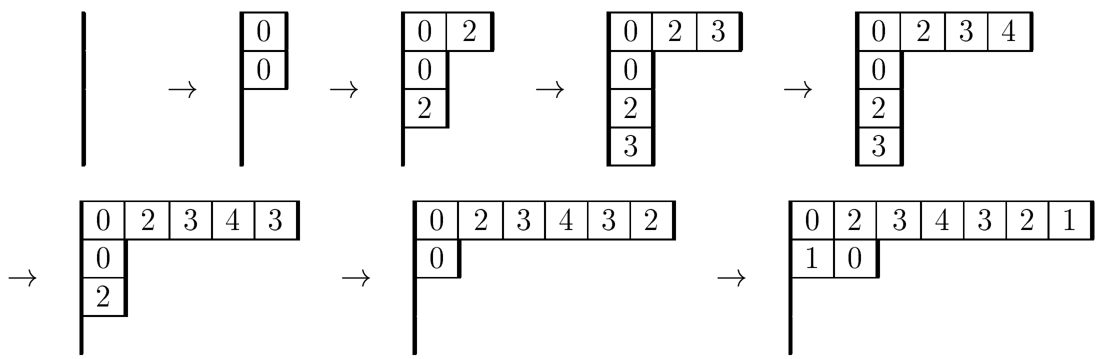

We note that the $T(w)$ produced by this means is independent of the particular expression for w that is used. Indeed, it does not matter whether the expression is *reduced.* Of course, this should be the case, because in the prescription of Sections 2.1, 2.2 and 2.3, $T(w)$ is seen to depend only on $\overline{w(\rho)-\rho}$. In Section 2.8, we show conversely how $T(w)$ may be used to produce a reduced expression for w.

Having now obtained $T(w)$, it is an easy matter to read $\overline{w(\rho)-\rho}$ from it. The generalised partition $\lambda(w) = (\lambda(w)_1, \lambda(w)_2, \ldots, \lambda(w)_n)$ is given by setting $\lambda(w)_i$ to be the displacement of the profile of $T(w)$ in the ith row from the vertical axis, with displacements to the right and left treated as positive and negative respectively. Then $\overline{w(\rho)-\rho} = \sum_{i=1}^{n} \lambda(w)_i \epsilon_i$.

In the next section, we show how $T(w)$ can also be used to obtain $D(w(\rho)-\rho)$, so that $w(\rho)-\rho$ is immediately known in full.

2.5 Depth charges

In order to obtain the value of $D(w(\rho)-\rho)$ from $T(w)$, we use an enhancement of the grids that were defined in Section 2.2. Every node in those grids is given a *charge* which is calculated using B_{ij} and C_{ij} defined by $B_{ij} = \lfloor (i-j)/\tilde{h}^\vee \rfloor$ and $C_{ij} = (i-j) \bmod \tilde{h}^\vee$. The charge $\zeta_{ij} \in \frac{1}{2}\mathbb{Z}$ of the node in the ith row and jth column of each grid is specified in the following table:

$$
\begin{array}{llll}
A_\ell^{(1)}: & \tilde{h}^\vee = \ell+1; & \zeta_{ij} = -B_{ij}; & \\
B_\ell^{(1)}: & \tilde{h}^\vee = 2\ell-1; & \zeta_{ij} = \begin{cases} \frac{1}{2} - B_{ij} & \text{if } C_{ij} \in \{0,1\}, \\ -B_{ij} & \text{otherwise;} \end{cases} & \\
C_\ell^{(1)}: & \tilde{h}^\vee = 2\ell+2; & \zeta_{ij} = \begin{cases} \frac{1}{2} - B_{ij} & \text{if } C_{ij} = 0, \\ -\frac{1}{2} - B_{ij} & \text{if } C_{ij} = \tilde{h}^\vee - 1, \\ -B_{ij} & \text{otherwise;} \end{cases} & \\
D_\ell^{(1)}: & \tilde{h}^\vee = 2\ell-2; & \zeta_{ij} = \begin{cases} \frac{1}{2} - B_{ij} & \text{if } C_{ij} \in \{0,1\}, \\ -B_{ij} & \text{otherwise;} \end{cases} & \\
A_{2\ell}^{(2)}: & \tilde{h}^\vee = 2\ell+1; & \zeta_{ij} = \begin{cases} \frac{1}{2} - B_{ij} & \text{if } C_{ij} = 0, \\ -\frac{1}{2} - B_{ij} & \text{if } C_{ij} = \tilde{h}^\vee - 1, \\ -B_{ij} & \text{otherwise;} \end{cases} & \\
A_{2\ell-1}^{(2)}: & \tilde{h}^\vee = 2\ell; & \zeta_{ij} = \begin{cases} \frac{1}{2} - B_{ij} & \text{if } C_{ij} \in \{0,1\}, \\ -B_{ij} & \text{otherwise;} \end{cases} & \\
D_{\ell+1}^{(2)}: & \tilde{h}^\vee = 2\ell; & \zeta_{ij} = \begin{cases} 1 - 2B_{ij} & \text{if } C_{ij} = 0, \\ -2B_{ij} & \text{otherwise.} \end{cases} &
\end{array}
\tag{2.6}
$$

In the enhanced grid, the charge ζ_{ij} is displayed as a subscript of the corresponding colour.

As in Section 2.2, we illustrate this definition with the $\ell = 4$ case of each of the seven sequences of $\mathbf{g}$. In each case, we again show the first 15 columns of the grid to the right of the vertical axis and the first five columns to the left. Here, we suppress the indication of unordered and tied entries for typographical reasons.

$$
A_4^{(1)}: \quad
\begin{array}{ccccc|ccccccccccccccc}
0_{\bar{1}} & 4_0 & 3_0 & 2_0 & 1_0 & 0_0 & 4_1 & 3_1 & 2_1 & 1_1 & 0_1 & 4_2 & 3_2 & 2_2 & 1_2 & 0_2 & 4_3 & 3_3 & 2_3 & 1_3 \\
1_{\bar{1}} & 0_{\bar{1}} & 4_0 & 3_0 & 2_0 & 1_0 & 0_0 & 4_1 & 3_1 & 2_1 & 1_1 & 0_1 & 4_2 & 3_2 & 2_2 & 1_2 & 0_2 & 4_3 & 3_3 & 2_3 \\
2_{\bar{1}} & 1_{\bar{1}} & 0_{\bar{1}} & 4_0 & 3_0 & 2_0 & 1_0 & 0_0 & 4_1 & 3_1 & 2_1 & 1_1 & 0_1 & 4_2 & 3_2 & 2_2 & 1_2 & 0_2 & 4_3 & 3_3 \\
3_{\bar{1}} & 2_{\bar{1}} & 1_{\bar{1}} & 0_{\bar{1}} & 4_0 & 3_0 & 2_0 & 1_0 & 0_0 & 4_1 & 3_1 & 2_1 & 1_1 & 0_1 & 4_2 & 3_2 & 2_2 & 1_2 & 0_2 & 4_3 \\
4_{\bar{1}} & 3_{\bar{1}} & 2_{\bar{1}} & 1_{\bar{1}} & 0_{\bar{1}} & 4_0 & 3_0 & 2_0 & 1_0 & 0_0 & 4_1 & 3_1 & 2_1 & 1_1 & 0_1 & 4_2 & 3_2 & 2_2 & 1_2 & 0_2
\end{array}
$$

$$
B_4^{(1)}: \quad
\begin{array}{ccccc|ccccccccccccccc}
3_0 & 4_0 & 3_0 & 2_0 & 1_{\frac{1}{2}} & 0_{\frac{1}{2}} & 2_1 & 3_1 & 4_1 & 3_1 & 2_1 & 1_{\frac{3}{2}} & 0_{\frac{3}{2}} & 2_2 & 3_2 & 4_2 & 3_2 & 2_2 & 1_{\frac{5}{2}} & 0_{\frac{5}{2}} \\
2_0 & 3_0 & 4_0 & 3_0 & 2_0 & 1_{\frac{1}{2}} & 0_{\frac{1}{2}} & 2_1 & 3_1 & 4_1 & 3_1 & 2_1 & 1_{\frac{3}{2}} & 0_{\frac{3}{2}} & 2_2 & 3_2 & 4_2 & 3_2 & 2_2 & 1_{\frac{5}{2}} \\
0_{\frac{\bar{1}}{2}} & 2_0 & 3_0 & 4_0 & 3_0 & 2_0 & 1_{\frac{1}{2}} & 0_{\frac{1}{2}} & 2_1 & 3_1 & 4_1 & 3_1 & 2_1 & 1_{\frac{3}{2}} & 0_{\frac{3}{2}} & 2_2 & 3_2 & 4_2 & 3_2 & 2_2 \\
1_{\frac{\bar{1}}{2}} & 0_{\frac{\bar{1}}{2}} & 2_0 & 3_0 & 4_0 & 3_0 & 2_0 & 1_{\frac{1}{2}} & 0_{\frac{1}{2}} & 2_1 & 3_1 & 4_1 & 3_1 & 2_1 & 1_{\frac{3}{2}} & 0_{\frac{3}{2}} & 2_2 & 3_2 & 4_2 & 3_2
\end{array}
$$

$$
C_4^{(1)}: \quad
\begin{array}{ccccc|ccccccccccccccc}
4_0 & 4_0 & 3_0 & 2_0 & 1_0 & 0_{\frac{1}{2}} & 0_{\frac{1}{2}} & 1_1 & 2_1 & 3_1 & 4_1 & 4_1 & 3_1 & 2_1 & 1_1 & 0_{\frac{3}{2}} & 0_{\frac{3}{2}} & 1_2 & 2_2 & 3_2 \\
3_0 & 4_0 & 4_0 & 3_0 & 2_0 & 1_0 & 0_{\frac{1}{2}} & 0_{\frac{1}{2}} & 1_1 & 2_1 & 3_1 & 4_1 & 4_1 & 3_1 & 2_1 & 1_1 & 0_{\frac{3}{2}} & 0_{\frac{3}{2}} & 1_2 & 2_2 \\
2_0 & 3_0 & 4_0 & 4_0 & 3_0 & 2_0 & 1_0 & 0_{\frac{1}{2}} & 0_{\frac{1}{2}} & 1_1 & 2_1 & 3_1 & 4_1 & 4_1 & 3_1 & 2_1 & 1_1 & 0_{\frac{3}{2}} & 0_{\frac{3}{2}} & 1_2 \\
1_0 & 2_0 & 3_0 & 4_0 & 4_0 & 3_0 & 2_0 & 1_0 & 0_{\frac{1}{2}} & 0_{\frac{1}{2}} & 1_1 & 2_1 & 3_1 & 4_1 & 4_1 & 3_1 & 2_1 & 1_1 & 0_{\frac{3}{2}} & 0_{\frac{3}{2}}
\end{array}
$$

$$
D_4^{(1)}: \quad
\begin{array}{ccccc|ccccccccccccccc}
2_0 & 4_0 & 3_0 & 2_0 & 1_{\frac{1}{2}} & 0_{\frac{1}{2}} & 2_1 & 4_1 & 3_1 & 2_1 & 1_{\frac{3}{2}} & 0_{\frac{3}{2}} & 2_2 & 4_2 & 3_2 & 2_2 & 1_{\frac{5}{2}} & 0_{\frac{5}{2}} & 2_3 & 4_3 \\
0_{\frac{\bar{1}}{2}} & 2_0 & 4_0 & 3_0 & 2_0 & 1_{\frac{1}{2}} & 0_{\frac{1}{2}} & 2_1 & 4_1 & 3_1 & 2_1 & 1_{\frac{3}{2}} & 0_{\frac{3}{2}} & 2_2 & 4_2 & 3_2 & 2_2 & 1_{\frac{5}{2}} & 0_{\frac{5}{2}} & 2_3 \\
1_{\frac{\bar{1}}{2}} & 0_{\frac{\bar{1}}{2}} & 2_0 & 4_0 & 3_0 & 2_0 & 1_{\frac{1}{2}} & 0_{\frac{1}{2}} & 2_1 & 4_1 & 3_1 & 2_1 & 1_{\frac{3}{2}} & 0_{\frac{3}{2}} & 2_2 & 4_2 & 3_2 & 2_2 & 1_{\frac{5}{2}} & 0_{\frac{5}{2}} \\
2_{\bar{1}} & 1_{\frac{\bar{1}}{2}} & 0_{\frac{\bar{1}}{2}} & 2_0 & 4_0 & 3_0 & 2_0 & 1_{\frac{1}{2}} & 0_{\frac{1}{2}} & 2_1 & 4_1 & 3_1 & 2_1 & 1_{\frac{3}{2}} & 0_{\frac{3}{2}} & 2_2 & 4_2 & 3_2 & 2_2 & 1_{\frac{5}{2}}
\end{array}
$$

$$
A_8^{(2)}: \quad
\begin{array}{ccccc|ccccccccccccccc}
3_0 & 4_0 & 3_0 & 2_0 & 1_0 & 0_{\frac{1}{2}} & 0_{\frac{1}{2}} & 1_1 & 2_1 & 3_1 & 4_1 & 3_1 & 2_1 & 1_1 & 0_{\frac{3}{2}} & 0_{\frac{3}{2}} & 1_2 & 2_2 & 3_2 & 4_2 \\
2_0 & 3_0 & 4_0 & 3_0 & 2_0 & 1_0 & 0_{\frac{1}{2}} & 0_{\frac{1}{2}} & 1_1 & 2_1 & 3_1 & 4_1 & 3_1 & 2_1 & 1_1 & 0_{\frac{3}{2}} & 0_{\frac{3}{2}} & 1_2 & 2_2 & 3_2 \\
1_0 & 2_0 & 3_0 & 4_0 & 3_0 & 2_0 & 1_0 & 0_{\frac{1}{2}} & 0_{\frac{1}{2}} & 1_1 & 2_1 & 3_1 & 4_1 & 3_1 & 2_1 & 1_1 & 0_{\frac{3}{2}} & 0_{\frac{3}{2}} & 1_2 & 2_2 \\
0_{\frac{\bar{1}}{2}} & 1_0 & 2_0 & 3_0 & 4_0 & 3_0 & 2_0 & 1_0 & 0_{\frac{1}{2}} & 0_{\frac{1}{2}} & 1_1 & 2_1 & 3_1 & 4_1 & 3_1 & 2_1 & 1_1 & 0_{\frac{3}{2}} & 0_{\frac{3}{2}} & 1_2
\end{array}
$$

$$
A_7^{(2)}: \quad
\begin{array}{ccccc|ccccccccccccccc}
4_0 & 4_0 & 3_0 & 2_0 & 1_{\frac{1}{2}} & 0_{\frac{1}{2}} & 2_1 & 3_1 & 4_1 & 4_1 & 3_1 & 2_1 & 1_{\frac{3}{2}} & 0_{\frac{3}{2}} & 2_2 & 3_2 & 4_2 & 4_2 & 3_2 & 2_2 \\
3_0 & 4_0 & 4_0 & 3_0 & 2_0 & 1_{\frac{1}{2}} & 0_{\frac{1}{2}} & 2_1 & 3_1 & 4_1 & 4_1 & 3_1 & 2_1 & 1_{\frac{3}{2}} & 0_{\frac{3}{2}} & 2_2 & 3_2 & 4_2 & 4_2 & 3_2 \\
2_0 & 3_0 & 4_0 & 4_0 & 3_0 & 2_0 & 1_{\frac{1}{2}} & 0_{\frac{1}{2}} & 2_1 & 3_1 & 4_1 & 4_1 & 3_1 & 2_1 & 1_{\frac{3}{2}} & 0_{\frac{3}{2}} & 2_2 & 3_2 & 4_2 & 4_2 \\
0_{\frac{\bar{1}}{2}} & 2_0 & 3_0 & 4_0 & 4_0 & 3_0 & 2_0 & 1_{\frac{1}{2}} & 0_{\frac{1}{2}} & 2_1 & 3_1 & 4_1 & 4_1 & 3_1 & 2_1 & 1_{\frac{3}{2}} & 0_{\frac{3}{2}} & 2_2 & 3_2 & 4_2
\end{array}
$$

$$
D_5^{(2)}: \quad
\begin{array}{ccccc|ccccccccccccccc}
3_0 & 4_0 & 3_0 & 2_0 & 1_0 & 0_1 & 1_2 & 2_2 & 3_2 & 4_2 & 3_2 & 2_2 & 1_2 & 0_3 & 1_4 & 2_4 & 3_4 & 4_4 & 3_4 & 2_4 \\
2_0 & 3_0 & 4_0 & 3_0 & 2_0 & 1_0 & 0_1 & 1_2 & 2_2 & 3_2 & 4_2 & 3_2 & 2_2 & 1_2 & 0_3 & 1_4 & 2_4 & 3_4 & 4_4 & 3_4 \\
1_0 & 2_0 & 3_0 & 4_0 & 3_0 & 2_0 & 1_0 & 0_1 & 1_2 & 2_2 & 3_2 & 4_2 & 3_2 & 2_2 & 1_2 & 0_3 & 1_4 & 2_4 & 3_4 & 4_4 \\
0_{\bar{1}} & 1_0 & 2_0 & 3_0 & 4_0 & 3_0 & 2_0 & 1_0 & 0_1 & 1_2 & 2_2 & 3_2 & 4_2 & 3_2 & 2_1 & 1_2 & 0_3 & 1_4 & 2_4 & 3_4
\end{array}
$$

It should be noted, quite generally, that on reading the coloured grids from left to right, a change in the value of the depth charge occurs only between certain nodes that are associated with the left hand end of the corresponding Dynkin diagram. Specifically, there is an increase of one between the 0 and ℓ-nodes for $\mathbf{g} = A_\ell^{(1)}$, of $\frac{1}{2}$ between the 0 and 1-nodes for $\mathbf{g} = C_\ell^{(1)}$ and $A_{2\ell}^{(2)}$, of one between the 0 and 1-nodes for $\mathbf{g} = D_{\ell+1}^{(2)}$, and of $\frac{1}{2}$ between both 2 and 0-nodes and 2 and 1-nodes for the cases $\mathbf{g} = B_\ell^{(1)}$, $D_\ell^{(1)}$ and $A_{2\ell-1}^{(2)}$.

With each entry in $T(w)$ assigned the corresponding charge, let $d(w)$ be the signed sum of the charges contained within $T(w)$, that is the sum of the charges to the right of the vertical axis minus the sum of those to the left of the vertical axis, which are for the most part negative. Then, as will be proved later, $d(w) = D(w(\rho) - \rho)$. Since the shape, that is to say the row lengths, of $T(w)$ determine the generalised partition $\lambda(w)$, it follows from (2.1) and (2.2) that $T(w)$ completely determines

$$
w(\rho) - \rho = \sum_{i=1}^{n} \lambda(w)_i \epsilon_i - d(w)\delta, \tag{2.7}
$$

as claimed.

We illustrate this rule in the following three examples, the first two of which deal with the cases from Examples 2.4.5 and 2.4.6 respectively.

Example 2.5.1 *Let* $\mathbf{g} = A_4^{(1)}$ *and* $w = s_0 s_3 s_4 s_3 s_1 s_0$. *With the enhanced grid,* $T(w)$ *takes the form:*

$$T(w) = \begin{array}{ccc|ccc} & & & 0_0 & 4_1 & 3_1 \\ & & & 1_0 & 0_0 & \\ 0_{\bar{1}} & 4_0 & 3_0 & & & \\ & & & & & \\ & 1_{\bar{1}} & 0_{\bar{1}} & & & \end{array}.$$

This gives $d(w) = (0+1+1+0+0) - (-1+0+0-1-1) = 5$. *Then, since* $\lambda(w) = (3, 2, -3, 0, -2)$, *from (2.7) we obtain* $w(\rho) - \rho = 3\epsilon_1 + 2\epsilon_2 - 3\epsilon_3 - 2\epsilon_5 - 5\delta$.

Example 2.5.2 *Let* $\mathbf{g} = B_4^{(1)}$ *and* $w = s_0 s_2 s_3 s_4 s_3 s_2 s_1$. *With the enhanced grid,* $T(w)$ *takes the form:*

$$T(w) = \begin{array}{|ccccccc} 0_{\frac{1}{2}} & 2_1 & 3_1 & 4_1 & 3_1 & 2_1 & 1_{\frac{3}{2}} \\ 1_{\frac{1}{2}} & 0_{\frac{1}{2}} & & & & & \\ & & & & & & \\ & & & & & & \end{array}.$$

This gives $d(w) = \frac{1}{2} + 1 + 1 + 1 + 1 + 1 + \frac{3}{2} + \frac{1}{2} + \frac{1}{2} = 8$. *Then, since* $\lambda(w) = (7, 2, 0, 0)$, *from (2.7) we obtain* $w(\rho) - \rho = 7\epsilon_1 + 2\epsilon_2 - 8\delta$.

Example 2.5.3 *Let* $\mathbf{g} = D_4^{(1)}$ *and* $w = s_0 s_2 s_4 s_3 s_2$. *With the enhanced grid,* $T(w)$ *takes the form:*

$$T(w) = \begin{array}{c|ccccc} & 0_{\frac{1}{2}} & 2_1 & 4_1 & 3_1 & 2_1 \\ & 0_{\frac{1}{2}} & & & & \\ & & & & & \\ 4_0 & 3_0 & & & & \end{array}.$$

This gives $d(w) = \frac{1}{2} + 1 + 1 + 1 + 1 + \frac{1}{2} + 0 - 0 = 5$. *Then, since* $\lambda(w) = (5, 1, 0, 0)$, *from (2.7) we obtain* $w(\rho) - \rho = 5\epsilon_1 + \epsilon_2 - 5\delta$.

2.6 Stretched coloured diagrams

Let Λ be any integral weight of the form $\Lambda = -D(\Lambda)\delta + \sum_{j=0}^{\ell} m_j(\Lambda)\Lambda_j$, with $m_j(\Lambda) \in \mathbb{Z}_{\geq 0}$ for $j \in I$. Then, given $T(w)$, the value of $w(\Lambda) - \Lambda$ is obtained by first constructing $T^\Lambda(w)$ from $T(w)$ by stretching horizontally each node coloured j by a factor of $m_j(\Lambda)$ to give a sequence of $m_j(\Lambda)$ j-nodes, each carrying their original depth charge. In effect, each j-node in $T(w)$ is simply multiplied by $m_j(\Lambda)$ to form $T^\Lambda(w)$. Now let $\lambda^\Lambda(w)_i$ be the length of the ith row of $T^\Lambda(w)$ taken positive or negative depending on whether the row extends to the left or right of the vertical axis. Let $d^\Lambda(w)$ be the signed sum of the depth charges in $T^\Lambda(w)$. With this notation:

$$w(\Lambda) - \Lambda = \sum_{i=1}^{n} \lambda^\Lambda(w)_i \epsilon_i - d^\Lambda(w)\delta. \tag{2.8}$$

Example 2.6.1 *For $\mathbf{g} = A_4^{(1)}$ and $w = s_0s_3s_4s_3s_1s_0$, $T(w)$ is stated in Example 2.5.1. With $\Lambda = 3\Lambda_0 + \Lambda_1 + 4\Lambda_2 + 5\Lambda_4$, the stretched coloured diagram $T^\Lambda(w)$ takes the form:*

$$T^\Lambda(w) = \begin{array}{cccccccc|cccccccc}
 & & & & & & & & 0_0 & 0_0 & 0_0 & 4_1 & 4_1 & 4_1 & 4_1 & 4_1 \\
 & & & & & & & & 1_0 & 0_0 & 0_0 & 0_0 & & & & \\
0_{\bar{1}} & 0_{\bar{1}} & 0_{\bar{1}} & 4_0 & 4_0 & 4_0 & 4_0 & 4_0 & & & & & & & & \\
 & & & & & & & & & & & & & & & \\
 & & & & 1_{\bar{1}} & 0_{\bar{1}} & 0_{\bar{1}} & 0_{\bar{1}} & & & & & & & &
\end{array}.$$

Thus $\lambda^\Lambda(w) = (8, 4, -8, 0, -4)$ and $d^\Lambda(w) = 12$. From (2.8), we then obtain $w(\Lambda) - \Lambda = 8\epsilon_1 + 4\epsilon_2 - 8\epsilon_3 - 4\epsilon_5 - 12\delta$.

Example 2.6.2 *For $\mathbf{g} = B_4^{(1)}$ and $w = s_0s_2s_3s_4s_3s_2s_1$, $T(w)$ is stated in Example 2.5.2. With $\Lambda = 3\Lambda_1 + 2\Lambda_2 + 3\Lambda_3$, the stretched coloured diagram $T^\Lambda(w)$ takes the form:*

$$T^\Lambda(w) = \begin{array}{|ccccccccccccc}
2_1 & 2_1 & 3_1 & 3_1 & 3_1 & 3_1 & 3_1 & 3_1 & 2_1 & 2_1 & 1_{\frac{3}{2}} & 1_{\frac{3}{2}} & 1_{\frac{3}{2}} \\
1_{\frac{1}{2}} & 1_{\frac{1}{2}} & 1_{\frac{1}{2}} & & & & & & & & & & \\
 & & & & & & & & & & & & \\
 & & & & & & & & & & & &
\end{array}.$$

Thus $\lambda^\Lambda(w) = (13, 3, 0, 0)$ and $d^\Lambda(w) = 16$. From (2.8), we then obtain $w(\Lambda) - \Lambda = 13\epsilon_1 + 3\epsilon_2 - 16\delta$.

In those cases in which $T(w)$ has been augmented with a pair $\boxed{i}\boxed{j}$ in the ith row, the stretching process places $m_i(\Lambda)$ nodes coloured i immediately to the left of the vertical axis in the ith row of $T^\Lambda(w)$, and $m_j(\Lambda)$ nodes coloured j immediately to their right. In accordance with the corresponding entries in $T(w)$, each of these colours receives a depth charge of $\frac{1}{2}$ if $i = 1$ and a depth charge of 0 if $i = \ell$. In these cases, we naturally set $\lambda^\Lambda(w)_i = m_j(\Lambda) - m_i(\Lambda)$. We encounter this situation in the following example.

Example 2.6.3 *For $\mathbf{g} = D_4^{(1)}$ and $w = s_0s_2s_4s_3s_2$, $T(w)$ is stated in Example 2.5.3. With $\Lambda = 3\Lambda_0 + \Lambda_3 + 4\Lambda_4$, the stretched coloured diagram $T^\Lambda(w)$ takes the form:*

$$T^\Lambda(w) = \begin{array}{cccc|cccccccc}
 & & & & 0_{\frac{1}{2}} & 0_{\frac{1}{2}} & 0_{\frac{1}{2}} & 4_1 & 4_1 & 4_1 & 4_1 & 3_1 \\
 & & & & 0_{\frac{1}{2}} & 0_{\frac{1}{2}} & 0_{\frac{1}{2}} & & & & & \\
 & & & & & & & & & & & \\
4_0 & 4_0 & 4_0 & 4_0 & 3_0 & & & & & & &
\end{array}.$$

Thus $\lambda^\Lambda(w) = (8, 3, 0, -3)$ and $d^\Lambda(w) = 8$. From (2.8), we then obtain $w(\Lambda) - \Lambda = 8\epsilon_1 + 3\epsilon_2 - 3\epsilon_4 - 8\delta$.

2.7 Characterisation for affine Weyl-Coxeter elements

In this section, we provide characterisations of the sets of generalised partitions $\{\lambda(w)|w \in W\}$ and coloured diagrams $\{T(w)|w \in W\}$. We give the latter characterisation first, and from this the former follows.

To characterise $\{T(w)|w \in W\}$, we introduce the notion of *edge-balanced*. This notion describes a particular distribution of the nodes adjacent to the profile of a coloured diagram T. Naturally, it depends on which $\mathbf{g}$ is under consideration.

If $\mathbf{g} = A_\ell^{(1)}$, we say that T is edge-balanced if the $\ell + 1$ segments of the profile of T bisect each of the following pairs exactly once:

$$\boxed{1}\boxed{0}, \quad \boxed{2}\boxed{1}, \quad \boxed{3}\boxed{2}, \quad \ldots, \quad \boxed{\ell}\boxed{\ell{-}1}, \quad \boxed{0}\boxed{\ell}.$$

If $\mathbf{g} = C_\ell^{(1)}$, $A_{2\ell}^{(2)}$ or $D_{\ell+1}^{(2)}$, we say that T is edge-balanced if the ℓ segments of the profile of T bisect each of the following pairs exactly once, with any pair reversed:

$$\boxed{1}\boxed{0}, \quad \boxed{2}\boxed{1}, \quad \boxed{3}\boxed{2}, \quad \ldots, \quad \boxed{\ell}\boxed{\ell{-}1}.$$

If $\mathbf{g} = B_\ell^{(1)}$ or $A_{2\ell-1}^{(2)}$, we say that T is edge-balanced if the ℓ segments of the profile of T bisect each of the following pairs exactly once, with any pair reversed:

$$\boxed{1}\boxed{0}, \quad \boxed{2}\boxed{1{\sim}0}, \quad \boxed{3}\boxed{2}, \quad \ldots, \quad \boxed{\ell}\boxed{\ell{-}1}.$$

Here, we say that the profile bisects the pair $\boxed{k}\boxed{i{\sim}j}$ if k is adjacent to the profile, and either element of the associated pair i and j is adjacent to the profile on the other side. If $\mathbf{g} = D_\ell^{(1)}$, we say that T is edge-balanced if the ℓ segments of the profile of T bisect each of the following pairs exactly once, with any pair reversed:

$$\boxed{1}\boxed{0}, \quad \boxed{2}\boxed{1{\sim}0}, \quad \boxed{3}\boxed{2}, \quad \ldots, \quad \boxed{\ell{-}2}\boxed{\ell{-}3}, \quad \boxed{\ell \sim \ell{-}1}\boxed{\ell{-}2}, \quad \boxed{\ell}\boxed{\ell{-}1}.$$

We can now state that $T(w)$ is edge-balanced for all $w \in W$.

Conversely, in the cases for which $\mathbf{g} = C_\ell^{(1)}$, $A_{2\ell}^{(2)}$ or $D_{\ell+1}^{(2)}$, if T is an edge-balanced coloured diagram, then there exists a unique $w \in W$ such that $T = T(w)$. In the cases for which $\mathbf{g} = B_\ell^{(1)}$, $D_\ell^{(1)}$ or $A_{2\ell-1}^{(2)}$, if T is an edge-balanced even-handed coloured diagram, then there exists a unique $w \in W$ such that $T = T(w)$. Finally, in the case $\mathbf{g} = A_\ell^{(1)}$, if T is an edge-balanced weight-balanced coloured diagram, then there again exists a unique $w \in W$ such that $T = T(w)$.

Example 2.7.1 *Let $\mathbf{g} = B_4^{(1)}$ and consider the following coloured diagram:*

$$T = \begin{array}{|c|c|c|c|c|c|c|c|c|}
\cline{4-5}
\multicolumn{3}{c|}{} & 1_{\frac{1}{2}} & 0_{\frac{1}{2}} & \multicolumn{4}{c}{} \\
\cline{4-9}
\multicolumn{4}{c|}{} & 1_{\frac{1}{2}} & 0_{\frac{1}{2}} & 2_1 & 3_1 & 4_1 \\
\cline{1-9}
2_0 & 3_0 & 4_0 & 3_0 & \multicolumn{5}{c}{} \\
\cline{1-5}
\multicolumn{4}{c|}{} & 3_0 & \multicolumn{4}{c}{} \\
\cline{5-5}
\end{array}.$$

From top to bottom, the profile of T bisects the pairs $\boxed{1}\boxed{0}$, $\boxed{4}\boxed{3}$, $\boxed{1{\sim}0}\boxed{2}$ *and* $\boxed{3}\boxed{2}$. *Then, by the above definition, T is edge-balanced. Note also that T is even-handed, and that this would not be the case if the augmented pair* $\boxed{1}\boxed{0}$ *were omitted from the first row. The above result then states that there exists $w \in W$ such that $T = T(w)$. In Section 2.8, we will obtain an explicit expression for this w in terms of the Coxeter generators of $B_4^{(1)}$.*

By examining the grids pertaining to each $\mathbf{g}$, and in particular their periodic nature, we are now able to immediately characterise $\{\lambda(w)|w \in W\}$. To do this, we introduce the sets $\mathcal{P}(\mathbf{g})$ of generalised partitions defined by:

$$
\begin{aligned}
\mathcal{P}(A_\ell^{(1)}) &= \{(\lambda_1, \lambda_2, \ldots, \lambda_{\ell+1}) \mid \textstyle\sum_{i=1}^{\ell+1} \lambda_i = 0, \\
&\qquad \{(\lambda_i - i) \operatorname{mod} (\ell+1)\}_{i=1}^{\ell+1} = \{0, 1, \ldots, \ell\}\}, \\
\mathcal{P}(B_\ell^{(1)}) &= \{(\lambda_1, \lambda_2, \ldots, \lambda_\ell) \mid \\
&\qquad \{|(\lambda_i - i + \ell) \operatorname{mod} (2\ell-1) - \ell + 1|\}_{i=1}^{\ell} = \{0, 1, \ldots, \ell-1\}\}; \\
\mathcal{P}(C_\ell^{(1)}) &= \{(\lambda_1, \lambda_2, \ldots, \lambda_\ell) \mid \\
&\qquad \{|(\lambda_i - i + \ell) \operatorname{mod} (2\ell+2) - \ell|\}_{i=1}^{\ell} = \{1, 2 \ldots, \ell\}\}; \\
\mathcal{P}(D_\ell^{(1)}) &= \{(\lambda_1, \lambda_2, \ldots, \lambda_\ell) \mid \\
&\qquad \{|(\lambda_i - i + \ell) \operatorname{mod} (2\ell-2) - \ell + 1|\}_{i=1}^{\ell} = \{0, 1, \ldots, \ell-1\}\}; \\
\mathcal{P}(A_{2\ell}^{(2)}) &= \{(\lambda_1, \lambda_2, \ldots, \lambda_\ell) \mid \\
&\qquad \{|(\lambda_i - i + \ell) \operatorname{mod} (2\ell+1) - \ell|\}_{i=1}^{\ell} = \{1, 2 \ldots, \ell\}\}; \\
\mathcal{P}(A_{2\ell-1}^{(2)}) &= \{(\lambda_1, \lambda_2, \ldots, \lambda_\ell) \mid \\
&\qquad \{|(\lambda_i - i + \ell) \operatorname{mod} (2\ell) - \ell|\}_{i=1}^{\ell} = \{0, 1, \ldots, \ell-1\}\}; \\
\mathcal{P}(D_{\ell+1}^{(2)}) &= \{(\lambda_1, \lambda_2, \ldots, \lambda_\ell) \mid \\
&\qquad \{|(\lambda_i - i + \ell) \operatorname{mod} (2\ell) - \ell + \tfrac{1}{2}|\}_{i=1}^{\ell} = \{\tfrac{1}{2}, \tfrac{3}{2}, \ldots, \ell - \tfrac{1}{2}\}\}.
\end{aligned}
$$

Note that in each case, we calculate modulo $\tilde{h}^\vee$, where the values of $\tilde{h}^\vee$ for each of the seven cases are given in (2.4).

With the above definitions, we can now state that $\{\lambda(w) \mid w \in W\} = \mathcal{P}(\mathbf{g})$. Moreover, for each generalised partition $\lambda \in \mathcal{P}(\mathbf{g})$, there is a unique $w \in W$ such that $\lambda(w) = \lambda$.

The set $\{T(w) \mid w \in W\}$ is now obtained from $\{\lambda(w) \mid w \in W\}$ by the means described in Section 2.3.

2.8 Reduced expressions

Let $w \in W$. If $w = s_{i_1} s_{i_2} \cdots s_{i_t}$ and t is the smallest value for which such an expression exists, then $s_{i_1} s_{i_2} \cdots s_{i_t}$ is said to be a *reduced* expression for w. The *length* $\ell(w)$ of w is then defined by $\ell(w) = t$. It is then the case that $\ell(ws_k) = \ell(w) \pm 1$ for all $k \in I$. Here, we show that $T(w)$ may be used to produce a reduced expression for w.

We first define the notion of a *k-shift*. If the profile in a particular row of a coloured diagram T is adjacent to k-nodes, performing a k-shift on that row moves the profile so that it lies on the other side of those k-nodes. The k-shift is described as *leftward* or *rightward* if the k-nodes in T lie to the left or to the right, respectively, of the profile.

We also describe the k-shift as *single* or *double* if a lone k-node or a tied pair of k-nodes, respectively, is adjacent to the profile. If the profile in a particular row is not adjacent to a k-node, a k-shift on that row leaves it unchanged. We say that T is obtained from a k-shift on a coloured diagram T' if each row of T is obtained from a k-shift on the corresponding row of T'.

The description in Section 2.4 then shows that if $w' \in W$ and $w = w's_k$ for $k \in I$, then $T(w)$ is obtained from $T(w')$ by a k-shift.

We write $T(w) \succ T(w')$, if $T(w)$ is obtained from $T(w')$ in one of the following four ways:

- a single rightward k-shift in row i and a single leftward k-shift in row j for $i < j$;
- a single rightward k-shift in each of rows i and j for $i \neq j$;
- a single rightward k-shift in row i;
- a double rightward k-shift in row i.

Conversely, we write $T(w) \prec T(w')$, if $T(w)$ is obtained from $T(w')$ in one of the following four ways:

- a single leftward k-shift in row i and a single rightward k-shift in row j for $i < j$;
- a single leftward k-shift in each of rows i and j for $i \neq j$;
- a single leftward k-shift in row i;
- a double leftward k-shift in row i.

We see that $T(w) \succ T(w')$ if and only if $T(w') \prec T(w)$. In fact, as shown later, $T(w)$ is necessarily obtained from $T(w')$ in one of the eight ways given above. Thus either $T(w) \succ T(w')$ or $T(w) \prec T(w')$.

With w' and w as above, we also show that $\ell(w) = \ell(w') + 1$ if and only if either:

- $d(w) > d(w')$; or
- $d(w) = d(w')$ *and* $T(w) \prec T(w')$.

Armed with this fact, we can now find a reduced expression for $w \in W$. In the first step, we seek $k \in I$ such that $\ell(ws_k) = \ell(w) - 1$. Note that there is necessarily at least one such value. On setting $w' = ws_k$ so that $w = w's_k$, each such value can be located by comparing $T(w)$ and $T(w')$ according to the above criterion. Set $k_1 = k$. If $T(w')$ is not the trivial coloured diagram, we now repeat this procedure with w' in place of w. In this way, we locate $k_2 \in I$ such that $\ell(ws_{k_1}s_{k_2}) = \ell(ws_{k_1}) - 1$. Eventually, this must lead to the trivial coloured diagram $T(1)$, implying that $ws_{k_1}s_{k_2} \cdots s_{k_{t-1}}s_{k_t} = 1$, and hence $w = s_{k_t}s_{k_{t-1}} \cdots s_{k_2}s_{k_1}$. By construction, this is necessarily a reduced expression for w. In fact, by choosing between the different values of k that arise at each step, all reduced expressions for w can be produced in this way.

Example 2.8.1 *Let $\mathbf{g} = B_4^{(1)}$ and consider the coloured diagram T given in Example 2.7.1. As stated in that example, there exists $w \in W$ for which $T = T(w)$. Here, we use the above method to find a reduced expression for w.*

First note that $d(w) = 4$. Using the method of Section 2.4, we obtain:

$T(ws_0) =$ 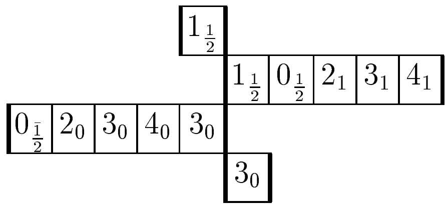 ,

$T(ws_1) =$ 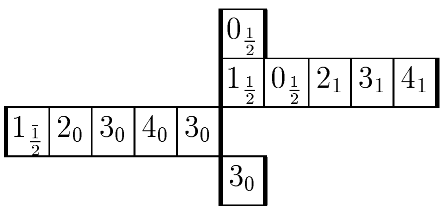 , $T(ws_2) =$ 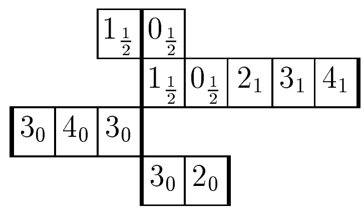 ,

$T(ws_3) =$ 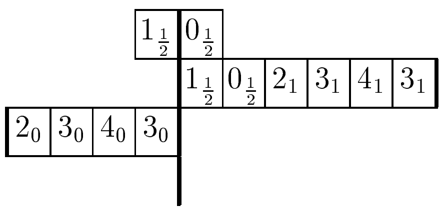 , $T(ws_4) =$ 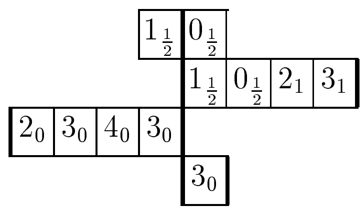 .

Thus $d(ws_0) = 4$, $d(ws_1) = 5$, $d(ws_2) = 4$, $d(ws_3) = 5$ and $d(ws_4) = 3$. In the cases for which $d(ws_k) = d(w)$, we see that $T(w) \succ T(ws_0)$ and $T(w) \prec T(ws_2)$. We therefore conclude that $\ell(ws_k) < \ell(w)$ for $k \in \{2,4\}$ and $\ell(ws_k) > \ell(w)$ for $k \in \{0,1,3\}$.

The calculation of a reduced expression for w proceeds recursively, using now either ws_2 or ws_4 in place of w. We choose ws_4. Using $T(ws_4)$ given above, we produce:

$T(ws_4s_3) =$ 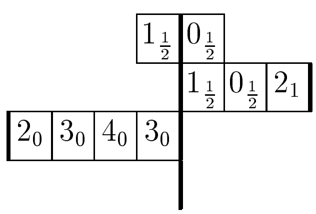 .

We then see that $d(ws_4s_3) = 2 < d(ws_4)$ and therefore $\ell(ws_4s_3) < \ell(ws_4)$. In the other cases resulting from $T(ws_4)$, it may be verified that $d(ws_4s_0) = 3$, $d(ws_4s_1) = 4$, $d(ws_4s_2) = 3$ and that $T(ws_4) \succ T(ws_4s_0)$ and $T(ws_4) \prec T(ws_4s_2)$. Thus $\ell(ws_4s_k) < \ell(ws_4)$ if and only if $k \in \{2,3\}$. We choose $k = 3$.

From $T(ws_4s_3)$ we obtain, in particular,

$T(ws_4s_3s_2) =$ 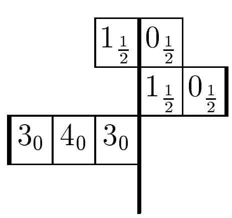 .

We then see that $d(ws_4s_3s_2) = 1 < d(ws_4s_3)$ and therefore $\ell(ws_4s_3s_2) < \ell(ws_4s_3)$. In the other cases $k \neq 2$, it may be verified that either $d(ws_4s_3s_k) > d(ws_4s_3)$ or that $T(ws_4s_3) \succ T(ws_4s_3s_k)$, and thus $\ell(ws_4s_3s_k) > \ell(ws_4s_3)$. So now we must proceed using $T(ws_4s_3s_2)$. This yields:

$T(ws_4s_3s_2s_0) =$ 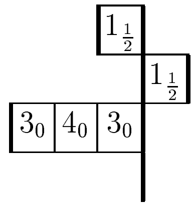 .

We see that $d(ws_4s_3s_2s_0) = 0 < d(ws_4s_3s_2)$. Additionally, $d(ws_4s_3s_2s_k) = 1 = d(ws_4s_3s_2)$ and $T(ws_4s_3s_2) \prec T(ws_4s_3s_2s_k)$, and $d(ws_4s_3s_2s_4) = 1$ and $T(ws_4s_3s_2) \succ T(ws_4s_3s_2s_4)$. Therefore, $\ell(ws_4s_3s_2s_k) < \ell(ws_4s_3s_2)$ if and only if $k \in \{0, 1, 3\}$. Choosing $k = 0$, we may now proceed:

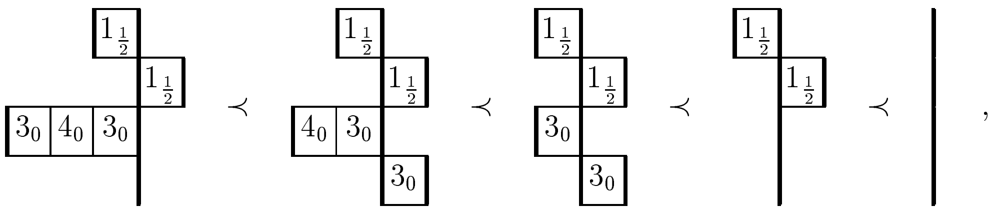

where, in each instance, the signed sum of the depth charges is 0. Altogether we thus have $ws_4s_3s_2s_0s_3s_4s_3s_1 = 1$, whereupon $w = s_1s_3s_4s_3s_0s_2s_3s_4$ is a reduced expression for w. Of course, it is one of many such expressions, and each one can be obtained by making appropriate choices in the above iterative process.

2.9 Coloured diagrams for coset representatives of natural subgroup

For each affine Lie algebra $\mathbf{g}$, we let $\overline{\mathbf{g}}$ be the maximal Lie subalgebra of $\mathbf{g}$ whose Dynkin diagram is obtained from that of $\mathbf{g}$ by omitting the node labelled 0. The Lie algebra $\overline{\mathbf{g}}$ is finite-dimensional and simple. For those cases in which $\mathbf{g}$ is a classical affine Lie algebra, these natural embeddings $\mathbf{g} \supset \overline{\mathbf{g}}$ are as follows:

$$A_\ell^{(1)} \supset A_\ell,\ B_\ell^{(1)} \supset B_\ell,\ C_\ell^{(1)} \supset C_\ell,\ D_\ell^{(1)} \supset D_\ell,\ A_{2\ell}^{(2)} \supset B_\ell,\ A_{2\ell-1}^{(2)} \supset C_\ell,\ D_{\ell+1}^{(2)} \supset B_\ell.$$

If we denote the Weyl-Coxeter group of $\overline{\mathbf{g}}$ by $\overline{W}$, it follows that $\overline{W} \subset W$. In fact, if $\{s_0, s_1, s_2, \ldots, s_\ell\}$ is the set of Coxeter generators of W, then $\{s_1, s_2, \ldots, s_\ell\}$ is the set of Coxeter generators of $\overline{W}$. Note that even though W is of infinite order, $\overline{W}$ is of finite order.

In what follows, we are especially interested in a particular set, W_s, of right coset representatives of $\overline{W}$ in W defined as follows:

Definition 2.9.1 *Let $\overline{I} = I \backslash \{0\}$, and set*

$$W_s = \{w \in W \mid \ell(s_iw) \geq \ell(w) \text{ for all } i \in \overline{I}\}. \tag{2.9}$$

It can be shown that W_s contains precisely one element from each right coset $\overline{W}w$. It can also be shown that each $w \in W_s$ is the unique element of minimal length in the coset $\overline{W}w$. Consequently, W_s is termed the set of minimal right coset representatives of $\overline{W}$ in W.

Let $w' \in W_s$ and $w = w's_k$ for $k \in I$. Later, we show that in the case for which $\ell(w) > \ell(w')$, then $w \in W_s$ if and only if $T(w) \succ T(w')$. On the other hand, in the case for which $\ell(w) < \ell(w')$, then necessarily $w \in W_s$ *and* $T(w) \prec T(w')$. These facts enable W_s to be constructed recursively by length, starting with $1 \in W_s$. Indeed, if we define:

$$W_s^{(t)} = \{w \in W_s \mid \ell(w) = t\} \tag{2.10}$$

for $t \in \mathbb{Z}_{\geq 0}$, we have the following:

Proposition 2.9.2 $W_s^{(0)} = \{1\}$. *For* $t > 0$

$$W_s^{(t)} = \{w = w's_k \mid w' \in W_s^{(t-1)},\ k \in I,\ T(w) \succ T(w')\}. \tag{2.11}$$

Thus for $t > 0$, for each pair $w' \in W_s^{(t-1)}$ and $k \in I$, we can now construct $W_s^{(t)}$ by constructing $T(w's_k)$ from $T(w')$. If $T(w's_k) \succ T(w')$ then $w's_k \in W_s^{(t)}$. All $w \in W_s^{(t)}$ necessarily arise in this way.

The above iteration process can be conveniently depicted on a directed rooted graph: the vertices of the graph are labelled by $T(w)$ for $w \in W_s$ with the root vertex labelled by the trivial coloured diagram $T(1)$, and a directed edge links $T(w')$ to $T(w)$ whenever $w = w's_k$ with $\ell(w) > \ell(w')$. We call the graph obtained in this way the Bruhat graph for W_s. In the cases $\mathbf{g} = C_3^{(1)}$, $B_3^{(1)}$, $D_4^{(1)}$ and $A_2^{(1)}$, the upper portions of the Bruhat graphs for W_s are displayed in Figs. 2, 3, 4 and 5 respectively. In each case, all the vertices that correspond to the elements of $W_s^{(t)}$ for some fixed t, and as such lie at a distance t from the root vertex, have been placed on the same horizontal level as one another.

2.10 Cores for coset representatives of natural subgroup

In this section, we characterise of the set of (generalised) partitions $\{\lambda(w)|w \in W_s\}$ in terms of their $\tilde{h}^\vee$-cores. For a definition of a p-core see [10, §2.7] or [19, p12], for example. These cores will be elements of one of the sets $\mathcal{F}, \mathcal{A}, \mathcal{C}, \mathcal{E}$ that we now specify. First, define $\mathcal{F}$ to be the set of all (genuine) partitions. Using Frobenius notation for partitions [17, §5.1 and §11.9], we now define:

$$\begin{aligned}
\mathcal{A} &= \left\{\alpha \in \mathcal{F} \mid \alpha = \left(\begin{smallmatrix} a_1 & a_2 & a_3 & \cdots & a_t \\ a_1+1 & a_2+1 & a_3+1 & \cdots & a_t+1 \end{smallmatrix}\right)\right\}\ ; \\
\mathcal{C} &= \left\{\alpha \in \mathcal{F} \mid \alpha = \left(\begin{smallmatrix} b_1+1 & b_2+1 & b_3+1 & \cdots & b_t+1 \\ b_1 & b_2 & b_3 & \cdots & b_t \end{smallmatrix}\right)\right\}\ ; \\
\mathcal{E} &= \left\{\alpha \in \mathcal{F} \mid \alpha = \left(\begin{smallmatrix} a_1 & a_2 & a_3 & \cdots & a_t \\ a_1 & a_2 & a_3 & \cdots & a_t \end{smallmatrix}\right)\right\}\ .
\end{aligned}$$

The characterisation then involves the sets $\mathcal{P}^+(\mathbf{g})$ of generalised partitions or partition pairs defined by:

$$\mathcal{P}^+(B_\ell^{(1)}) = \{\lambda \in \mathcal{F} \mid \lambda \equiv \zeta \bmod (2\ell-1), \zeta \in \mathcal{A}, \ell(\lambda) \leq \ell, \ell(\zeta) \leq \ell\};$$

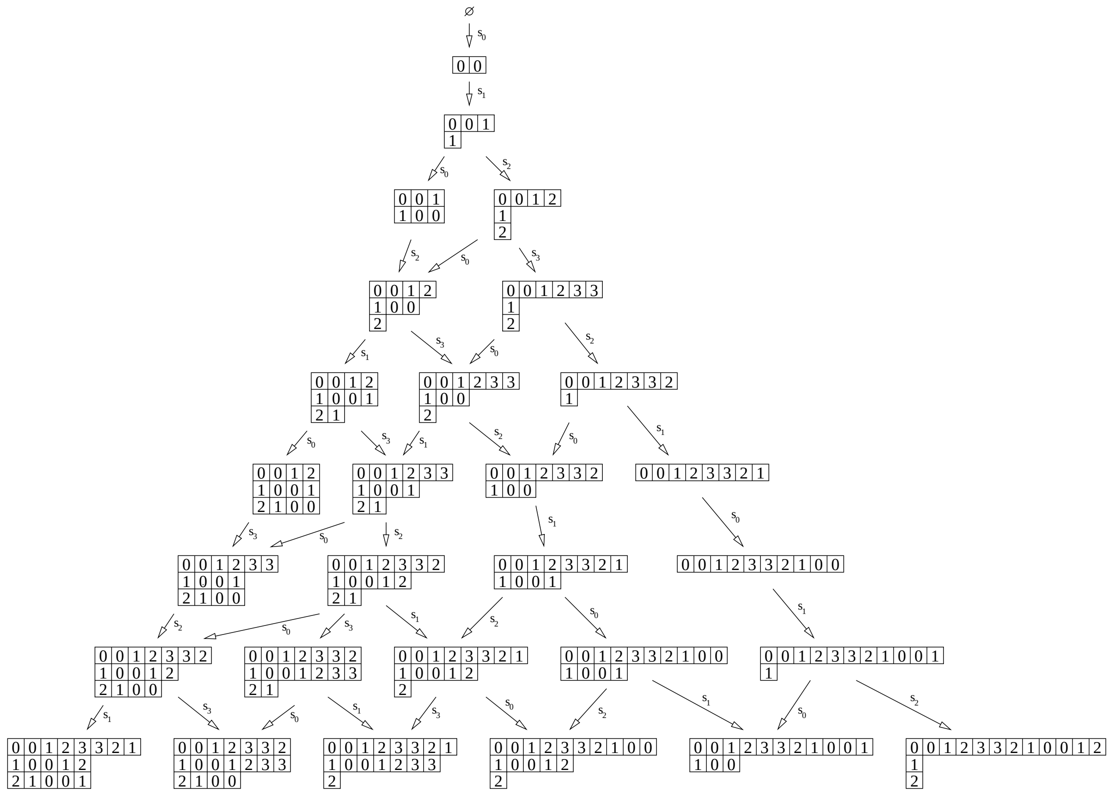

Figure 2: Top of Bruhat graph for W_s in the case $\mathbf{g} = C_3^{(1)}$

$$\begin{aligned}
\mathcal{P}^+(C_\ell^{(1)}) &= \{\lambda \in \mathcal{F} \mid \lambda \equiv \zeta \bmod (2\ell+2), \zeta \in \mathcal{C}, \ell(\lambda) \le \ell, \ell(\zeta) \le \ell\};\\
\mathcal{P}^+(A_{2\ell}^{(2)}) &= \{\lambda \in \mathcal{F} \mid \lambda \equiv \zeta \bmod (2\ell+1), \zeta \in \mathcal{C}, \ell(\lambda) \le \ell, \ell(\zeta) \le \ell\};\\
\mathcal{P}^+(A_{2\ell-1}^{(2)}) &= \{\lambda \in \mathcal{F} \mid \lambda \equiv \zeta \bmod (2\ell), \zeta \in \mathcal{A}, \ell(\lambda) \le \ell, \ell(\zeta) \le \ell\};\\
\mathcal{P}^+(D_{\ell+1}^{(2)}) &= \{\lambda \in \mathcal{F} \mid \lambda \equiv \zeta \bmod (2\ell), \zeta \in \mathcal{E}, \ell(\lambda) \le \ell, \ell(\zeta) \le \ell\};\\
\mathcal{P}^+(D_\ell^{(1)}) &= \{(\lambda_1, \lambda_2, \ldots, \lambda_{\ell-1}, \lambda_\ell) \mid (\lambda_1, \lambda_2, \ldots, \lambda_{\ell-1}, |\lambda_\ell|) \in \mathcal{F},\\
&\qquad (\lambda_1, \lambda_2, \ldots, \lambda_{\ell-1}, |\lambda_\ell|) \equiv \zeta \bmod (2\ell-2), \zeta \in \mathcal{A}, \ell(\zeta) < \ell\};\\
\mathcal{P}^+(A_\ell^{(1)}) &= \{(\mu;\nu) \mid \mu \in \mathcal{F}, \nu \in \mathcal{F}, |\mu| = |\nu|, \ell(\mu)+\ell(\nu) \le \ell+1,\\
&\qquad \mu \equiv \zeta \bmod (\ell+1), \nu \equiv \zeta' \bmod (\ell+1), \zeta \in \mathcal{F}, \ell(\zeta)+\ell(\zeta') \le \ell+1\}.
\end{aligned}$$

Here, if λ and ζ are partitions then we write $\lambda \equiv \zeta \bmod p$ to indicate that λ and ζ have the same p-core. $\ell(\lambda)$ is the number of non-zero parts of the partition λ.

Note that for $\mathbf{g} = B_\ell^{(1)}$, $C_\ell^{(1)}$, $A_{2\ell}^{(2)}$, $A_{2\ell-1}^{(2)}$ or $D_{\ell+1}^{(2)}$, the set $\mathcal{P}^+(\mathbf{g})$ is comprised of genuine partitions, and for $\mathbf{g} = D_\ell^{(1)}$, only the ℓth part of each member of $\mathcal{P}^+(\mathbf{g})$ is permitted to be negative. In the $\mathbf{g} = A_\ell^{(1)}$ case, the definition above is in terms of pairs $(\mu;\nu)$ where μ and ν are both genuine partitions. We will use the notation $\lambda = (\mu;\nu)$ to mean that

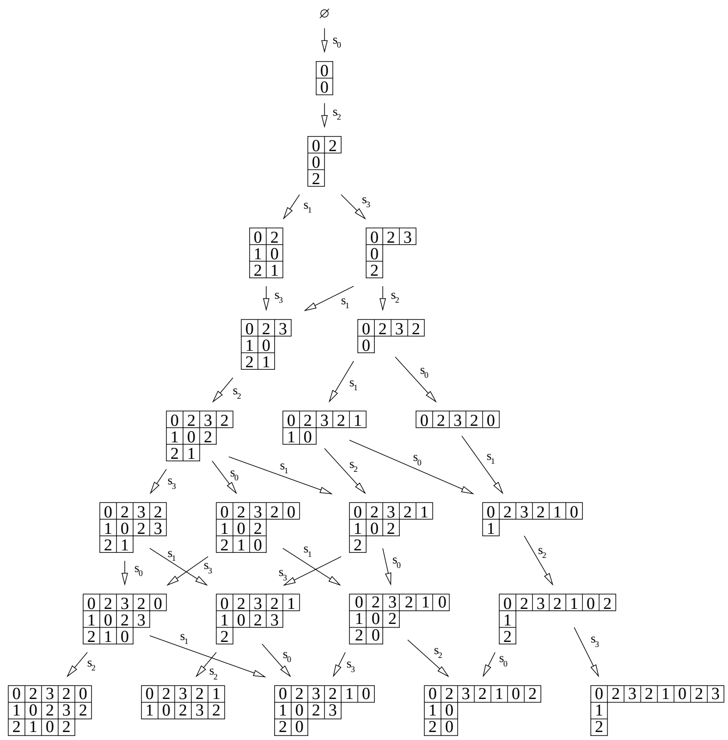

Figure 3: Top of Bruhat graph for W_s in the case $\mathbf{g} = B_3^{(1)}$

$\mu, \nu \in \mathcal{F}$ with $\ell(\mu) + \ell(\nu) \leq n$ where $n = \ell + 1$, and λ is the generalised partition for which $\lambda_i = \mu_i$ for $1 \leq i \leq \ell(\mu)$, $\lambda_i = 0$ for $\ell(\mu) < i \leq n - \ell(\nu)$, and $\lambda_i = -\nu_{n+1-i}$ for $n - \ell(\nu) < i \leq n$ so that $\lambda = (\mu_1, \mu_2, \ldots, \mu_{\ell(\mu)}, 0, \ldots, 0, -\nu_{\ell(\nu)}, \ldots, -\nu_2, -\nu_1)$.

With the above definitions, we can now state:

Proposition 2.10.1 *If $\mathbf{g} = B_\ell^{(1)}$, $C_\ell^{(1)}$, $D_\ell^{(1)}$, $A_{2\ell}^{(2)}$, $A_{2\ell-1}^{(2)}$ or $D_{\ell+1}^{(2)}$, then $\{\lambda(w) \mid w \in W_s\} = \mathcal{P}^+(\mathbf{g})$. Moreover, for each generalised partition $\lambda \in \mathcal{P}^+(\mathbf{g})$, there is a unique $w \in W_s$ such that $\lambda(w) = \lambda$.*

If $\mathbf{g} = A_{n-1}^{(1)}$, then $\{\lambda(w) \mid w \in W_s\} = \mathcal{P}^+(\mathbf{g})$. Moreover, for each generalised partition $(\mu; \nu) \in \mathcal{P}^+(\mathbf{g})$, there is a unique $w \in W_s$ such that $\lambda(w) = (\mu; \nu)$.

The set $\{T(w) \mid w \in W_s\}$ is now obtained from $\{\lambda(w) \mid w \in W_s\}$ by the means described in Section 2.3. To recapitulate briefly, for each $\lambda(w)$, the corresponding $F(w)$ is superposed on the grid for $\mathbf{g}$. This yields $T(w)$ unless $\mathbf{g} = B_\ell^{(1)}$, $D_\ell^{(1)}$ or $A_{2\ell-1}^{(2)}$. In these cases it is further required to ensure that $T(w)$ is even-handed by, where necessary, either interchanging unordered pairs, or where appropriate in the $D_\ell^{(1)}$ case, by augmenting the ℓth row with $\boxed{\ell}\boxed{\ell{-}1}$.

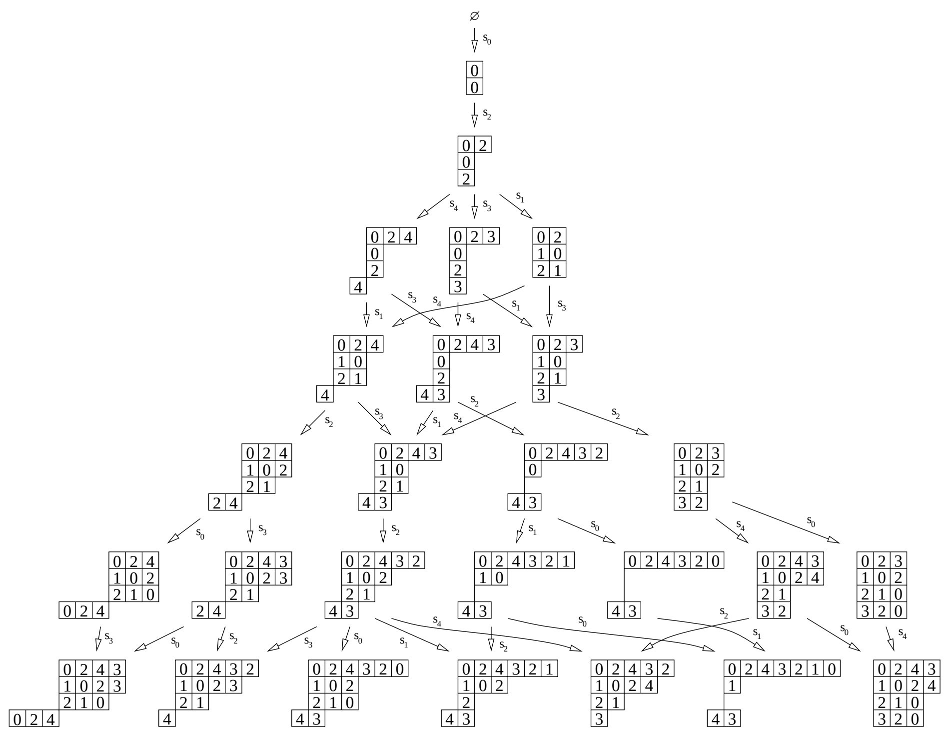

Figure 4: Top of Bruhat graph for W_s in the case $\mathbf{g} = D_4^{(1)}$

3 Background

In the following sections, we prove all the assertions made in Section 1. In this section, we gather together the parts of the theory of affine Lie algebras, simple Lie algebras and Coxeter groups that we use. We draw extensively on the texts [12, 7].

3.1 Affine Lie algebras

The classification theorem of Kac and Moody shows that each affine Lie algebra $\mathbf{g}$ is isomorphic to one of:

$$A_\ell^{(1)};\ B_\ell^{(1)};\ C_\ell^{(1)};\ D_\ell^{(1)};\ A_{2\ell}^{(2)};\ A_{2\ell+1}^{(2)};\ D_{\ell+1}^{(2)};$$
$$E_6^{(1)};\ E_7^{(1)};\ E_8^{(1)};\ F_4^{(1)};\ G_2^{(1)};\ E_6^{(2)};\ D_4^{(3)},$$

where $\ell \in \mathbb{Z}_{>0}$, with some restrictions of the form $\ell \geq \ell_{\min} \geq 1$. The first seven cases are known as *classical* affine Lie algebras. Each of their ranks is ℓ. The final seven cases are known as *exceptional* affine Lie algebras. Their ranks are 6,7,8,4,2,4,2 respectively. Those cases with superscript (1) are also known as *untwisted* (or *direct*) affine Lie algebras. The others are known as *twisted* affine Lie algebras.

To each affine Lie algebra $\mathbf{g}$ of rank ℓ, the classification theorem associates an $(\ell + 1) \times (\ell + 1)$ *generalised Cartan matrix* $A = (A_{ij})_{i,j\in I}$, where $I = \{0, 1, 2, \ldots, \ell\}$. The

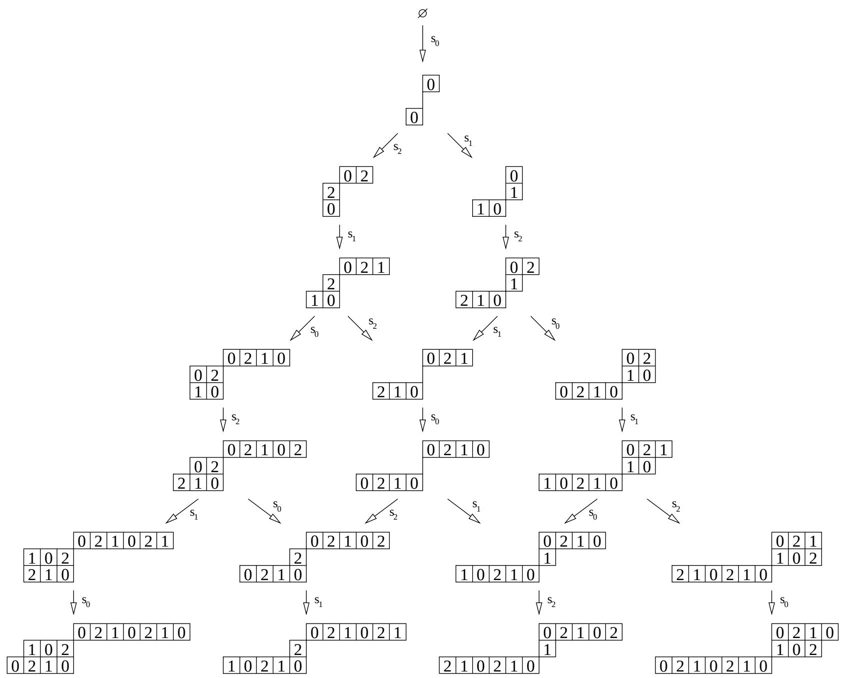

Figure 5: Top of Bruhat graph for W_s in the case $\mathbf{g} = A_2^{(1)}$

affine Lie algebra $\mathbf{g}$ is then the complex Lie algebra generated by the set of elements $\{d, e_i, f_i, h_i : i \in I\}$ subject to the relations:

$$\begin{array}{ll} [h_i, h_j] = 0, & [e_i, f_j] = \delta_{ij} h_i, \\ [h_i, e_j] = A_{ij} e_j, & [h_i, f_j] = -A_{ij} f_j, \\ (\operatorname{ad} e_i)^{1-A_{ij}} e_j = 0 \text{ for } i \neq j, & (\operatorname{ad} f_i)^{1-A_{ij}} f_j = 0 \text{ for } i \neq j, \end{array} \tag{3.1}$$

and

$$[d, h_i] = 0, \qquad [d, e_i] = \delta_{i0} e_i, \qquad [d, f_i] = -\delta_{i0} f_i. \tag{3.2}$$

The generalised Cartan matrices of the affine Lie algebras may be found in [3, App. N]. They are often encoded in directed multigraphs known as Dynkin diagrams. The Dynkin diagram of an affine Lie algebra of rank ℓ has $\ell + 1$ vertices labelled α_j for $j \in I$. If, for $i \neq j$, the vertices α_i and α_j are not linked then $A_{ij} = A_{ji} = 0$. Otherwise, α_i and α_j are linked: if no arrow points from α_j to α_i then $A_{ij} = -1$, and if an arrow points from α_j to α_i then $A_{ij} = -m$ where m is the multiplicity of the edge linking α_i and α_j. As usual, $A_{ii} = 2$ for all $i \in I$. The Dynkin diagrams of the classical affine Lie algebras are listed in Table 1.

The Cartan subalgebra $\mathbf{h}$ of $\mathbf{g}$ is the $(\ell + 2)$-dimensional algebra with basis $\{d, h_i \,|\, i \in I\}$. Its dual $\mathbf{h}^*$ has basis $\{\Lambda_0, \alpha_i \,|\, i \in I\}$ where for $i, j \in I$, $\alpha_j(h_i) = A_{ij}$, $\alpha_j(d) = \delta_{j0}$, $\Lambda_0(h_i) = \delta_{i0}$ and $\Lambda_0(d) = 0$. $\{\alpha_i \,|\, i \in I\}$ is the set of simple roots of $\mathbf{g}$.

For each of the affine Lie algebras, the generalised Cartan matrix A has corank 1. The marks c_i for $i \in I$ are the smallest positive integers such that $\sum_{j=0}^{\ell} c_j A_{ij} = 0$ for all $i \in I$. Similarly, the comarks $c_i^\vee$ for $i \in I$ are the smallest positive integers such that $\sum_{i=0}^{\ell} c_i^\vee A_{ij} = 0$ for all $j \in I$. In this paper, we use a labelling of the simple roots such that $c_0 = 1$ for each $\mathbf{g}$, while $c_0^\vee = 1$ for each $\mathbf{g}$ except $A_{2\ell}^{(2)}$ for which $c_0^\vee = 2$. This follows the convention of [20, 3] but not of [12].

The Coxeter number h and the dual Coxeter number $h^\vee$ of $\mathbf{g}$ are defined by $h = \sum_{i=0}^{\ell} c_i$ and $h^\vee = \sum_{i=0}^{\ell} c_i^\vee$ respectively. In (2.3), we defined $\tilde{h}^\vee = 2h^\vee$ if $\mathbf{g} = C_\ell^{(1)}$ and $\tilde{h}^\vee = h^\vee$ otherwise, and in (2.5), for each $i \in I$, we defined $\tilde{c}_i^\vee = 2c_i^\vee$ if $\mathbf{g} = C_\ell^{(1)}$ and $\tilde{c}_i^\vee = c_i^\vee$ otherwise. Note that $\tilde{h}^\vee = \sum_{i=0}^{\ell} \tilde{c}_i^\vee$.

The null root δ is defined by $\delta = \sum_{i=0}^{\ell} c_i\alpha_i$, whereupon $\delta(h_i) = 0$ for all $i \in I$, and $\delta(d) = c_0 = 1$. From $c_0 = 1$, it also follows that $\delta = \alpha_0 + \theta$ with $\theta = \sum_{i=1}^{\ell} c_i\alpha_i$.

3.2 Weight basis of $\mathbf{h}^*$

Having defined Λ_0 above, for $j \in I\backslash\{0\}$, the Dynkin weight Λ_j is defined by $\Lambda_j(d) = 0$ and $\Lambda_j(h_i) = \delta_{ij}$ for each $i \in I$. It immediately follows that

$$\alpha_k = \sum_{j\in I} A_{jk}\Lambda_j + \delta_{k0}\delta. \tag{3.3}$$

Moreover, $\{\delta, \Lambda_j \,|\, j \in I\}$ is a basis for $\mathbf{h}^*$. The *integral weight lattice* of $\mathbf{g}$ is defined by $P = \mathbb{C}\delta + \sum_{i=0}^{\ell} \mathbb{Z}\Lambda_i$. The *dominant integral weight lattice* of $\mathbf{g}$ is defined by $P^+ = \mathbb{C}\delta + \sum_{i=0}^{\ell} \mathbb{Z}_{\geq 0}\Lambda_i$.

Since $\{\delta, \Lambda_j \,|\, j \in I\}$ is a basis for $\mathbf{h}^*$, for any $\lambda \in \mathbf{h}^*$ we can write:

$$\lambda = -D(\lambda)\delta + \sum_{i=0}^{\ell} m_i(\lambda)\Lambda_i, \tag{3.4}$$

where $D(\lambda) = -\lambda(d)$ and $m_i(\lambda) = \lambda(h_i)$ for all $i \in I$. We refer to $D(\lambda)$ as the *depth* of λ. We also define the *level* of λ by $L(\lambda) = \sum_{i=0}^{\ell} c_i^\vee m_i(\lambda)$, or equivalently by $L(\lambda) = \lambda(c)$ where $c \in \mathbf{h}$ is defined by $c = \sum_{i=0}^{\ell} c_i^\vee h_i$. Then D and L are linear operators on $\mathbf{h}^*$.

We now immediately obtain $L(\Lambda_i) = c_i^\vee$ and $D(\Lambda_i) = 0$ for $i \in I$, and $L(\delta) = \delta(c) = \sum_{i=0}^{\ell} c_i^\vee\delta(h_i) = 0$ and $D(\delta) = -\delta(d) = -1$. Using (3.3), we then also obtain $L(\alpha_k) = \sum_{j=0}^{\ell} A_{jk}c_j^\vee = 0$ and $D(\alpha_k) = -\delta_{k0}$ for $k \in I$. The *Weyl vector* ρ of $\mathbf{g}$ is defined by $\rho = \sum_{i=0}^{\ell} \Lambda_i$. Then $L(\rho) = h^\vee$ and $D(\rho) = 0$.

Now define $\overline{\mathbf{h}}^* = \mathrm{span}\{\alpha_1, \alpha_2, \ldots, \alpha_\ell\}$, so that $\mathbf{h}^* = \overline{\mathbf{h}}^* \oplus \mathbb{C}\Lambda_0 \oplus \mathbb{C}\delta$.

Lemma 3.2.1 *Let $\lambda \in \mathbf{h}^*$. Then*

$$\lambda = \overline{\lambda} + \tilde{L}(\lambda)\Lambda_0 - D(\lambda)\delta, \tag{3.5}$$

where $\overline{\lambda} \in \overline{\mathbf{h}}^*$ and $\tilde{L}(\lambda) = L(\lambda)/c_0^\vee$.

Proof: In accordance with the above decomposition of $\mathbf{h}^*$, we can write $\lambda = \overline{\lambda} + m\Lambda_0 - p\delta$ for some $m, p \in \mathbb{C}$, with $\overline{\lambda} \in \overline{\mathbf{h}}^*$. Then $D(\lambda) = p$ since $D(\alpha_j) = 0$ for all $j \in I\backslash\{0\}$, $D(\Lambda_0) = 0$ and $D(\delta) = -1$. Similarly, $L(\lambda) = mc_0^\vee$ since $L(\alpha_j) = 0$ for all $j \in I\backslash\{0\}$, $L(\Lambda_0) = c_0^\vee$ and $L(\delta) = 0$. These results immediately imply (3.5). □

3.3 Root systems and natural basis of $\mathbf{h}^*$

As usual, an element $\alpha \in \mathbf{h}^*\backslash\{0\}$ is said to be a root of $\mathbf{g}$ if there exists non-zero $e_\alpha \in \mathbf{g}$ such that $[h, e_\alpha] = \alpha(h)e_\alpha$ for all $h \in \mathbf{h}$. The set of all roots is denoted Δ. In the case of affine Lie algebras $\mathbf{g}$, Δ has infinite cardinality. As usual, we can write $\Delta = \Delta^+ \cup \Delta^-$, where the set Δ^- of negative roots is obtained from the set Δ^- of positive roots by $\Delta^- = \{-\alpha \,|\, \alpha \in \Delta^+\}$. On the other hand, we can write $\Delta = \Delta_{re} \cup \Delta_{im}$, where Δ_{re} is a set of real roots, and Δ_{im} is a set of imaginary roots given by $\Delta_{im} = \{m\delta \,|\, m \in \mathbb{Z}\backslash\{0\}\}$. We also define $\Delta^\pm_{re} = \Delta^\pm \cap \Delta_{re}$ and $\Delta^\pm_{im} = \Delta^\pm \cap \Delta_{im}$, whereupon $\Delta_{re} = \Delta^+_{re} \cup \Delta^-_{re}$. and $\Delta_{im} = \Delta^+_{im} \cup \Delta^-_{im}$.

In this paper, we concentrate on the classical affine Lie algebras $\mathbf{g} = A^{(1)}_\ell$, $B^{(1)}_\ell$, $C^{(1)}_\ell$, $D^{(1)}_\ell$, $A^{(2)}_{2\ell}$, $A^{(2)}_{2\ell-1}$, $D^{(2)}_{\ell+1}$. In all cases other than $\mathbf{g} = A^{(1)}_\ell$ we set $n = \ell$, while for $\mathbf{g} = A^{(1)}_\ell$ we set $n = \ell + 1$. We now embed $\overline{\mathbf{h}}^*$ in E^n, where E^n is the n-dimensional Euclidean vector space having basis vectors $\epsilon_1, \epsilon_2, \ldots, \epsilon_n$. Then $\mathbf{h}^* \subset E^n \oplus \mathbb{C}\delta \oplus \mathbb{C}\Lambda_0$. The following theorem (selecting details from [12, Theorems 7.4 and 8.3]) specifies the simple roots and the positive real and imaginary roots of each classical affine Lie algebra $\mathbf{g}$ in the corresponding natural basis.

Theorem 3.3.1 *In terms of δ and the Euclidean basis elements $\epsilon_1, \epsilon_2, \ldots, \epsilon_n$, the simple roots $\alpha_0, \alpha_1, \ldots, \alpha_\ell$ of $\mathbf{g}$ are as tabulated below. For all $\mathbf{g}$, the set Δ^+_{im} of positive imaginary roots is given by*

$$\Delta^+_{im} = \{m\delta \,|\, m \in \mathbb{Z}_{>0}\}.$$

For untwisted $\mathbf{g}$, the set Δ^+_{re} of positive real roots is given by:

$$\Delta^+_{re} = \Delta^+_0 \cup \{m\delta \pm \alpha \,|\, m \in \mathbb{Z}_{>0}, \alpha \in \Delta^+_0\},$$

and for twisted $\mathbf{g}$ by:

$$\Delta^+_{re} = \Delta^+_0 \cup \{2m\delta \pm \alpha \,|\, m \in \mathbb{Z}_{>0}, \alpha \in \Delta^+_0\} \cup \{(2m-1)\delta \pm \alpha \,|\, m \in \mathbb{Z}_{>0}, \alpha \in \Delta^+_1\},$$

with Δ^+_0 and Δ^+_1 also as tabulated below.

$$\begin{aligned}
A^{(1)}_\ell: \quad & \alpha_0 = \delta - \theta \textit{ where } \theta = \epsilon_1 - \epsilon_{\ell+1}, \\
& \alpha_1 = \epsilon_1 - \epsilon_2,\ \alpha_2 = \epsilon_2 - \epsilon_3,\ \ldots,\ \alpha_\ell = \epsilon_\ell - \epsilon_{\ell+1}; \\
& \Delta^+_0 = \{\epsilon_i - \epsilon_j \,|\, 1 \le i < j \le \ell + 1\}. \\
B^{(1)}_\ell: \quad & \alpha_0 = \delta - \theta \textit{ where } \theta = \epsilon_1 + \epsilon_2, \\
& \alpha_1 = \epsilon_1 - \epsilon_2,\ \alpha_2 = \epsilon_2 - \epsilon_3,\ \ldots,\ \alpha_{\ell-1} = \epsilon_{\ell-1} - \epsilon_\ell, \\
& \alpha_\ell = \epsilon_\ell; \\
& \Delta^+_0 = \{\epsilon_i \pm \epsilon_j,\ \epsilon_k \,|\, 1 \le i < j \le \ell, 1 \le k \le \ell\}. \\
C^{(1)}_\ell: \quad & \alpha_0 = \delta - \theta \textit{ where } \theta = 2\epsilon_1, \\
& \alpha_1 = \epsilon_1 - \epsilon_2,\ \alpha_2 = \epsilon_2 - \epsilon_3,\ \ldots,\ \alpha_{\ell-1} = \epsilon_{\ell-1} - \epsilon_\ell, \\
& \alpha_\ell = 2\epsilon_\ell; \\
& \Delta^+_0 = \{\epsilon_i \pm \epsilon_j,\ 2\epsilon_k \,|\, 1 \le i < j \le \ell, 1 \le k \le \ell\}.
\end{aligned}$$

$$
\begin{aligned}
D_\ell^{(1)}: \quad & \alpha_0 = \delta - \theta \textit{ where } \theta = \epsilon_1 + \epsilon_2, \\
& \alpha_1 = \epsilon_1 - \epsilon_2,\ \alpha_2 = \epsilon_2 - \epsilon_3,\ \ldots,\ \alpha_{\ell-1} = \epsilon_{\ell-1} - \epsilon_\ell, \\
& \alpha_\ell = \epsilon_{\ell-1} + \epsilon_\ell; \\
& \Delta_0^+ = \{\epsilon_i \pm \epsilon_j \,|\, 1 \le i < j \le \ell\}. \\
A_{2\ell}^{(2)}: \quad & \alpha_0 = \delta - \theta \textit{ where } \theta = 2\epsilon_1, \\
& \alpha_1 = \epsilon_1 - \epsilon_2,\ \alpha_2 = \epsilon_2 - \epsilon_3,\ \ldots,\ \alpha_{\ell-1} = \epsilon_{\ell-1} - \epsilon_\ell, \\
& \alpha_\ell = \epsilon_\ell; \\
& \Delta_0^+ = \{\epsilon_i \pm \epsilon_j,\, \epsilon_k \,|\, 1 \le i < j \le \ell, 1 \le k \le \ell\}, \\
& \Delta_1^+ = \{\epsilon_i \pm \epsilon_j,\, \epsilon_k,\, 2\epsilon_k \,|\, 1 \le i < j \le \ell, 1 \le k \le \ell\}. \\
A_{2\ell-1}^{(2)}: \quad & \alpha_0 = \delta - \theta \textit{ where } \theta = \epsilon_1 + \epsilon_2, \\
& \alpha_1 = \epsilon_1 - \epsilon_2,\ \alpha_2 = \epsilon_2 - \epsilon_3,\ \ldots,\ \alpha_{\ell-1} = \epsilon_{\ell-1} - \epsilon_\ell, \\
& \alpha_\ell = 2\epsilon_\ell; \\
& \Delta_0^+ = \{\epsilon_i \pm \epsilon_j,\, 2\epsilon_k \,|\, 1 \le i < j \le \ell, 1 \le k \le \ell\}, \\
& \Delta_1^+ = \{\epsilon_i \pm \epsilon_j \,|\, 1 \le i < j \le \ell\}. \\
D_{\ell+1}^{(2)}: \quad & \alpha_0 = \delta - \theta \textit{ where } \theta = \epsilon_1, \\
& \alpha_1 = \epsilon_1 - \epsilon_2,\ \alpha_2 = \epsilon_2 - \epsilon_3,\ \ldots,\ \alpha_{\ell-1} = \epsilon_{\ell-1} - \epsilon_\ell, \\
& \alpha_\ell = \epsilon_\ell; \\
& \Delta_0^+ = \{\epsilon_i \pm \epsilon_j,\, \epsilon_k \,|\, 1 \le i < j \le \ell, 1 \le k \le \ell\}, \\
& \Delta_1^+ = \{\epsilon_k \,|\, 1 \le k \le \ell\}.
\end{aligned}
$$

In the cases $\mathbf{g} = A_\ell^{(1)}$, $B_\ell^{(1)}$, $C_\ell^{(1)}$ and $D_\ell^{(1)}$, it will be notationally convenient to set $\Delta_1^+ = \Delta_0^+$. Note then that $\Delta_1^+ \subseteq \Delta_0^+$ except when $\mathbf{g} = A_{2\ell}^{(2)}$, in which case $\Delta_0^+ \subseteq \Delta_1^+$. With Δ_0^+ and Δ_1^+ as specified above, we also define $\Delta_0^- = \{-\alpha \,|\, \alpha \in \Delta_0^+\}$ and $\Delta_1^- = \{-\alpha \,|\, \alpha \in \Delta_1^+\}$.

Note that $\mathbf{h}^* = E^n \oplus \mathbb{C}\delta \oplus \mathbb{C}\Lambda_0$ except in the case $\mathbf{g} = A_\ell^{(1)}$, for which $\mathbf{h}^* = E^n \oplus \mathbb{C}\delta \oplus \mathbb{C}\Lambda_0/(\epsilon_1+\epsilon_2+\cdots+\epsilon_n)$. In this latter case, it is then convenient to set $\epsilon_1+\epsilon_2+\cdots+\epsilon_n = 0$. Then $\overline{\mathbf{h}}^* = \mathrm{span}\{\epsilon_1, \epsilon_2, \ldots, \epsilon_n\}$ for each classical $\mathbf{g}$. It is now clear that (1.1) follows from (3.5) since $L(\lambda) = c_0^\vee \tilde{L}(\lambda)$ and $c_0^\vee = 1$ for all $\mathbf{g}$ other than $\mathbf{g} = A_{2\ell}^{(2)}$, for which $c_0^\vee = 2$.

3.4 Bilinear form on $\mathbf{h}^*$

A non-degenerate symmetric bilinear form $(\cdot|\cdot)$ on $E^n \oplus \mathbb{C}\delta \oplus \mathbb{C}\Lambda_0$ is specified by setting $(\epsilon_i|\epsilon_j) = \delta_{ij}$ for $1 \le i,j \le n$; $(\epsilon_i|\delta) = (\epsilon_i|\Lambda_0) = 0$ for $1 \le i \le n$; $(\Lambda_0|\Lambda_0) = (\delta|\delta) = 0$ and $(\delta|\Lambda_0) = \frac{1}{2}(\alpha_0|\alpha_0)$. After defining $\alpha_i^\vee = 2\alpha_i/(\alpha_i|\alpha_i)$, it may then be checked that the expressions in Theorem 3.3.1 satisfy $(\Lambda_0|\alpha_i^\vee) = \delta_{0i}$ for $i \in I$, and $(\alpha_i^\vee|\alpha_j) = A_{ij}$ for $i,j \in I$. It follows that $(\alpha_i^\vee|\delta) = (\alpha_i|\delta) = 0$ for $i \in I$. In addition, because $(\alpha_i^\vee|\alpha_j) = \alpha_j(h_i)$, $(\alpha_i^\vee|\Lambda_0) = \Lambda_0(h_i)$ and $\mathbf{h}^*$ has basis $\{\Lambda_0, \alpha_j | j \in I\}$, it follows that $(\alpha_i^\vee|\Lambda_j) = \Lambda_j(h_i) = \delta_{ij}$ for all $i,j \in I$.

One important distinction between real and imaginary roots is that for all $\alpha \in \Delta_{re}$ we have $(\alpha|\alpha) > 0$, whereas for all $\alpha \in \Delta_{im}$ we have $(\alpha|\alpha) = 0$. Note also that for any $\lambda \in \mathbf{h}^*$ we have $\overline{\lambda} = \sum_{i=1}^{n} \lambda_i \epsilon_i$ where $\lambda_i = (\lambda \,|\, \epsilon_i) = (\overline{\lambda} \,|\, \epsilon_i)$ for $i = 1, 2, \ldots, n$.

3.5 The Weyl group of g as a Coxeter group

Here, we review some basic facts and results about the Weyl-Coxeter group of an affine Lie algebra $\mathbf{g}$.

If $\alpha \in \Delta_{re}$ the action $s_\alpha : \mathbf{h}^* \to \mathbf{h}^*$ is defined by:

$$s_\alpha(\eta) = \eta - (\eta \,|\, \alpha^\vee)\alpha, \tag{3.6}$$

for all $\eta \in \mathbf{h}^*$. Note that $s_\alpha = s_{m\alpha}$ for $m \in \mathbb{Z}\backslash\{0\}$. The group W generated by $\{s_\alpha \,|\, \alpha \in \Delta_{re}\}$ is the Weyl-Coxeter group of $\mathbf{g}$. The following facts are easily established:

$$(w(\eta) \,|\, w(\zeta)) = (\eta \,|\, \zeta), \tag{3.7}$$

$$s_\alpha^2 = 1, \tag{3.8}$$

$$w s_\alpha w^{-1} = s_{w(\alpha)}, \tag{3.9}$$

$$w(\alpha) = -\alpha \text{ if and only if } w = s_\alpha, \tag{3.10}$$

for all $w \in W$, $\eta, \zeta \in \mathbf{h}^*$ and $\alpha \in \Delta$.

It is customary to set $s_i = s_{\alpha_i}$ for $i \in I$. Then $S = \{s_i \,|\, i \in I\}$ is a minimal generating set for W, and (W, S) is a *Coxeter system*. This is a consequence of the fact that:

$$(s_i s_j)^{m_{ij}} = 1 \tag{3.11}$$

for all $i, j \in I$ where the m_{ij} are certain positive integers. The relations (3.11) actually provide a presentation of W. It follows that there is a homomorphism sgn : $W \to \{\pm 1\}$ given by $\mathrm{sgn}(w) = (-1)^t$ whenever $w = s_{i_1} s_{i_2} \cdots s_{i_t}$ with $i_j \in I$ for $j = 1, 2, \ldots, t$.

The length function $\ell : W \to \mathbb{Z}_{\geq 0}$ was defined in Section 2.8. It has the following properties (see [7, §5]):

$$\ell(w s_i) = \ell(w) \pm 1, \qquad \ell(s_i w) = \ell(w) \pm 1, \tag{3.12}$$

$$\ell(w^{-1}) = \ell(w), \tag{3.13}$$

$$\ell(w s_i) > \ell(w) \text{ if and only if } w(\alpha_i) \in \Delta^+, \tag{3.14}$$

for all $w \in W$ and $i \in I$. More precisely, we have

$$\ell(w s_i) > \ell(w) \text{ if and only if } w(\alpha_i) \in \Delta^+_{re}, \tag{3.15}$$

for all $w \in W$ and $i \in I$. This is a simple consequence of the fact that $\Delta^+ = \Delta^+_{re} \cup \Delta^+_{im}$ and the observation that $(w(\alpha_i)|w(\alpha_i)) = (\alpha_i|\alpha_i) > 0$, so that $w(\alpha_i) \notin \Delta^+_{im}$. Of course, the affine Weyl-Coxeter group W is not finite and $\ell(w)$ is not bounded.

We also note that not only Δ, but both Δ^+_{im} and Δ^-_{im}, are invariant under the action of W. Moreover,

$$s_i(\Delta^+\backslash\{\alpha_i\}) = \Delta^+\backslash\{\alpha_i\}. \tag{3.16}$$

It is easily checked that the Weyl-Coxeter groups of $B_\ell^{(1)}$ and $A_{2\ell-1}^{(2)}$ are isomorphic. Additionally, $C_\ell^{(1)}$, $A_{2\ell}^{(2)}$ and $D_{\ell+1}^{(2)}$ are mutually isomorphic. The Weyl-Coxeter groups of $A_\ell^{(1)}$, $B_\ell^{(1)}$, $C_\ell^{(1)}$ and $D_\ell^{(1)}$ are respectively isomorphic to the groups denoted $\tilde{A}_\ell$, $\tilde{B}_\ell$, $\tilde{C}_\ell$ and $\tilde{D}_\ell$ in [1, 7].

3.6 Weyl-Coxeter action on natural basis

Here we deduce the action of the generators $s_0, s_1, \ldots, s_\ell$ of W on the natural basis elements $\Lambda_0, \delta, \epsilon_1, \epsilon_2, \ldots, \epsilon_n$ of $\mathbf{h}^*$. Using (3.6) and the bilinear form of Section 3.4, we immediately obtain $s_i(\delta) = \delta$ for all $i \in I$, $s_0(\Lambda_0) = \Lambda_0 - \alpha_0 = \Lambda_0 - \delta + \theta$ and $s_i(\Lambda_0) = \Lambda_0$ for all $i \in I\backslash\{0\}$.

In the case of each classical affine algebra $\mathbf{g}$, the use of (3.6) together with the bilinear form defined in Section 3.4 and the data tabulated in Theorem 3.3.1, enables us to calculate $s_i(\epsilon_j)$ for $1 \leq j \leq n$ and all $i \in I$. For $i = 0$ and $i = \ell$ we find that $s_i(\epsilon_j)$ is dependent on the $\mathbf{g}$ in question. For $i = 0$, we obtain:

$$\begin{array}{ll} A_\ell^{(1)}: & s_0(\epsilon_{\ell+1}) = \epsilon_1 - \delta,\ s_0(\epsilon_1) = \epsilon_{\ell+1} + \delta; \\ B_\ell^{(1)}, D_\ell^{(1)}, A_{2\ell-1}^{(2)}: & s_0(\epsilon_1) = \delta - \epsilon_2,\ s_0(\epsilon_2) = \delta - \epsilon_1; \\ C_\ell^{(1)}, A_{2\ell}^{(2)}: & s_0(\epsilon_1) = \delta - \epsilon_1; \\ D_{\ell+1}^{(2)}: & s_0(\epsilon_1) = 2\delta - \epsilon_1, \end{array} \tag{3.17}$$

with $s_0(\epsilon_j) = \epsilon_j$ for the values of j not covered here. For $i = \ell$, we obtain:

$$\begin{array}{ll} A_\ell^{(1)}: & s_\ell(\epsilon_\ell) = \epsilon_{\ell+1},\ s_\ell(\epsilon_{\ell+1}) = \epsilon_\ell; \\ D_\ell^{(1)}: & s_\ell(\epsilon_\ell) = -\epsilon_{\ell-1},\ s_\ell(\epsilon_{\ell-1}) = -\epsilon_\ell; \\ B_\ell^{(1)}, C_\ell^{(1)}, A_{2\ell}^{(2)}, A_{2\ell-1}^{(2)}, D_{\ell+1}^{(2)}: & s_\ell(\epsilon_\ell) = -\epsilon_\ell, \end{array} \tag{3.18}$$

again with $s_\ell(\epsilon_j) = \epsilon_j$ for the values of j not covered here. Finally, for $i = 1, 2, \ldots, \ell - 1$ and all classical affine Lie algebras $\mathbf{g}$,

$$s_i(\epsilon_i) = \epsilon_{i+1},\ s_i(\epsilon_{i+1}) = \epsilon_i, \tag{3.19}$$

with $s_i(\epsilon_j) = \epsilon_j$ for $j \notin \{i, i+1\}$.

3.7 Natural simple Lie subalgebra $\overline{\mathbf{g}}$

Let $\overline{I} = I\backslash\{0\} = \{1, 2, \ldots, \ell\}$. Then any affine Lie algebra $\mathbf{g}$ generated by the elements $\{d, e_i, f_i, h_i \,|\, i \in I\}$ subject to the relations (3.1) and (3.2) possesses a subalgebra $\overline{\mathbf{g}}$ generated by the elements $\{e_i, f_i, h_i \,|\, i \in \overline{I}\}$ subject just to the relations (3.1). Moreover, the restriction of the generalised Cartan matrix $A = (A_{ij})_{i,j \in I}$ to the relevant submatrix $\overline{A} = (A_{ij})_{i,j \in \overline{I}}$ is such that $\overline{A}$ is the Cartan matrix of a finite-dimensional simple Lie algebra. Thus, the subalgebra $\overline{\mathbf{g}}$ of $\mathbf{g}$ is a finite-dimensional simple Lie algebra.

The classification theorem of Cartan and Killing [2, 15] shows that each simple Lie algebra $\overline{\mathbf{g}}$ is isomorphic to one of:

$$A_\ell;\ B_\ell;\ C_\ell;\ D_\ell;\ E_6;\ E_7;\ E_8;\ F_4;\ G_2,$$

where $\ell \geq 1, 2, 3, 4$ for $\mathbf{g} = A_\ell$, B_ℓ, C_ℓ, D_ℓ respectively. In each case, the rank is specified by the relevant subscript.

In fact, for each of the affine Lie algebras $\mathbf{g}$ the natural embeddings $\mathbf{g} \supset \overline{\mathbf{g}}$ arising as above are given by:

$$\begin{aligned}
&A_\ell^{(1)} \supset A_\ell;\ B_\ell^{(1)} \supset B_\ell;\ C_\ell^{(1)} \supset C_\ell;\ D_\ell^{(1)} \supset D_\ell;\\
&A_{2\ell}^{(2)} \supset B_\ell;\ A_{2\ell-1}^{(2)} \supset C_\ell;\ D_{\ell+1}^{(2)} \supset B_\ell;\\
&E_6^{(1)} \supset E_6;\ E_7^{(1)} \supset E_7;\ E_8^{(1)} \supset E_8;\ F_4^{(1)} \supset F_4;\ G_2^{(1)} \supset G_2;\\
&E_6^{(2)} \supset F_4;\ D_4^{(3)} \supset G_2.
\end{aligned}$$

The Cartan subalgebra $\overline{\mathbf{h}}$ of $\overline{\mathbf{g}}$ is the ℓ-dimensional algebra with basis $\{h_i | i \in \overline{I}\}$. Its dual has basis $\{\overline{\alpha_i} | i \in \overline{I}\}$ where for $i, j \in \overline{I}$, $\overline{\alpha}_j(h_i) = \overline{A}_{ij}$. By comparing the definition of $\overline{\alpha}_j$ with that of α_j, we see that we can identify $\overline{\alpha}_j = \alpha_j$ (in their actions on $\overline{\mathbf{h}}$) for $j \in \overline{I}$. Consequently, the dual of $\overline{\mathbf{h}}$ is precisely $\overline{\mathbf{h}}^*$ as defined in Section 3.2.

In view of the above embeddings and the fact that we are considering just the classical affine Lie algebras, we need only consider here the classical simple Lie algebras $\overline{\mathbf{g}} = A_\ell$, B_ℓ, C_ℓ and D_ℓ. In the following theorem, we state standard expressions (see [1, §4] and [7, §2.10]) for the simple roots of $\overline{\mathbf{g}}$ in terms of the Euclidean basis elements $\epsilon_1, \epsilon_2, \ldots, \epsilon_n$, where $n = \ell$ except for the case $\overline{\mathbf{g}} = A_\ell$ for which $n = \ell + 1$. These expressions may be obtained by suitably restricting the expressions of Theorem 3.3.1.

Theorem 3.7.1 *In terms of the Euclidean basis elements $\epsilon_1, \epsilon_2, \ldots, \epsilon_n$, the simple roots $\alpha_1,\ \alpha_2, \ldots, \alpha_\ell$ of $\overline{\mathbf{g}}$ are as tabulated below. The full set Δ_0 of roots of $\overline{\mathbf{g}}$ is given by $\Delta_0 = \Delta_0^+ \cup \Delta_0^-$, where the set Δ_0^+ of positive roots is tabulated below, and the set Δ_0^- of negative roots is defined by $\Delta_0^- = \{-\alpha | \alpha \in \Delta_0^+\}$.*

$$\begin{array}{ll}
A_\ell: & \alpha_1 = \epsilon_1 - \epsilon_2, \alpha_2 = \epsilon_2 - \epsilon_3, \ldots, \alpha_\ell = \epsilon_\ell - \epsilon_{\ell+1};\\
& \Delta_0^+ = \{\epsilon_i - \epsilon_j | 1 \leq i < j \leq \ell + 1\}.\\
B_\ell: & \alpha_1 = \epsilon_1 - \epsilon_2, \alpha_2 = \epsilon_2 - \epsilon_3, \ldots, \alpha_{\ell-1} = \epsilon_{\ell-1} - \epsilon_\ell,\\
& \alpha_\ell = \epsilon_\ell;\\
& \Delta_0^+ = \{\epsilon_i \pm \epsilon_j,\ \epsilon_k | 1 \leq i < j \leq \ell, 1 \leq k \leq \ell\}.\\
C_\ell: & \alpha_1 = \epsilon_1 - \epsilon_2, \alpha_2 = \epsilon_2 - \epsilon_3, \ldots, \alpha_{\ell-1} = \epsilon_{\ell-1} - \epsilon_\ell,\\
& \alpha_\ell = 2\epsilon_\ell;\\
& \Delta_0^+ = \{\epsilon_i \pm \epsilon_j,\ 2\epsilon_k | 1 \leq i < j \leq \ell, 1 \leq k \leq \ell\}.\\
D_\ell: & \alpha_1 = \epsilon_1 - \epsilon_2, \alpha_2 = \epsilon_2 - \epsilon_3, \ldots, \alpha_{\ell-1} = \epsilon_{\ell-1} - \epsilon_\ell,\\
& \alpha_\ell = \epsilon_{\ell-1} + \epsilon_\ell;\\
& \Delta_0^+ = \{\epsilon_i \pm \epsilon_j | 1 \leq i < j \leq \ell\}.
\end{array}$$

Note that for the embedding $\mathbf{g} \supset \overline{\mathbf{g}}$, the set of positive roots of $\overline{\mathbf{g}}$ coincides with the subset Δ_0^+ of roots of the affine Lie algebra $\mathbf{g}$ identified in Theorem 3.3.1. It is well known that any root $\alpha \in \Delta_0$ is either positive or negative, and that it may be correspondingly expressed as a linear sum of simple roots with either all non-negative or all non-positive integer coefficients, respectively. As can be seen from Theorem 3.3.1, any $\gamma \in \Delta_1^+$ of our classical affine algebras $\mathbf{g}$ is such that either $\gamma = \alpha$ or $\gamma = 2\alpha$ with $\alpha \in \Delta_0^+$ in both cases. It follows that for all $\gamma \in \Delta_0 \cup \Delta_1$ we have $\gamma = \sum_{i=0}^{\ell} r_i\alpha_i$ with either all $r_i \in \mathbb{Z}_{\geq 0}$ or all $r_i \in \mathbb{Z}_{\leq 0}$, corresponding to whether $\gamma \in \Delta_0^+ \cup \Delta_1^+$ or $\gamma \in \Delta_0^- \cup \Delta_1^-$, respectively.

Since $\overline{\Lambda_i} \in \overline{\mathbf{h}}^*$ and, via (3.5), $\overline{\Lambda_i}(h_j) = \Lambda_i(h_j) - (c_i^\vee/c_0^\vee)\Lambda_0(h_j) = \delta_{ij}$ for all $i, j \in \overline{I}$, it follows that for $i \in \overline{I}$, the weights $\overline{\Lambda_i}$ are the fundamental weights of the simple Lie subalgebra $\overline{\mathbf{g}}$. Therefore $\overline{\rho} = \sum_{i\in\overline{I}} \overline{\Lambda}_i$ is the Weyl vector of $\overline{\mathbf{g}}$. Also note that $(\overline{\Lambda_i}|\alpha_j^\vee) = (\Lambda_i|\alpha_j^\vee) - (c_i^\vee/c_0^\vee)(\Lambda_0|\alpha_j^\vee) = \delta_{ij}$ for all $i, j \in \overline{I}$.

The integral weight lattice of $\overline{\mathbf{g}}$ is defined by $\overline{P} = \sum_{i=1}^{\ell} \mathbb{Z}\overline{\Lambda}_i$. The dominant integral weight lattice of $\overline{\mathbf{g}}$ is defined by $\overline{P}^+ = \sum_{i=1}^{\ell} \mathbb{Z}_{\geq 0}\overline{\Lambda}_i$.

Lemma 3.7.2 *Let $\overline{\lambda} \in \overline{\mathbf{h}}^*$ and write $\overline{\lambda} = \sum_{i=1}^{n} \overline{\lambda}_i\epsilon_i$. Then $\overline{\lambda} \in \overline{P}^+$ if and only if $\overline{\lambda}_i - \overline{\lambda}_{i+1} \in \mathbb{Z}_{\geq 0}$ for $1 \leq i < n$* and

- $\sum_{i=1}^{n} \overline{\lambda}_i = 0$ *if* $\mathbf{g} = A_\ell$;
- $\overline{\lambda}_\ell \in \frac{1}{2}\mathbb{Z}_{\geq 0}$ *if* $\mathbf{g} = B_\ell$;
- $\overline{\lambda}_\ell \in \mathbb{Z}_{\geq 0}$ *if* $\mathbf{g} = C_\ell$;
- $\overline{\lambda}_\ell \in \frac{1}{2}\mathbb{Z}$ *and* $\overline{\lambda}_{\ell-1} \geq |\overline{\lambda}_\ell|$ *if* $\mathbf{g} = D_\ell$.

Proof: Let $m_i = (\overline{\lambda}|\alpha_i^\vee)$ for $1 \leq i \leq \ell$ so that $\overline{\lambda} = \sum_{i=1}^{\ell} m_i\overline{\Lambda}_i$. For $1 \leq i < n$, Theorem 3.7.1 gives $\alpha_i = \epsilon_i - \epsilon_{i+1}$, whereupon $m_i = (\sum_{j=1}^{n} \overline{\lambda}_j\epsilon_j|\epsilon_i - \epsilon_{i+1}) = \overline{\lambda}_i - \overline{\lambda}_{i+1}$.

Now, for $\mathbf{g} = B_\ell$, C_ℓ and D_ℓ, consider $i = n$ $(= \ell)$. For $\mathbf{g} = B_\ell$, we have $\alpha_\ell = \epsilon_\ell$ whereupon $m_\ell = 2(\overline{\lambda}|\epsilon_\ell) = 2\overline{\lambda}_\ell$. For $\mathbf{g} = C_\ell$, we have $\alpha_\ell = 2\epsilon_\ell$ whereupon $m_\ell = (\overline{\lambda}|\epsilon_\ell) = \overline{\lambda}_\ell$. For $\mathbf{g} = D_\ell$, we have $\alpha_\ell = \epsilon_{\ell-1} + \epsilon_\ell$ whereupon $m_\ell = (\overline{\lambda}|\epsilon_{\ell-1} + \epsilon_\ell) = \overline{\lambda}_{\ell-1} + \overline{\lambda}_\ell$ and $m_\ell - m_{\ell-1} = 2\overline{\lambda}_\ell$. Since each $m_i \in \mathbb{Z}_{\geq 0}$ for $\overline{\lambda} \in \overline{P}^+$, the required conditions follow.

For $\mathbf{g} = A_\ell$, each α_i is orthogonal to $\epsilon_1 + \epsilon_2 + \ldots + \epsilon_{\ell+1}$. It follows that $\overline{\mathbf{h}}^*$ is orthogonal to this vector because $\{\alpha_i \,|\, 1 \leq i \leq \ell\}$ is a basis for $\overline{\mathbf{h}}^*$. The required conditions then also follow for $\mathbf{g} = A_\ell$. $\square$

Let $\overline{W}$ be the subgroup of W generated by $S = \{s_i | i \in \overline{I}\}$. Then $(\overline{W}, \overline{S})$ is a Coxeter system, and $\overline{W}$ is the Weyl-Coxeter group of $\overline{\mathbf{g}}$. It is a finite Coxeter group, and has properties analogous to those of W given in Section 3.5. In particular, the action of $\overline{W}$ on $\overline{\mathbf{h}}^*$ is given by (3.6) where we restrict $\alpha \in \Delta_0$ and $\eta \in \overline{\mathbf{h}}^*$. We also note that length functions defined on W and $\overline{W}$ are compatible in that if $w \in \overline{W}$ and $\ell(w) = t$, then there exists $i_1, i_2, \ldots, i_t \in \overline{I}$ such that $w = s_{i_1}s_{i_2}\cdots s_{i_t}$ (see [7, Prop. 5.5]).

4 Unveiling the colours

4.1 Casting the rainbow

In this section, we prove that if $w \in W$ and $\Lambda \in \mathbf{h}^*$ then:

$$\overline{w(\Lambda) - \Lambda} = \sum_{i=1}^{n} \lambda^{\Lambda}(w)_i \epsilon_i, \tag{4.1}$$

where each $\lambda^{\Lambda}(w)_i$ is obtained from the coloured diagram $T(w)$ as described in Section 2.6. This will follow from Theorem 4.1.4 below. The proof of the full (2.8) will be obtained in Section 4.3 below.

The simplest way to proceed here is to adopt the description of $T(w)$ given in Section 2.4 as the definition of $T(w)$. In particular, if $w' \in W$, $k \in I$ and $w'' = w's_k$, then $T(w'')$ is obtained from $T(w')$ by a k-shift. By this means, $T(w)$ is built up recursively using any expression for w in terms of the generators $s_0, s_1, \ldots, s_\ell$ of W.

Once (4.1) has been established, it follows that:

$$\overline{w(\rho) - \rho} = \sum_{i=1}^{n} \lambda(w)_i \epsilon_i. \tag{4.2}$$

Thereupon, the above definition of $T(w)$ is consistent with that given in Sections 2.1, 2.2 and 2.3. This also shows that $T(w)$ is independent of the expression used to produce it in the previous paragraph.

For each coloured diagram T, $j \in I$ and $1 \le i \le n$, we let $n_{ij}(T)$ and $d_{ij}(T)$ denote respectively the number (positive or negative) of j-nodes and the signed sum of their charges in the ith row of T. As usual, nodes to the left of the vertical axis give a negative contribution. We also let $d_j(T) = \sum_{i=1}^{n} d_{ij}(T)$ for each $j \in I$, so that $d_j(T)$ is the signed sum of the charges of j-nodes throughout T. For $w \in W$, it will be useful to set $n_{ij}(w) = n_{ij}(T(w))$, $d_{ij}(w) = d_{ij}(T(w))$ and $d_j(w) = d_j(T(w))$. Our proofs below and in Section 4.3 proceed by relating these values to those defined in the next paragraph.

For each $w \in W$, we define the values $N_{ij}(w)$ and $P_j(w)$ for $j \in I$ and $1 \le i \le n$ by setting:

$$w(\Lambda_j) - \Lambda_j = \sum_{i=1}^{n} N_{ij}(w)\epsilon_i - P_j(w)\delta, \tag{4.3}$$

in accordance with (3.5) after noting that $L(w(\Lambda_j) - \Lambda_j) = 0$.

Now if $\Lambda \in \mathbf{h}^*$ and $m_j(\Lambda) = (\Lambda \mid \alpha_j^\vee)$ for $0 \le j \le \ell$, then $\Lambda = \sum_{j=0}^{\ell} m_j(\Lambda)\Lambda_j - D(\Lambda)\delta$, whereupon, since $w(\delta) = \delta$, (4.3) immediately implies that:

$$w(\Lambda) - \Lambda = \sum_{i=1}^{n} \sum_{j=0}^{\ell} m_j(\Lambda) N_{ij}(w)\epsilon_i - \sum_{j=0}^{\ell} m_j(\Lambda) P_j(w)\delta. \tag{4.4}$$

The following result provides useful recursive expressions for $N_{ij}(w)$ and $P_j(w)$.

Lemma 4.1.1 *Let $w' \in W$, $k \in I$ and $w = w's_k$. Then:*

$$N_{ij}(w) = \begin{cases} N_{ij}(w') - (\alpha_k|\epsilon_i) - \sum_{m=0}^{\ell} A_{mk} N_{im}(w') & \text{if } j = k; \\ N_{ij}(w') & \text{if } j \neq k, \end{cases} \tag{4.5}$$

for $1 \leq i \leq n$, and

$$P_j(w) = \begin{cases} P_j(w') + \delta_{k,0} - \sum_{m=0}^{\ell} A_{mk} P_m(w') & \text{if } j = k; \\ P_j(w') & \text{if } j \neq k. \end{cases} \tag{4.6}$$

If $w = 1$, then $N_{ij}(w) = P_j(w) = 0$ for $j \in I$ and $1 \leq i \leq n$.

Proof: Using (4.3), we calculate:

$$\begin{aligned} \sum_{i=1}^{n} N_{ij}(w)\epsilon_i - P_j(w)\delta = w(\Lambda_j) - \Lambda_j \\ &= w'(s_k(\Lambda_j) - \Lambda_j) + w'(\Lambda_j) - \Lambda_j \\ &= -\delta_{jk} w'(\alpha_k) + \sum_{i=1}^{n} N_{ij}(w')\epsilon_i - P_j(w')\delta. \end{aligned}$$

We then write $w'(\alpha_k) = \alpha_k + (w'(\alpha_k) - \alpha_k)$, so that, since $\alpha_k = \sum_{m=0}^{\ell} A_{mk}\Lambda_m + \delta_{k,0}\delta$ and $w'(\delta) = \delta$, we have:

$$\begin{aligned} w'(\alpha_k) &= \alpha_k + \sum_{m=0}^{\ell} A_{mk}(w'(\Lambda_m) - \Lambda_m) \\ &= \alpha_k + \sum_{m=0}^{\ell} A_{mk} \left(\sum_{i=1}^{n} N_{im}(w')\epsilon_i - P_m(w')\delta \right). \end{aligned}$$

After combining these results, (4.5) and (4.6) follow from the linear independence of $\delta, \epsilon_1, \epsilon_2, \ldots, \epsilon_n$.

The final statement is immediate. □

In order to show that $T(w)$, defined as described above, satisfies (4.1), we will use an induction argument. The induction step is encapsulated in the following lemma. In this lemma, and in Section 4.3, we make use of the notion of a k-block, which we now describe.

We define a k-block for all $\mathbf{g}$ and $k \in I$, except in a few instances. These instances are $\mathbf{g} = A_1^{(1)}$; $\mathbf{g} = A_2^{(2)}$; $k = 1$ for $\mathbf{g} = C_2^{(1)}, A_6^{(2)}$ and $D_3^{(2)}$; and $k = 2$ for $\mathbf{g} = B_3^{(1)}, D_4^{(1)}$ and $A_5^{(2)}$. Apart from these, a k-block is a finite contiguous portion of a row of the grid pertaining to $\mathbf{g}$, in which an m-node is present if and only if either $A_{mk} \neq 0$, or m and k are associated. All possible k-blocks are shown in Tables 2 and 3 (for $\mathbf{g} = A_\ell^{(1)}$, the labels on the nodes are taken modulo $\ell + 1$). Alongside each k-block is the portion of the corresponding Dynkin diagram comprised of all vertices labelled α_m whenever $A_{mk} \neq 0$ or k and m are associated. The value of A_{mk} pertaining to the α_mth vertex is displayed above that vertex.

Case	k-block	Linkage of α_kth node
1a	$\boxed{k+1}\boxed{k}\boxed{k-1}$	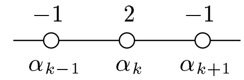
1b	$\boxed{k-1}\boxed{k}\boxed{k+1}$	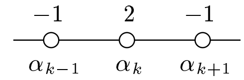
2a	$\boxed{k+1}\boxed{k}\boxed{k-1}\boxed{k}\boxed{k+1}$	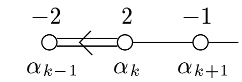
2b	$\boxed{k-1}\boxed{k}\boxed{k+1}\boxed{k}\boxed{k-1}$	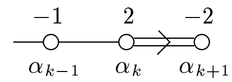
3a	$\boxed{k+1}\boxed{k}\boxed{k-1}\boxed{k-1}\boxed{k}\boxed{k+1}$	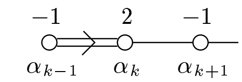
3b	$\boxed{k-1}\boxed{k}\boxed{k+1}\boxed{k+1}\boxed{k}\boxed{k-1}$	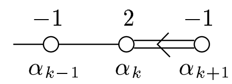
4a	$\boxed{k+1}\boxed{k}\boxed{k-1\sim k-2}\boxed{k}\boxed{k+1}$	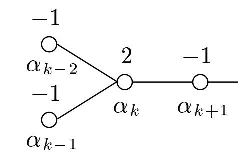
4b	$\boxed{k-1}\boxed{k}\boxed{k+2\sim k+1}\boxed{k}\boxed{k-1}$	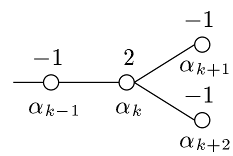

Table 2: k-blocks

Lemma 4.1.2 *Let T' and T be coloured diagrams with T obtained from T' by a k-shift, where $k \in I$. For $1 \le i \le n$, set $\vartheta_{ik}(T') = n_{ik}(T) - n_{ik}(T')$ and $\Sigma_{ik}(T') = \sum_{m=0}^{\ell} A_{mk} n_{im}(T')$. Then:*

$$\vartheta_{ik}(T') = -\Sigma_{ik}(T') - (\alpha_k|\epsilon_i). \tag{4.7}$$

Proof: We first claim that (4.7) holds when the ith row of T' is empty, so that this portion of the profile of T' coincides with the vertical axis,. In this case, the second term on the right of (4.7) is trivially 0. Note that here $\vartheta_{ik}(T')$ is non-zero only if the vertical axis is adjacent to a k-node. For $\mathbf{g} = A_\ell^{(1)}$, examination of the grid shows that $\vartheta_{ik}(T') = \delta_{i,k+1} - \delta_{ik} - \delta_{i-n,k}$ for $1 \le i \le n$. Using Theorem 3.3.1, we see that this equals $-(\alpha_k|\epsilon_i)$ and the claim holds. For $\mathbf{g} = C_\ell^{(1)}$, $A_{2\ell}^{(2)}$ or $D_{\ell+1}^{(2)}$, examination of the grids gives $\vartheta_{ik}(T') = \delta_{i,k+1} - \delta_{ik}$ for $1 \le i \le \ell$, except when $i = 1$ and $k = 0$ for $\mathbf{g} = C_\ell^{(1)}$ or $A_{2\ell}^{(2)}$, or when $i = k = \ell$ for $\mathbf{g} = C_\ell^{(1)}$. In the first of these excepted instances

Case	k-block	Linkage of α_kth node
5a	$\boxed{k+1}\boxed{k}\boxed{k+1}$	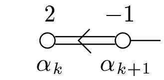
5b	$\boxed{k-1}\boxed{k}\boxed{k-1}$	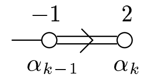
6a	$\boxed{k+1}\boxed{k}\boxed{k}\boxed{k+1}$	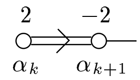
6b	$\boxed{k-1}\boxed{k}\boxed{k}\boxed{k-1}$	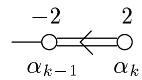
7a	$\boxed{k+1}\boxed{k\sim k-1}\boxed{k+1}$	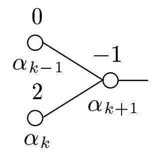
7b	$\boxed{k+2}\boxed{k+1\sim k}\boxed{k+2}$	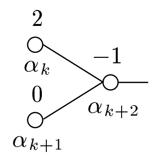
7c	$\boxed{k-2}\boxed{k\sim k-1}\boxed{k-2}$	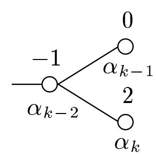
7d	$\boxed{k-1}\boxed{k+1\sim k}\boxed{k-1}$	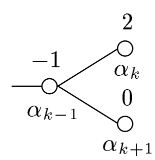

Table 3: k-blocks (cont.)

$\vartheta_{10}(T') = 2$, while in the second $\vartheta_{\ell\ell}(T') = -2$. In each instance, Theorem 3.3.1 shows that $\vartheta_{ik}(T') = -(\alpha_k|\epsilon_i)$, as required. For $\mathbf{g} = B_\ell^{(1)}$, $D_\ell^{(1)}$ or $A_{2\ell+1}^{(2)}$, examination of the grids gives $\vartheta_{ik}(T') = \delta_{i,k+1} - \delta_{ik}$ for $1 \le i \le \ell$, except when $i = 2$ and $k = 0$ for either $\mathbf{g}$, when $i = \ell - 1$ and $k = \ell$ for $\mathbf{g} = D_\ell^{(1)}$, or when $i = k = \ell$ for $\mathbf{g} = A_{2\ell+1}^{(2)}$. In the first of these excepted instances $\vartheta_{20}(T') = 1$, in the second $\vartheta_{\ell-1,\ell}(T') = -1$, and in the third $\vartheta_{\ell\ell}(T') = -2$. In each instance, Theorem 3.3.1 again shows that $\vartheta_{ik}(T') = -(\alpha_k|\epsilon_i)$, as required. In fact the requirement $\vartheta_{ik}(T') = -(\alpha_k|\epsilon_i)$ is sufficient to determine all the entries in the grid that are adjacent to the vertical axis, including tied pairs and unordered pairs.

We now claim that, whatever the length of the ith row of T', the values of the two sides of (4.7) change by the same amount when the profile is moved to the next possible position on its right. This claim will be verified below cases by case. Once verified, its iterative application shows that (4.7) holds for rows of positive length. Of course, the periodicity of the grids ensures that the two sides of the expression also change by the same amount when the profile is moved to the next possible position on its left. Thereupon, we conclude that (4.7) holds in all cases.

For convenience, we will denote the change in $\Sigma_{ik}(T')$ by $\Delta\Sigma$, and the change in $\vartheta_{ik}(T')$ by $\Delta\vartheta$. In particular, if the profile of the original T' moves to its right past n_j adjacent j-nodes then $\Delta\Sigma = n_j A_{jk}$, where of course n_j is either 1 or, in the case of a tied pair, 2. If in the ith row of the original T' the profile is not adjacent to any k-nodes then $\vartheta_{ik}(T') = 0$ since the ith row of T and T' must coincide. On the other hand if it is adjacent to n_k k-nodes in the ith row then $\vartheta_{ik}(T') = n_k$ or $-n_k$ according to whether these are to the right or to the left of the profile, since the ith row of T is necessarily formed by adding or deleting the n_k adjacent k-nodes to T'. It follows that $\Delta\vartheta$ may be read off the k-blocks rather easily as the profile of T' advances from left to right by first enumerating $\vartheta_{ik}(T')$ in accordance with the above rule, and then calculating differences in these values.

To prove our claim, we must show that $\Delta\vartheta = -\Delta\Sigma$ in every possible case. We first consider those cases for which k-blocks are defined. If the profile passes over a j-node which is not in a k-block then $\Delta\vartheta = 0$ since before and after the change, the profile is not adjacent to a k-node. On the other hand, $A_{jk} = 0$ for this case, which implies that $\Delta\Sigma = 0$, as required.

For each of the k-blocks listed in Tables 2 and 3, we examine $\Delta\vartheta$ and $\Delta\Sigma$ as the profile passes over a j-node that is in the k-block.

For cases 1a and 1b, there are three nodes to pass over. Thus there are four profile positions which yield $\vartheta_{ik} = (0, 1, -1, 0)$ in correspondence with the initial profile being not adjacent to a k-node, being to the left of a k-node, being to the right of a k-node, and finally being no longer adjacent to a k-node. These values give, in turn, the values $(1, -2, 1)$ for $\Delta\vartheta$. Reading the values of A_{jk} for the j-nodes $k+1$, k and $k+1$ from the accompanying Dynkin diagram immediately gives the values $(-1, 2, -1)$ for $\Delta\Sigma$. The above claim thus holds here.

For Cases 2a and 2b, we have $k = 1$ and $k = \ell - 1$ respectively. In either case, the six possible positions of profile give $\vartheta_{ik}(T') = (0, 1, -1, 1, -1, 0)$, so the five moves give $(1, -2, 2, -2, 1)$ for $\Delta\vartheta$ in agreement with the values $(-1, 2, -2, 2, -1)$ for $\Delta\Sigma$.

For Cases 3a and 3b, we have $k = 1$ and $k = \ell - 1$ respectively. Since the profile cannot lie in the central position between the two tied nodes, there are again five moves to consider. They give $(1, -2, 2, -2, 1)$ for $\Delta\vartheta$ and $(-1, 2, -2, 2, -1)$ for $\Delta\Sigma$.

For Cases 4a and 4b, we have $k = 2$ and $k = \ell - 2$ respectively. Here there are six moves to consider, with the order of the central interchangeable pair irrelevant. These moves give $(1, -2, 1, 1, -2, 1)$ for $\Delta\vartheta$ and $(-1, 2, -1, -1, 2, -1)$ for $\Delta\Sigma$.

For Cases 5a and 5b, we have $k = 0$ and $k = \ell$ respectively. The three moves give $(1, -2, 1)$ for $\Delta\vartheta$ and $(-1, 2, -1)$ for $\Delta\Sigma$.

For Cases 6a and 6b, we have $k = 0$ and $k = \ell$ respectively. Since the profile cannot lie in the central position between the two tied nodes, there are again three moves to consider. They give $(2, -4, 2)$ for $\Delta\vartheta$ and $(-2, 4, -2)$ for $\Delta\Sigma$.

For Case 7a, we have $k = 1$. If the unordered pair $1 \sim 0$ is ordered as shown one obtains $\vartheta_{ik}(T') = (0, 1, -1, -1, 0)$ so that the four moves give $(1, -2, 0, 1)$ for $\Delta\vartheta$. Correspondingly, we find $\Delta\Sigma = (-1, 2, 0, -1)$ as required. On the other hand if the unordered pair $1 \sim 0$ is actually reordered as $0 \sim 1$ then one obtains $\vartheta_{ik}(T') = (0, 1, 1, -1, 0)$, so that $\Delta\vartheta = (1, 0, -2, 1)$. This time we find $\Delta\Sigma = (-1, 0, 2, -1)$, again as required.

For Case 7b, we have $k = 0$. The details of this case read exactly as for Case 7a, except for the interchange of the $1 \sim 0$ and $0 \sim 1$ cases.

For Cases 7c and 7d, we have $k = \ell$ and $k = \ell - 1$ respectively. These cases are similar to Cases 7a and 7b respectively with the contributions corresponding to the configurations $1 \sim 0$ and $0 \sim 1$ cases now applying to the $\ell \sim \ell - 1$ and $\ell - 1 \sim \ell$ contributions, respectively.

The completes the verification of the claim that $\Delta\vartheta = -\Delta\Sigma$ in the cases for which k-blocks are defined. The cases for which there are no k-blocks are tabulated in Tables 4, 5, and 6. We tackle each of them in turn.

$\mathbf{g}$	grid	k	Dynkin graph	α_k	i	$-(\alpha_k\|\epsilon_i)$
$A_1^{(1)}$	$\begin{array}{\|c\|c\|}\hline 0 & 1 \\ \hline 1 & 0 \\ \hline\end{array}$	0	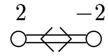 2, -2; α_k, α_{k+1}	$\delta - \epsilon_1 + \epsilon_2$	1 2	1 -1
		1	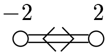 -2, 2; α_{k-1}, α_k	$\epsilon_1 - \epsilon_2$	1 2	-1 1
$A_2^{(2)}$	$\begin{array}{\|c c\|c\|}\hline 0 & 0 & 1 \\ \hline\end{array}$	0	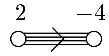 2, -4; α_k, α_{k+1}	$\delta - 2\epsilon_1$	1	2
		1	 -1, 2; α_{k-1}, α_k	ϵ_1	1	-1

Table 4: Data for $A_1^{(1)}$ and $A_2^{(2)}$

For $\mathbf{g} = A_1^{(1)}$, each row comprises a sequence of $\boxed{0|1}$ blocks. For $k = 0$, we obtain the values $(-2, 2)$ for $\Delta\vartheta$ and the values $(2, -2)$ for $\Delta\Sigma$, as the profile passes between the three valid positions. For $k = 1$, we obtain the values $(2, -2)$ for $\Delta\vartheta$ and the values $(-2, 2)$ for $\Delta\Sigma$.

For $\mathbf{g} = A_2^{(2)}$, the single row comprises a sequence of $\boxed{0|0|1}$ blocks. For $k = 0$, we obtain the values $(-4, 4)$ for $\Delta\vartheta$ and the values $(4, -4)$ for $\Delta\Sigma$, as the profile passes between the three valid positions. For $k = 1$, we obtain the values $(2, -2)$ for $\Delta\vartheta$ and the values $(-2, 2)$ for $\Delta\Sigma$.

$\mathbf{g}$	grid	k	Dynkin graph	α_k	i	$-(\alpha_k\|\epsilon_i)$
$C_2^{(1)}$	$\begin{array}{\|c\|c\|c\|c\|c\|c\|}\hline 0&0&1&2&2&1\\ \hline 1&0&0&1&2&2\\ \hline\end{array}$	1	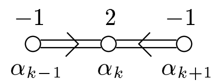	$\epsilon_1-\epsilon_2$	1 2	-1 1
$A_4^{(2)}$	$\begin{array}{\|c\|c\|c\|c\|c\|}\hline 0&0&1&2&1\\ \hline 1&0&0&1&2\\ \hline\end{array}$	1	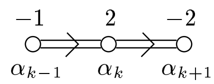	$\epsilon_1-\epsilon_2$	1 2	-1 1
$D_3^{(2)}$	$\begin{array}{\|c\|c\|c\|c\|}\hline 0&1&2&1\\ \hline 1&0&1&2\\ \hline\end{array}$	1	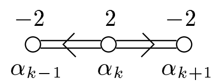	$\epsilon_1-\epsilon_2$	1 2	-1 1

Table 5: Data for $C_2^{(1)}$, $A_4^{(2)}$ and $D_3^{(2)}$ when $k=1$

For $\mathbf{g}=D_3^{(2)}$, each row comprises a sequence of $\boxed{0\|1\|2\|1}$ blocks. With $k=1$, as we pass between the five valid positions, we obtain the values $(2,-2,2,-2)$ for $\Delta\vartheta$ and the values $(-2,2,-2,2)$ for $\Delta\Sigma$.

For $\mathbf{g}=A_4^{(2)}$, each row comprises a sequence of $\boxed{0\|0\|1\|2\|1}$ blocks, and the details of this case are precisely the same as for the $\mathbf{g}=D_3^{(2)}$ case above.

For $\mathbf{g}=C_2^{(1)}$, each row comprises a sequence of $\boxed{0\|0\|1\|2\|2\|1}$ blocks, and once again the details are the same as for the $\mathbf{g}=D_3^{(2)}$ case.

$\mathbf{g}$	grid	k	Dynkin graph	α_k	i	$-(\alpha_k\|\epsilon_i)$
$B_3^{(1)}$	$\begin{array}{\|c\|c\|c\|c\|c\|}\hline 0&2&3&2&1\\ \hline 1&0&2&3&2\\ \hline 2&1&0&2&3\\ \hline\end{array}$	2	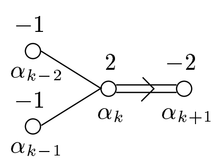	$\epsilon_2-\epsilon_3$	1 2 3	0 -1 1
$A_5^{(2)}$	$\begin{array}{\|c\|c\|c\|c\|c\|c\|}\hline 0&2&3&3&2&1\\ \hline 1&0&2&3&3&2\\ \hline 2&1&0&2&3&3\\ \hline\end{array}$	2	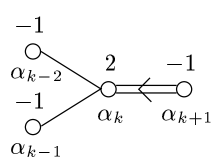	$\epsilon_2-\epsilon_3$	1 2 3	0 -1 1
$D_4^{(1)}$	$\begin{array}{\|c\|c\|c\|c\|c\|c\|}\hline 0&2&4&3&2&1\\ \hline 1&0&2&4&3&2\\ \hline 2&1&0&2&4&3\\ \hline 3&2&1&0&2&4\\ \hline\end{array}$	2	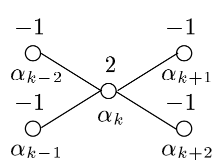	$\epsilon_2-\epsilon_3$	1 2 3 4	0 -1 1 0

Table 6: Data for $B_3^{(1)}$, $A_5^{(2)}$ and $D_4^{(1)}$ when $k=2$

For $\mathbf{g} = B_3^{(1)}$, each row comprises a sequence of $\boxed{1}\boxed{0}\boxed{2}\boxed{3}\boxed{2}$ blocks. Here $k = 2$ and the order of the pair $\boxed{1}\boxed{0}$ is irrelevant. As we pass between the six valid positions, we obtain the values $(1, 1, -2, 2, -2)$ for $\Delta\vartheta$ and the values $(-1, -1, 2, -2, 2)$ for $\Delta\Sigma$.

For $\mathbf{g} = A_5^{(2)}$, each row comprises a sequence of $\boxed{1}\boxed{0}\boxed{2}\boxed{3}\boxed{3}\boxed{2}$ blocks. The details of this case are then as for the $\mathbf{g} = B_3^{(1)}$ case above.

For $\mathbf{g} = D_4^{(1)}$, each row comprises a sequence of $\boxed{1}\boxed{0}\boxed{2}\boxed{4}\boxed{3}\boxed{2}$ blocks. Here $k = 2$ and the order of each pair $\boxed{1}\boxed{0}$ and $\boxed{4}\boxed{3}$ is irrelevant. As we pass over the six nodes, we obtain the values $(1, 1, -2, 1, 1, -2)$ for $\Delta\vartheta$ and the values $(-1, -1, 2, -1, -1, 2)$ for $\Delta\Sigma$.

This completes the verification of the above claim that $\Delta\vartheta = -\Delta\Sigma$ in all cases. To complete the proof, it remains to directly verify (4.7) where a row has been augmented. This occurs only if $i = 1$ and either $\mathbf{g} = B_\ell^{(1)}$, $D_\ell^{(1)}$ or $A_{2\ell+1}^{(2)}$, or if $i = \ell$ and $\mathbf{g} = D_\ell^{(1)}$. In the former case, $\vartheta_{ik}(T')$ takes the values $(-1, 1, 0)$ for $k = 0$, $k = 1$ and $k \geq 2$ respectively. Since $n_{10}(T') = 1$, $n_{11}(T') = -1$ and $n_{1k}(T') = 0$ for $k \geq 2$, and $(\alpha_0|\epsilon_1) = -1$, $(\alpha_1|\epsilon_1) = 1$ and $(\alpha_k|\epsilon_1) = 0$ for $k \geq 2$, it follows that (4.7) holds in this case. The latter case is similar. $\square$

Lemma 4.1.3 *If $w \in W$ then $N_{ij}(w) = n_{ij}(w)$ for $j \in I$ and $1 \leq i \leq n$.*

Proof: Let $w = w's_k$ so that $T = T(w)$ is obtained from $T' = T(w')$ by a k-shift. Let $j \in I$. Since T and T' differ by k-nodes, we have $n_{ij}(w) = n_{ij}(w')$ for $j \neq k$ and $1 \leq i \leq n$. For the $j = k$ case, Lemma 4.1.2 shows that:

$$n_{ik}(w) = n_{ik}(w') - (\alpha_k|\epsilon_i) - \sum_{m=0}^{\ell} A_{mk} n_{im}(w'). \tag{4.8}$$

Comparing this with (4.5) shows that $N_{ij}(w)$ and $n_{ij}(w)$ satisfy identical recurrence relations. Since there exists an expression $w = s_{i_1} s_{i_2} \cdots s_{i_t}$ in terms of the generators of $\mathbf{g}$, and $N_{ij}(1) = n_{ij}(1) = 0$ for $j \in I$ and $1 \leq i \leq n$, it follows that $N_{ij}(w) = n_{ij}(w)$ for all $j \in I$ and $1 \leq i \leq n$. $\square$

Theorem 4.1.4 *Let $w \in W$ and $\Lambda \in \mathbf{h}^*$. Then:*

$$\overline{w(\Lambda) - \Lambda} = \sum_{i=1}^{n} \sum_{j=0}^{\ell} m_j(\Lambda) n_{ij}(w) \epsilon_i, \tag{4.9}$$

where $m_j(\Lambda) = (\Lambda \,|\, \alpha_j^\vee)$ for $j \in I$.

Proof: This follows immediately from (4.4) after noting that Lemma 4.1.3 shows that $N_{ij}(w) = n_{ij}(w)$ for $j \in I$ and $1 \leq i \leq n$. $\square$

Using the notation of Section 2.6, this result can be written in the form (4.1).

4.2 Properties of the profiles

We now examine the profiles of the coloured diagrams $T(w)$, for $w \in W$.

Lemma 4.2.1 *For $w \in W$ and $1 \le h \le n$, let i be such that $\overline{w(\epsilon_h)} = \pm\epsilon_i$. Then the pair that straddles the vertical axis in the hth row of the grid, is that pair which straddles the profile of $T(w)$ in the ith row. Moreover, the pair is reversed if and only if $\overline{w(\epsilon_h)} = -\epsilon_i$.*

Proof: First note that that the existence of an i such that $\overline{w(\epsilon_h)} = \pm\epsilon_i$ follows from the specification of the action of W on $\epsilon_1, \epsilon_2, \ldots, \epsilon_n$ given in Section 3.6. In fact, this action shows that $w(\epsilon_h) = \pm\epsilon_i + m\delta$ for some $m \in \mathbb{Z}$. Then $w^{-1}(\epsilon_i) = \pm\epsilon_h - m\delta$.

For $k \in I$, let $w' = ws_k$. For $1 \le i \le n$ and $j \in I$, Lemma 4.1.2 shows that there are $N_{ij}(w)$ nodes coloured j in the ith row of $T(w)$, and $N_{ij}(w')$ nodes coloured j in the ith row of $T(w')$. Use of (4.3) gives $(w(\Lambda_j) - \Lambda_j \,|\, \epsilon_i) = N_{ij}(w)$ and $(w'(\Lambda_j) - \Lambda_j \,|\, \epsilon_i) = N_{ij}(w')$, whereupon:

$$\begin{aligned} N_{ij}(w') - N_{ij}(w) &= (w'(\Lambda_j) - w(\Lambda_j) \,|\, \epsilon_i) = (w(s_k(\Lambda_j) - \Lambda_j) \,|\, \epsilon_i) \\ &= -\delta_{jk}(w(\alpha_k) \,|\, \epsilon_i) = -\delta_{jk}(\alpha_k \,|\, w^{-1}(\epsilon_i)) \\ &= -\delta_{jk}(\alpha_k \,|\, \pm\epsilon_h - m\delta) = \mp\delta_{jk}(\alpha_k \,|\, \epsilon_h). \end{aligned}$$

The presence of δ_{jk} here confirms that $T(w')$ and $T(w)$ differ only by k-nodes. This expression implies that $(\alpha_k|\epsilon_h) < 0$ if and only if a k-node is adjacent and to the right of the profile in the ith row of $T(w)$, and $(\alpha_k|\epsilon_h) > 0$ if and only if a k-node is adjacent and to the left of the profile in the ith row of $T(w)$. We will compare this with the special case $w = 1$, for which $\overline{w(\epsilon_k)} = \epsilon_k$ and

$$N_{hk}(w') - N_{hk}(w) = N_{hk}(s_k) - N_{hk}(1) = -(\alpha_k|\epsilon_h).$$

The comparison shows that the nodes neighbouring the profile in the hth row of $T(1)$ are precisely those neighbouring the profile in the ith row of $T(w)$. Moreover, we see that the pair is reversed if and only if $\overline{w(\epsilon_h)} = -\epsilon_i$. □

Corollary 4.2.2 *If $w \in W$ then $T(w)$ is edge-balanced.*

Proof: First note that $T(1)$ is edge-balanced. Lemma 4.2.1 shows that the pairs which straddle the profile of $T(w)$ are a permutation of those which straddle the profile of $T(1)$, with some of those pairs reversed. It follows that $T(w)$ is edge-balanced. □

Corollary 4.2.3 *If $\mathbf{g} = A_\ell^{(1)}$ and $w \in W$ then $T(w)$ is colour-balanced.*

Proof: Let $w' \in W$ and $k \in I$. By Corollary 4.2.2, the profile of $T(w')$ contains a unique segment which bisects a pair $\boxed{k}\boxed{k{-}1}$ and a unique segment which bisects a pair $\boxed{k{+}1}\boxed{k}$. No other segment of the profile is adjacent to a k-node. Thus, since $T(w's_k)$ is obtained from $T(w')$ by a k-shift, only the two rows in which the profile of $T(w')$ bisects these configurations change. For $\boxed{k}\boxed{k{-}1}$ the profile shifts one position to the left, and for $\boxed{k{+}1}\boxed{k}$ the profile shifts by one position to the right. Therefore, whether the two k-nodes in question are to the right of the vertical axis, to the left of the vertical axis, or one is on each side, the difference between the numbers of k-nodes to the left and right of the vertical axis in $T(w's_k)$ is precisely the same as that for $T(w')$.

Thus, after recursively constructing $T(w)$ from the trivial $T(1)$ using an expression for w in terms of the generators $s_0, s_1, \ldots, s_\ell$, the resultant $T(w)$ necessarily contains the same number of k-nodes to the left and right of the vertical axis, for all $k \in I$. $\square$

Corollary 4.2.4 *If $\mathbf{g} = B_\ell^{(1)}$, $D_\ell^{(1)}$ or $A_{2\ell-1}^{(2)}$, and $w \in W$ then $T(w)$ is even-handed.*

Proof: Let $w' \in W$ and first consider $k \in \{0, 1\}$. By Corollary 4.2.2, the profile of $T(w')$ contains a unique segment which bisects a pair $\boxed{1}\boxed{0}$ and a unique segment which bisects $\boxed{2}\boxed{1{\sim}0}$. No other segment of the profile is adjacent to a 0- or a 1-node. Thus, since $T(w's_k)$ is obtained from $T(w')$ by a k-shift, only the two rows in which the profile of $T(w')$ bisects these configurations change. In each of these rows, a k-node is either appended or removed. Thus the difference between the number of k-nodes in $T(w's_k)$ and $T(w')$ is either -2, 0, or 2. In particular, the difference is even. Thus, after recursively constructing $T(w)$ from the trivial $T(1)$ using an expression for w in terms of the generators $s_0, s_1, \ldots, s_\ell$, the resultant $T(w)$ necessarily contains an even number of k-nodes. The argument for $\mathbf{g} = D_\ell^{(1)}$ and $k \in \{\ell - 1, \ell\}$ is similar. $\square$

Although we don't use this fact, it is interesting to note that for $\mathbf{g} = D_\ell^{(1)}$, the number of reversals in the pairs that straddle the profile of each $T(w)$ is necessarily even. To see this, note that apart from the first row, each of the rows of $T(w)$ in which the profile bisects an unreversed pair $\boxed{k}\boxed{k{-}1}$ for $2 \le k \le \ell - 1$ contains as many complete $\boxed{1}\boxed{0}$ pairs as $\boxed{\ell}\boxed{\ell{-}1}$ pairs. The same is true of that row in which the profile bisects the pair $\boxed{1}\boxed{0}$, either reversed or unreversed. And, again apart from the first row, each of the rows of $T(w)$ in which the profile bisects a reversed pair $\boxed{k{-}1}\boxed{k}$ for $2 \le k \le \ell - 1$ contains one more complete $\boxed{1}\boxed{0}$ pair than $\boxed{\ell}\boxed{\ell{-}1}$ pairs. The same is true of that row in which the profile bisects the pair $\boxed{\ell}\boxed{\ell{-}1}$, either reversed or unreversed. In the case of the first row of $T(w)$, the number of complete $\boxed{1}\boxed{0}$ pairs is one fewer than that which would be obtained above. Let the pair $\boxed{1}\boxed{0}$ be bisected by the profile of $T(w)$ such that $\boxed{1}$ (resp. $\boxed{0}$) is to the left. The even-handed requirement then dictates that there are necessarily an odd (resp. even) number of complete $\boxed{1}\boxed{0}$ pairs in $T(w)$. Then, if the number of reversed bisected pairs $\boxed{k{-}1}\boxed{k}$ for $2 \le k \le \ell - 1$ is even, the comparison above between the number of complete $\boxed{1}\boxed{0}$ and $\boxed{\ell}\boxed{\ell{-}1}$ pairs, shows that there is also an odd (resp. even) number of complete $\boxed{\ell}\boxed{\ell{-}1}$ pairs in $T(w)$. The even-handed requirement then dictates that the $\boxed{\ell}\boxed{\ell{-}1}$ pair is bisected by the profile of $T(w)$ such that $\boxed{\ell}$ (resp. $\boxed{\ell{-}1}$) is to the left. Thus either both or neither of $\boxed{0}\boxed{1}$ and $\boxed{\ell{-}1}\boxed{\ell}$ appear straddling the profile, which together with the even number of reversed bisected pairs $\boxed{k{-}1}\boxed{k}$ for $2 \le k \le \ell - 1$, implies that there are an even number of reversals altogether. Similarly, there are an even number of reversals altogether if there is an odd number of reversed bisected pairs $\boxed{k{-}1}\boxed{k}$ for $2 \le k \le \ell - 1$, when exactly one of the reversed bisected pairs $\boxed{0}\boxed{1}$ and $\boxed{\ell{-}1}\boxed{\ell}$ appears.

This fact can be attributed to the influence of the Weyl-Coxeter group $\overline{W}$ of $\overline{\mathbf{g}}$ on the profile. In this $\mathbf{g} = D_\ell^{(1)}$ case, we have $\overline{\mathbf{g}} = D_\ell$ and $\overline{W}$ may be realised as the group of signed permutations of $\epsilon_1, \epsilon_2, \dots, \epsilon_\ell$, with always an even number of sign changes.

4.3 Setting the depth charges

In this section, we prove that the charges of the nodes in the stretched coloured diagram $T^\Lambda(w)$ defined in Section 2.6 yields the depth factor $d^\Lambda(w)$. Recall that $N_{ij}(w)$ and $P_j(w)$ are defined by (4.3), and that $d_{ij}(w)$, $d_{ij}(T)$, $n_{ij}(w)$, $n_{ij}(T)$ and $d_j(w)$ are also defined in Section 4.1.

We will use the notation:

$$\delta(i,\boxed{1}\boxed{0}) = \begin{cases} 1 & \text{if in the } i\text{th row, the profile of } T' \text{ bisects } \boxed{1}\boxed{0} \text{ or } \boxed{0}\boxed{1}; \\ 0 & \text{otherwise.} \end{cases}$$

$$\delta^+(i,\boxed{1}\boxed{0}) = \begin{cases} 1 & \text{if in the } i\text{th row, the profile of } T' \text{ bisects } \boxed{1}\boxed{0}; \\ 0 & \text{otherwise.} \end{cases}$$

Similar notation will be used for other pairs of nodes.

Lemma 4.3.1 *Let T' and T be coloured diagrams with T obtained from T' by a k-shift, where $k \in I$. Let $1 \le i \le n$ and set:*

$$\hat{\vartheta}_{ik}(T') = d_{ik}(T) - d_{ik}(T')$$

and

$$\hat{\Sigma}_{ik}(T') = \sum_{m=0}^{\ell} A_{mk} d_{im}(T').$$

Then, for $\mathbf{g} = A_\ell^{(1)}$,

$$\hat{\vartheta}_{ik}(T') = -\hat{\Sigma}_{ik}(T') + \delta_{k0}\delta^+(i,\boxed{0}\boxed{\ell}) + (\delta_{k\ell} - \delta_{k0}) n_{i0}(T'); \tag{4.10}$$

for $\mathbf{g} = C_\ell^{(1)}$, $A_{2\ell}^{(2)}$ or $D_{\ell+1}^{(2)}$,

$$\hat{\vartheta}_{ik}(T') = -\hat{\Sigma}_{ik}(T') + \delta_{k0}\delta(i,\boxed{1}\boxed{0}); \tag{4.11}$$

and for $\mathbf{g} = B_\ell^{(1)}$, $D_\ell^{(1)}$ or $A_{2\ell+1}^{(2)}$,

$$\hat{\vartheta}_{ik}(T') = -\hat{\Sigma}_{ik}(T') + \begin{cases} \frac{1}{2}\delta(i,\boxed{1}\boxed{0}) + \frac{1}{2}\delta(i,\boxed{2}\boxed{1\sim 0}) & \textit{if } k=0; \\ \frac{1}{2}\delta(i,\boxed{1}\boxed{0}) + \frac{1}{2}\delta(i,\boxed{2}\boxed{1\sim 0}) - \delta_{i1} & \textit{if } k=1; \\ \frac{1}{2}\delta_{i1} - \frac{1}{2}\delta(i,\boxed{1}\boxed{0}) & \textit{if } k=2; \\ 0 & \textit{if } k \ge 3. \end{cases} \tag{4.12}$$

Proof: We first claim that (4.10), (4.11) and (4.12) each hold when the ith row of T' is empty. Note that here, the left side of each expression is non-zero only if the vertical axis is adjacent to a k-node that has non-zero charge. Examination of the depth charged grids with tied pairs and unordered pairs identified shows that for $\mathbf{g} = A_\ell^{(1)}$, we have $\hat{\vartheta}_{n0}(T') = 1$; for $\mathbf{g} = C_\ell^{(1)}$, $A_{2\ell}^{(2)}$ or $D_{\ell+1}^{(2)}$, we have $\hat{\vartheta}_{10}(T') = 1$; and for $\mathbf{g} = B_\ell^{(1)}$, $D_\ell^{(1)}$ or $A_{2\ell+1}^{(2)}$, we have $\hat{\vartheta}_{10}(T') = \hat{\vartheta}_{20}(T') = \frac{1}{2}$ and $\hat{\vartheta}_{11}(T') = -\hat{\vartheta}_{21}(T') = -\frac{1}{2}$; with $\hat{\vartheta}_{ik}(T') = 0$ in all other cases. Each of the final two terms on the right side of (4.10) is 0, whereas $\delta_{k0}\delta^+(i, \boxed{0|\ell})$ is non-zero only if $k = 0$ and $i = n$. Thus (4.10) holds here. The final term on the right side of (4.11) is 0, whereas $\delta_{k0}\delta(i, \boxed{1|0})$ is non-zero only if $k = 0$ and $i = 1$. Thus (4.11) holds here. The first term on the right side of (4.12) is 0. The remaining terms give 0 for $k \geq 2$. For $k \in \{0, 1\}$, they are seen to be non-zero only if $i \in \{1, 2\}$, and moreover are in agreement with the above values for $\hat{\vartheta}_{ik}(T')$. The above claim is thus verified.

We now claim that, whatever the length of the ith row of T', the values of the two sides of each of (4.10), (4.11) and (4.12) change by the same amount when the profile is moved to the next possible position on its right. This claim will be verified below by considering many cases. Once verified, its iterative application shows that each of (4.10), (4.11) and (4.12) holds for rows of positive length. Of course, the periodicity of the grids ensures that the two sides of each of these expressions also change by the same amount when the profile is moved to the next possible position on its left. Thereupon, we conclude that (4.10), (4.11) and (4.12) hold in all cases.

This procedure parallels that adopted in the proof of Lemma 4.1.2 and we therefore use a similar notation whereby we denote the change in $\hat{\Sigma}_{ik}(T')$ by $\Delta\hat{\Sigma}$, and the change in $\hat{\vartheta}_{ik}(T')$ by $\Delta\hat{\vartheta}$. This means in particular that if the profile in the ith row has to its right n_j adjacent j-nodes, each of charge d_j, then $\Delta\hat{\Sigma} = n_j A_{jk} d_j = d_j \Delta\Sigma$. In addition, if in the ith row of the original T' the profile is not adjacent to any k-nodes then $\hat{\vartheta}_{ik}(T') = 0$ since the ith row of T and T' must coincide. On the other hand if it is adjacent to n_k k-nodes each of charge d_k in the ith row then $\hat{\vartheta}_{ik}(T') = n_k d_k$ or $-n_k d_k$ according to whether these are to the right or to the left of the profile, since the ith row of T is necessarily formed by adding or deleting the n_k adjacent k-nodes to T'. It follows that $\Delta\hat{\vartheta}$ may be read off the k-blocks rather easily as the profile of T' advances from left to right by first enumerating $\hat{\vartheta}_{ik}(T')$ in accordance with the above rule, and then calculating differences in these values.

We now consider those cases for which k-blocks are defined. If the profile passes over a j-node which is not in a k-block then $\Delta\hat{\vartheta} = 0$ since before and after the change, the profile is not adjacent to a k-node. To see that the right sides of (4.10), (4.11) and (4.12) are similarly unchanged, first note that $A_{jk} = 0$ implies that $\Delta\Sigma = 0$. The claim then holds for (4.11) since when $k = 0$, each $\boxed{1|0}$ is in a k-block. For (4.10), it holds because when $k = 0$, $\boxed{0|\ell}$ is in a k-block; and when $k \in \{0, \ell\}$, each 0-node is within a k-block. For (4.12), it holds because when $k \in \{0, 1, 2\}$, each $\boxed{1|0}$ and each $\boxed{2|1{\sim}0}$ is in a k-block.

For each of the k-blocks listed in Tables 2 and 3, we now examine the changes when the profile passes over a j-node that is in the k-block. For convenience, hereafter, we consider the charge of the leftmost node of a k-block to be r. The other charges are then determined. The only changes in charge occur between 0 and ℓ, between 0 and 1, and between the unordered pair $1 \sim 0$ and 2. This is the origin of the terms involving these nodes in (4.10)-(4.12). In particular, if the k-block contains no 0-node, then each of its charges is r. In such a case there are no variations of the factors appearing in (4.10)-(4.12) other than $\hat{\theta}_{ik}(T')$ and $\hat{\Sigma}_{ik}(T')$, as the profile of T' advances across the k-block. In addition we have $\Delta\hat{\Sigma} = r\Delta\Sigma$ and $\Delta\hat{\vartheta} = r\Delta\vartheta$. Since $\Delta\vartheta = -\Delta\Sigma$, as shown in the proof of Lemma 4.1.2, we immediately have $\Delta\hat{\vartheta} = -\Delta\hat{\Sigma}$, as required. This constancy of r over a k-block covers all cases other than those associated with the left hand end of the Dynkin diagram of $\mathbf{g}$ where the vertex 0 appears.

For cases 1a and 1b, for example, if $k \notin \{0, 1, \ell\}$. There are three nodes to pass over, all of depth charge r. These give the values $(r, -2r, r)$ for $\Delta\hat{\vartheta}$ and the values $(-r, 2r, -r)$ for $\Delta\hat{\Sigma}$. The above claim thus holds here.

The instances $k \in \{0, \ell\}$ of Cases 1a and 1b only arise if $\mathbf{g} = A_\ell^{(1)}$, and then Case 1b does not arise. For $\mathbf{g} = A_\ell^{(1)}$, only (4.10) applies. For $k = 1$, each of the charges in the k-block is r, whereupon the previous argument deals with this case. For $k = 0$, the charges read $(r, r, r+1)$ from left to right. Then the three nodes give the values $(r, -2r, r)$ for $\Delta\hat{\vartheta}$ and the values $(-r, 2r, -r-1)$ for $\Delta\hat{\Sigma}$. Since $\delta^+(i, \boxed{0}\boxed{\ell})$ increases by $(0, 1, -1)$ and $n_{i0}(T')$ by $(0, 1, 0)$ as the profile passes over the same three nodes, the above claim is verified here. For $k = \ell$, the charges read $(r, r+1, r+1)$ from left to right. Then the three nodes give the values $(r+1, -2r-2, r+1)$ for $\Delta\hat{\vartheta}$ and the values $(-r, 2r+2, -r-1)$ for $\Delta\hat{\Sigma}$. Since $n_{i0}(T')$ changes by $(1, 0, 0)$ as the profile passes over the same three nodes, the above claim is verified here. This deals with all cases that arise for $\mathbf{g} = A_\ell^{(1)}$.

Hereafter, we deal only with $\mathbf{g} \neq A_\ell^{(1)}$, for which we anticipate from the statement of Lemma 4.3.1 that $\Delta\hat{\vartheta} = -\Delta\hat{\Sigma}$, except in the case $k = 0$ for $\mathbf{g} = C_\ell^{(1)}$, $A_{2\ell}^{(2)}$ or $D_{\ell+1}^{(2)}$, and the cases $k = 0$, 1 or 2 for $\mathbf{g} = \mathbf{g} = B_\ell^{(1)}$, $D_\ell^{(1)}$ or $A_{2\ell+1}^{(2)}$. Note that Cases 2a and 5a only arise for $\mathbf{g} = D_{\ell+1}^{(2)}$, that Cases 3a and 6a only arise for $\mathbf{g} = C_\ell^{(1)}$ and $A_{2\ell}^{(2)}$, and that Cases 4a, 7a and 7b only arise for $\mathbf{g} = B_\ell^{(1)}$, $D_\ell^{(1)}$ or $A_{2\ell+1}^{(2)}$. All the other Cases 2b, 3b, 4b, 5b, 6b, 7c and 7d involve the right hand end of the Dynkin diagrams so that the charges in the k-block are all r and they involve no 0-nodes.

For Case 2a, we have $k = 1$ and the charges read $(r, r, r+1, r+2, r+2)$ left to right. The five moves give $(r, -2r, 2r+2, -2r-4, r+2)$ for $\Delta\hat{\vartheta}$ and $(-r, 2r, -2r-2, 2r+4, -r-2)$ for $\Delta\hat{\Sigma}$. Since $k = 1$ this gives $\Delta\hat{\vartheta} = -\Delta\hat{\Sigma}$, as required by (4.11).

For Case 2b, we have $k = \ell - 1$ and the charges in the k-block are all r. The five moves give $(r, -2r, 2r, -2r, r)$ for $\Delta\hat{\vartheta}$ and $(-r, 2r, -2r, 2r, -r)$ for $\Delta\hat{\Sigma}$.

For Case 3a, we have $k = 1$ and the charges read $(r, r, r + \frac{1}{2}, r + \frac{1}{2}, r + 1, r + 1)$ left to right. The five possible moves give $(r, -2r, 2r+1, -2r-2, r+1)$ for $\Delta\hat{\vartheta}$ and $(-r, 2r, -2r-1, 2r+2, -r-1)$ for $\Delta\hat{\Sigma}$.

For Case 3b, we have $k = \ell - 1$ and the charges in the k-block are all r. The five moves give $(r, -2r, 2r, -2r, r)$ for $\Delta\hat{\vartheta}$ and $(-r, 2r, -2r, 2r, -r)$ for $\Delta\hat{\Sigma}$.

For Case 4a, we have $k = 2$ and the charges read $(r, r, r + \frac{1}{2}, r + \frac{1}{2}, r + 1, r + 1)$ left to right. Noting that the order of the pair $\boxed{1}\boxed{0}$ is irrelevant here, the six possible moves give $(r, -2r, r, r+1, -2r-2, r+1)$ for $\Delta\hat{\vartheta}$ and $(-r, 2r, -r - \frac{1}{2}, -r - \frac{1}{2}, 2r+2, -r-1)$ for $\Delta\hat{\Sigma}$. Since $\delta(i, \boxed{1}\boxed{0})$ increases by $(0, 0, 1, -1, 0, 0)$ for the same six moves, the claim holds here for (4.12).

For Case 4b, we have $k = \ell - 2$ and the charges in the k-block are all r. Again noting the irrelevance of the unordered pair, the six moves give $(r, -2r, r, r, -2r, r)$ for $\Delta\hat{\vartheta}$ and $(-r, 2r, -r, -r, 2r, -r)$ for $\Delta\hat{\Sigma}$.

For Case 5a, we have $k = 0$ and the charges read $(r, r+1, r+2)$ left to right. The three moves give $(r+1, -2r-2, r+1)$ for $\Delta\hat{\vartheta}$ and $(-r, 2r+2, -r-2)$ for $\Delta\hat{\Sigma}$. Since $\delta(i, \boxed{1}\boxed{0})$ increases by $(1, 0, -1)$ for the same three moves, the claim holds here for (4.11).

For Case 5b, we have $k = \ell$ and the charges in the k-block are all r. The three moves give $(r, -2r, r)$ for $\Delta\hat{\vartheta}$ and $(-r, 2r, r)$ for $\Delta\hat{\Sigma}$.

For Case 6a, we have $k = 0$ and the charges read $(r, r+\frac{1}{2}, r+\frac{1}{2}, r+1)$ left to right. The three moves give $(2r+1, -4r-2, 2r+1)$ for $\Delta\hat{\vartheta}$ and $(-2r, 4r+2, -2r)$ for $\Delta\hat{\Sigma}$. Since $\delta(i, \boxed{1}\boxed{0})$ increases by $(1, 0, -1)$ for the same three moves, the claim holds here for (4.11).

For Case 6b, we have $k = \ell$ and the charges in the k-block are all r. The three moves give $(2r, -4r, 2r)$ for $\Delta\hat{\vartheta}$ and $(-2r, 4r, 2r)$ for $\Delta\hat{\Sigma}$.

For Case 7a, we have $k = 1$ and the charges read $(r, r+\frac{1}{2}, r+\frac{1}{2}, r+1)$ left to right. The four moves give $(r+\frac{1}{2}, -2r-1, 0, r+\frac{1}{2})$ or $(r+\frac{1}{2}, 0, -2r-1, r+\frac{1}{2})$ for $\Delta\hat{\vartheta}$, according to the central nodes being ordered $1 \sim 0$ or $0 \sim 1$, respectively. The four moves also give $(-r, 2r+1, 0, -r-1)$ and $(-r, 0, 2r+1, -r-1)$ for $\Delta\hat{\Sigma}$, in the corresponding cases. Since $\delta(i, \boxed{1}\boxed{0})$ increases by $(0, 1, -1, 0)$ and $\boxed{2}\boxed{1{\sim}0}$ increases by $(1, -1, 1, -1)$ for the same four moves, the claim holds here for (4.12).

For Case 7b, we have $k = 0$. The details of this case read exactly as for Case 7a, except for the interchange of values of the cases $1 \sim 0$ and $0 \sim 1$.

For Case 7c, we have $k = \ell$ and the charges in the k-block are all r. The four moves give $(r, -2r, 0, r)$ or $(r, 0, -2r, r)$ for $\Delta\hat{\vartheta}$ and $(-r, 2r, 0, -r)$ or $(-r, 0, 2r, -r)$ for $\Delta\hat{\Sigma}$, according to the central nodes being ordered $\ell \sim \ell - 1$ or $\ell - 1 \sim \ell$, respectively.

For Case 7d, we have $k = \ell - 1$. The details of this case read exactly as for Case 7c, except for the interchange of the cases $\ell \sim \ell - 1$ and $\ell - 1 \sim \ell$.

This completes the verification of the claim in the cases for which k-blocks are defined. The cases for which there are no k-blocks are tabulated in Tables 4, 5, and 6. We tackle each of them in turn.

For $\mathbf{g} = A_1^{(1)}$, each row comprises a sequence of $\boxed{1_r}\boxed{0_r}$ blocks, with r increasing by 1 as we pass from one block to that on its right. First consider $k = 1 = \ell$. As the profile passes over the two nodes, we obtain the values $(-2r, 2r+1)$ for $\Delta\hat{\vartheta}$ and the values $(2r, -2r)$ for $\Delta\hat{\Sigma}$. Since $n_{i0}(T')$ increases by $(0, 1)$ as the profile passes over the same two nodes, both sides of (4.10) change by the same amount, and the claim is verified in this case. For $k = 0$, we obtain the values $(2r-1, -2r)$ for $\Delta\hat{\vartheta}$ and the values $(-2r, 2r)$ for $\Delta\hat{\Sigma}$, as the profile passes over the two nodes. Then, since $n_{i0}(T')$ increases by $(0, 1)$ and $\delta^+(i, \boxed{0}\boxed{\ell})$ increases by $(-1, 1)$, as the profile passes over the same two nodes, again both sides of (4.10) change by the same amount, and the claim is verified here.

For $\mathbf{g} = A_2^{(2)}$, the single row comprises a sequence of $\boxed{0_r}\boxed{0_r}\boxed{1_{r+1/2}}$ blocks, with r increasing by 1 as we pass from one block to that on its right. First consider $k = 1 = \ell$. As the profile passes between the three valid positions, we obtain the values $(2r, -2r-1)$ for $\Delta\hat{\vartheta}$ and the values $(-2r, 2r+1)$ for $\Delta\hat{\Sigma}$. For $k = 0$, we obtain the values $(-4r, 4r+2)$ for

$\Delta\hat{\vartheta}$ and the values $(4r, -4r-2)$ for $\Delta\hat{\Sigma}$. Since $\delta(i, \boxed{1}\boxed{0}) = 1$ in all cases, the claim holds here for (4.11) and $k \in \{0, 1\}$ as required.

For $\mathbf{g} = D_3^{(2)}$, each row comprises a sequence of $\boxed{0_{r-1}}\boxed{1_r}\boxed{2_r}\boxed{1_r}$ blocks, with r increasing by 2 as we pass from one block to that on its right. With $k = 1$, as we pass over the four nodes, we obtain the values $(2r-2, -2r, 2r, -2r)$ for $\Delta\hat{\vartheta}$ and the values $(-2r+2, 2r, -2r, 2r)$ for $\Delta\hat{\Sigma}$.

For $\mathbf{g} = A_4^{(2)}$, each row comprises a sequence of $\boxed{0_{r-1/2}}\boxed{0_{r-1/2}}\boxed{1_r}\boxed{2_r}\boxed{1_r}$ blocks, with r increasing by 1 as we pass from one block to that on its right. With $k = 1$, as we pass between the five valid positions, we obtain the values $(2r-1, -2r, 2r, -2r)$ for $\Delta\hat{\vartheta}$ and the values $(-2r+1, 2r, -2r, 2r)$ for $\Delta\hat{\Sigma}$.

For $\mathbf{g} = C_2^{(1)}$, each row comprises a sequence of $\boxed{0_{r-1/2}}\boxed{0_{r-1/2}}\boxed{1_r}\boxed{2_r}\boxed{2_r}\boxed{1_r}$ blocks, with r increasing by 1 as we pass from one block to that on its right. Here $k = 1$ and the details of this case are then as for the $\mathbf{g} = A_4^{(2)}$ case above.

For $\mathbf{g} = B_3^{(1)}$, each row comprises a sequence of $\boxed{1_{r-1/2}}\boxed{0_{r-1/2}}\boxed{2_r}\boxed{3_r}\boxed{2_r}$ blocks, with r increasing by 1 as we pass from one block to that on its right. Here $k = 2$ and the order of the pair $\boxed{1}\boxed{0}$ is irrelevant. As we pass between the six valid positions, we obtain the values $(r-1, r, -2r, 2r, -2r)$ for $\Delta\hat{\vartheta}$ and the values $(-r+\frac{1}{2}, -r+\frac{1}{2}, 2r, -2r, 2r)$ for $\Delta\hat{\Sigma}$. Then, since $\delta(i, \boxed{1}\boxed{0})$ changes by $(1, -1, 0, 0, 0)$, the claim holds here for (4.12).

For $\mathbf{g} = A_5^{(2)}$, each row comprises a sequence of $\boxed{1_{r-1/2}}\boxed{0_{r-1/2}}\boxed{2_r}\boxed{3_r}\boxed{3_r}\boxed{2_r}$ blocks, with r increasing by 1 as we pass from one block to that on its right. Once again $k = 2$ and the details of this case are then as for the $\mathbf{g} = B_3^{(1)}$ case above.

For $\mathbf{g} = D_4^{(1)}$, each row comprises a sequence of $\boxed{1_{r-1/2}}\boxed{0_{r-1/2}}\boxed{2_r}\boxed{4_r}\boxed{3_r}\boxed{2_r}$ blocks, with r increasing by 1 as we pass from one block to that on its right. Here $k = 2$ and the order of each pair $\boxed{1}\boxed{0}$ and $\boxed{4}\boxed{3}$ is irrelevant. As we pass over the six nodes, we obtain the values $(r-1, r, -2r, r, r, -2r)$ for $\Delta\hat{\vartheta}$ and the values $(-r+\frac{1}{2}, -r+\frac{1}{2}, 2r, -r, -r, 2r)$ for $\Delta\hat{\Sigma}$. Then, since $\delta(i, \boxed{1}\boxed{0})$ changes by $(1, -1, 0, 0, 0, 0)$, the claim holds here for (4.12).

This completes the verification of the above claim in all cases. To complete the proof, it remains to directly verify (4.12) where a row has been augmented. This occurs only if $i = 1$ and either $\mathbf{g} = B_\ell^{(1)}$, $D_\ell^{(1)}$ or $A_{2\ell+1}^{(2)}$, or if $i = \ell$ and $\mathbf{g} = D_\ell^{(1)}$. In the former case, $\hat{\vartheta}_{ik}(T')$ takes the values $(-\frac{1}{2}, \frac{1}{2}, 0)$ for $k = 0$, $k = 1$ and $k \geq 2$ respectively Since $d_{10} = \frac{1}{2}$, $d_{11} = -\frac{1}{2}$ and $d_{1k} = 0$ for $k \geq 2$, and $\delta(i, \boxed{1}\boxed{0}) = 1$, it follows that (4.12) holds in this case. In the latter case, both sides of (4.12) are immediately seen to be 0. $\square$

Lemma 4.3.2 *If $w \in W$ then $P_j(w) = d_j(w)$ for each $j \in I$.*

Proof: Let $w = w' s_k$ so that $T = T(w)$ is obtained from $T' = T(w')$ by a k-shift. Let $j \in I$. Since T and T' differ by k-nodes, we have $d_{ij}(w) = d_{ij}(w')$ for $j \neq k$ and $1 \leq i \leq n$. Summing these results over i for $1 \leq i \leq n$ gives $d_j(w) = d_j(w')$ for $j \in I \backslash \{k\}$. For the $j = k$ case, we claim that:

$$d_k(w) = d_k(w') + \delta_{k0} - \sum_{m=0}^{\ell} A_{mk} d_m(w'). \tag{4.13}$$

Assuming the veracity of this claim, (4.6) shows that $d_j(w)$ and $P_j(w)$ satisfy identical recurrence relations. Since there exists an expression $w = s_{i_1}s_{i_2}\cdots s_{i_t}$ in terms of the generators of $\mathbf{g}$, and $P_j(1) = d_j(1) = 0$ for $j \in I$, it follows that $P_j(w) = d_j(w)$ for all $j \in I$.

We now establish the above claim using the results of Lemma 4.3.1. In each of the cases (4.10), (4.11) and (4.12), we perform a sum over i for $1 \le i \le n$. Since $\hat{\vartheta}_{ik}(T') = d_{ik}(T) - d_{ik}(T')$, each left side yields $d_k(T) - d_k(T')$ under this summation.

For $\mathbf{g} = C_\ell^{(1)}$, $A_{2\ell}^{(2)}$ or $D_{\ell+1}^{(2)}$, the right side of (4.11) yields $\delta_{k0} - \sum_{m=0}^{\ell} A_{mk}d_m(T')$ under this summation, after noting that, by Lemma 4.2.2, $\delta(i, \boxed{1}\boxed{0}) = 1$ for precisely one value of i, and 0 otherwise. The claim (4.13) now follows because $d_j(T') = d_j(w')$ and $d_j(T) = d_j(w)$ for $j \in I$.

For $\mathbf{g} = B_\ell^{(1)}$, $D_\ell^{(1)}$ or $A_{2\ell+1}^{(2)}$, the claim (4.13) follows from (4.12) and Lemma 4.2.2 in a similar way.

For $\mathbf{g} = A_\ell^{(1)}$, (4.10) and Lemma 4.2.2 similarly yield:

$$d_k(w) = d_k(w') + \delta_{k0} + (\delta_{k\ell} - \delta_{k0})\sum_{i=1}^{n} n_{i0}(w') - \sum_{m=0}^{\ell} A_{mk}d_m(w'). \tag{4.14}$$

Corollary 4.2.3 states that $T(w')$ is colour-balanced, whereupon $\sum_{i=1}^{n} n_{i0}(w') = 0$ in particular. The claim (4.13) then follows from (4.14). $\square$

Theorem 4.3.3 *Let $w \in W$ and $\Lambda \in \mathbf{h}^*$. Let $d^\Lambda(w) = \sum_{j=0}^{\ell} m_j(\Lambda)d_j(w)$ and let $\lambda^\Lambda(w)_i = \sum_{j=0}^{\ell} m_j(\Lambda)n_{ij}(w)$ for $1 \le i \le n$. Then:*

$$w(\Lambda) - \Lambda = \sum_{i=1}^{n} \lambda^\Lambda(w)_i\epsilon_i + d^\Lambda(w)\delta.$$

Proof: Since $N_{ij}(w) = n_{ij}(w)$ by Theorem 4.1.3, and $P_j(w) = d_j(w)$ by Lemma 4.3.2, this follows directly from (4.4). $\square$

On examining the definition of T^Λ in Section 2.6, this proves the result (2.8).

4.4 Recursive generation

In this section, we show that if $w, w' \in W$ with $w = w's_k$, then $T(w)$ differs from $T(w')$ as described in Section 2.8.

Lemma 4.4.1 *Let $w' \in W$ and $w = w's_k$ for $k \in I$. Then either $T(w) \succ T(w')$ or $T(w) \prec T(w')$. Moreover, if $\ell(w) = \ell(w') + 1$ then $d(w) \ge d(w')$, and if $d(w) = d(w')$ then $T(w) \prec T(w')$. On the other hand, if $\ell(w) = \ell(w') - 1$ then $d(w) \le d(w')$, and if $d(w) = d(w')$ then $T(w) \succ T(w')$.*

Proof: Let $j \in I$. Using the definition (4.3) for both $w, w' \in W$, we obtain:

$$\begin{aligned}\sum_{i=1}^{n}(N_{ij}(w) - N_{ij}(w'))\epsilon_i - (P_j(w) - P_j(w'))\delta &= w(\Lambda_j) - w'(\Lambda_j)\\ &= w'(s_k(\Lambda_j) - \Lambda_j) = -\delta_{jk} w(\alpha_k).\end{aligned}$$

Since $w'(\alpha_k) \in \Delta_{re}$, Theorem 3.3.1 shows that $w'(\alpha_k) = -m\delta + \gamma$ with $m \in \mathbb{Z}$ and $\gamma \in \Delta_0 \cup \Delta_1$. On the one hand, this gives $P_j(w) - P_j(w') = -\delta_{jk} m$, so that $d_j(w) - d_j(w') = -\delta_{jk} m$ by Lemma 4.3.2, which when summed over $j \in I$ gives $d(w) - d(w') = -m$. On the other hand, $\sum_{i=1}^{n}(N_{ij}(w) - N_{ij}(w'))\epsilon_i = -\delta_{jk}\gamma$, which when summed over $j \in I$, gives $\sum_{i=1}^{n}(\lambda_i(w) - \lambda_i(w'))\epsilon_i = -\gamma$ via Theorem 4.1.4. Theorem 3.3.1 shows that $\gamma \in \{\pm(\epsilon_p - \epsilon_q), \pm(\epsilon_p + \epsilon_q), \pm 2\epsilon_p, \pm\epsilon_q | 1 \leq p, q \leq n; p < q\}$, whereby one of the following holds:

- $\lambda_i(w) - \lambda_i(w') = \mp(\delta_{ip} - \delta_{iq})$,
- $\lambda_i(w) - \lambda_i(w') = \mp(\delta_{ip} + \delta_{iq})$,
- $\lambda_i(w) - \lambda_i(w') = \mp 2\delta_{ip}$,
- $\lambda_i(w) - \lambda_i(w') = \mp \delta_{ip}$,

where $1 \leq p, q \leq n$ and, in the first two cases, $p < q$. Since $T(w)$ is obtained from $T(w')$ by a k-shift, this shows that either $T(w) \prec T(w')$ (the '$-$' case of '$\mp$' above) or $T(w) \succ T(w')$ (the '$+$' case of '$\mp$' above)

Now if $\ell(w) > \ell(w')$ then $w'(\alpha_k) \in \Delta_{re}^{+}$. Theorem 3.3.1 then shows that $w'(\alpha_k) = -m\delta + \gamma$ with $m \leq 0$ and if $m = 0$ then $\gamma \in \Delta_0^{+}$. This latter case corresponds to the '$-$' case of '$\mp$' in the bulleted items above. Then $T(w) \prec T(w')$.

Similarly, if $\ell(w) < \ell(w')$ then $w'(\alpha_k) = -m\delta + \gamma \in \Delta_{re}^{-}$. with $m \geq 0$ and if $m = 0$ then $\gamma \in \Delta_0^{-}$. This latter case corresponds to the '$+$' case of '$\mp$' in the bulleted items above. Then $T(w) \succ T(w')$. $\square$

The depth $d(T)$ of a coloured diagram T is defined to be the signed sum of the depth charges in T with, as before, those to the left side of the vertical axis providing a negative contribution. This may be used to define a total order on the set of coloured diagrams. Let T and T' be coloured diagrams with corresponding generalised partitions λ and λ'. We first define $\lambda' > \lambda$ if there exists h such that $\lambda'_h > \lambda_h$ and $\lambda'_i = \lambda_i$ for $1 \leq i < h$. We then define $T' < T$ if either $d(T') < d(T)$, or both $d(T') = d(T)$ and $\lambda' > \lambda$. It is easily verified that this induces a total order on coloured diagrams.

Lemma 4.4.2 *Let $w, w' \in W$. If $T(w) = T(w')$ then $w = w'$.*

Proof: Let $w = s_{i_1} s_{i_2} \cdots s_{i_t}$. Then $T(1) < T(s_{i_1}) < T(s_{i_1} s_{i_2}) < \cdots < T(w)$ by Lemma 4.4.1. In particular, if $w \neq 1$ then $T(w) \neq T(1)$.

Since $T(w) = T(w')$, the recursive construction process implies that $T(wu) = T(w'u)$ for all $u \in W$. In particular, if $u = w^{-1}$, it follows that $T(1) = T(w'w^{-1})$ and therefore, by the previous paragraph, that $w'w^{-1} = 1$. Then $w' = w$ as required. $\square$

4.5 Proving the characterisation

To characterise the set $\{\lambda(w)|w \in W\}$, we use the structure of the grids. To this end, define:

$$\Delta = \begin{cases} -1 & \text{if } \mathbf{g} = B_\ell^{(1)}, D_\ell^{(1)}, A_{2\ell-1}^{(2)}; \\ 0 & \text{if } \mathbf{g} = D_{\ell+1}^{(2)}; \\ 1 & \text{if } \mathbf{g} = C_\ell^{(1)}, A_{2\ell}^{(2)}. \end{cases} \tag{4.15}$$

Lemma 4.5.1 *Let the generalised partition λ be superposed on the grid for a particular $\mathbf{g}$.*

Let $\mathbf{g} \in \{A_\ell^{(1)}, C_\ell^{(1)}, A_{2\ell}^{(2)}, D_{\ell+1}^{(2)}\}$. If the unreversed pair $\boxed{k{+}1}\boxed{k}$ straddles the profile of λ in the ith row then:

$$\lambda_i - i \equiv -(k+1) \ (\mathrm{mod}\, \tilde{h}^\vee), \tag{4.16}$$

and if the reversed pair $\boxed{k}\boxed{k{+}1}$ straddles the profile of λ in the ith row then:

$$\lambda_i - i \equiv k + \Delta \ (\mathrm{mod}\, \tilde{h}^\vee) \tag{4.17}$$

(in the $\mathbf{g} = A_\ell^{(1)}$ case, we identify 0-nodes with n-nodes).

For $\mathbf{g} = \{B_\ell^{(1)}, D_\ell^{(1)}, A_{2\ell-1}^{(2)}\}$, the same statement holds if for $k = 1$, the pair $\boxed{k{+}1}\boxed{k}$ is interpreted as either $\boxed{2}\boxed{1}$ or $\boxed{2}\boxed{0}$, and the pair $\boxed{k}\boxed{k{+}1}$ is interpreted as either $\boxed{1}\boxed{2}$ or $\boxed{0}\boxed{2}$; and if for $k = \ell - 2$ and $\mathbf{g} = D_\ell^{(1)}$, the pair $\boxed{k{+}1}\boxed{k}$ is interpreted as either $\boxed{\ell{-}1}\boxed{\ell{-}2}$ or $\boxed{\ell}\boxed{\ell{-}2}$, and the pair $\boxed{k}\boxed{k{+}1}$ is interpreted as either $\boxed{\ell{-}2}\boxed{\ell{-}1}$ or $\boxed{\ell{-}2}\boxed{\ell}$.

The above statement also holds for associated pairs, whether they are regarded as reversed or unreversed.

Proof: These results follow immediately from the structure of the grids given in Section 2.2. □

In what follows, we will use without comment, the extended interpretations of Lemma 4.5.1 that relate to the $\mathbf{g} = \{B_\ell^{(1)}, D_\ell^{(1)}, A_{2\ell-1}^{(2)}\}$ cases.

Theorem 4.5.2 *Let the generalised partition λ be edge-balanced, and if $\mathbf{g} = A_\ell^{(1)}$ then additionally $\sum_{i=1}^n \lambda_i = 0$. Then there exists a unique $w \in W$ such that $\lambda = \lambda(w)$.*

Proof: Let T be the coloured diagram obtained by superposing λ on the appropriate grid. Where there are unordered pairs, the order of each of those bisected by the profile of T is chosen so that T is even-handed, with augmented pairs added as appropriate (see Section 2.3). This defines T uniquely. Below, we seek $w \in W$ such that $T = T(w)$. The even-handed requirement above ensures that we don't fall foul of Corollary 4.2.4. If we can find $w \in W$ such that $T = T(w)$ then Lemma 4.4.2 shows w is unique. It would then follow that $\lambda = \lambda(w)$ for unique w.

If λ is the zero partition then $w = 1$ uniquely. So assume hereafter that λ is not zero. In the first part of this proof, we will construct a coloured diagram T' by emulating the action of s_k on T for a suitable k. We let λ' be the generalised partition corresponding to

T'. In each case, it will be verified that $T' < T$, where for the purpose of this proof, we define $T' < T$ if the list of the absolute values of the parts of λ' written in non-increasing order lexicographically precedes the corresponding list for λ.

Let $p = \max\{|\lambda_i|\}_{i=1}^n$, so that p is the largest absolute part in λ. We now examine the set of node-pairs that are bisected by the profile of λ in rows of length $\pm p$. We define the set $\mathcal{E}_U^+$ to comprise all r with $1 \le r \le n$ such that the unreversed pair $\boxed{r}\boxed{r{-}1}$ is bisected by the profile in a row of length $+p$, and the set $\mathcal{E}_R^-$ to comprise all r with $1 \le r \le n$ such that the reversed pair $\boxed{r{-}1}\boxed{r}$ is bisected by the profile in a row of length $-p$. Similarly, we define the set $\mathcal{E}_R^+$ to comprise all r with $0 \le r \le n-1$ such that the reversed pair $\boxed{r}\boxed{r{+}1}$ is bisected by the profile in a row of length $+p$, and the set $\mathcal{E}_U^-$ to comprise all r with $0 \le r \le n-1$ such that the unreversed pair $\boxed{r{+}1}\boxed{r}$ is bisected by the profile in a row of length $-p$.

In the case of $\mathbf{g} = A_\ell^{(1)}$, we use the above definitions after identifying an n-node with a 0-node. Note that at least one of the above four sets is non-empty, and if $\mathbf{g} = A_\ell^{(1)}$ then $\mathcal{E}_R^\pm = \emptyset$.

If $\mathbf{g} = B_\ell^{(1)}$, $C_\ell^{(1)}$, $A_{2\ell}^{(2)}$, $A_{2\ell-1}^{(2)}$ or $D_{\ell+1}^{(2)}$, and $\ell \in \mathcal{E}_R^- \cup \mathcal{E}_U^+$ then take $k = \ell$. If $\mathbf{g} = C_\ell^{(1)}$, $A_{2\ell}^{(2)}$ or $D_{\ell+1}^{(2)}$, and $0 \in \mathcal{E}_U^- \cup \mathcal{E}_R^+$ then take $k = 0$. In each of these cases, we form T' from T by a single k-shift. We then immediately see that $T' < T$ as required.

Otherwise, if $\mathbf{g} \ne A_\ell^{(1)}$, we select k such that $1 \le k \le \ell-1$ for which either $k \in \mathcal{E}_R^- \cup \mathcal{E}_U^+$ but $k+1 \notin \mathcal{E}_R^- \cup \mathcal{E}_U^+$, or $k \in \mathcal{E}_U^- \cup \mathcal{E}_R^+$ but $k-1 \notin \mathcal{E}_U^- \cup \mathcal{E}_R^+$. Such k exists because one of the four sets is non-empty, $\ell \notin \mathcal{E}_R^- \cup \mathcal{E}_U^+$, $0 \notin \mathcal{E}_U^- \cup \mathcal{E}_R^+$. For the $\mathbf{g} = A_\ell^{(1)}$ case, we select k such that $1 \le k \le n$ for which either $k \in \mathcal{E}_U^+$ but $k+1 \notin \mathcal{E}_U^+$, or $k \in \mathcal{E}_U^-$ but $k-1 \notin \mathcal{E}_U^-$. Such k exists because either $\mathcal{E}_U^-$ or $\mathcal{E}_U^+$ is non empty and $\sum_{i=1}^n \lambda_i = 0$ implies that $\mathcal{E}_U^- \ne \{1, 2, \dots, n\} \ne \mathcal{E}_U^+$.

We now obtain T' by performing a k-shift on T. To see that $T' < T$, let j be the row in which the profile bisects the identified pair. Then $|\lambda_j| = p$ and $|\lambda'_j| = p-1$. Since λ is edge-balanced, there exists h with $h \ne j$ such that the profile in the hth row is adjacent to a k-node. The choice of p implies that $|\lambda_h| \le p$. If $|\lambda_h| \le p-2$ then $|\lambda'_h| \le p-1$, whereupon we immediately have $T' < T$ as required. It remains to consider $|\lambda_h| \in \{p, p-1\}$.

To proceed, we consider separately the alternative ways of originally selecting k. For $k \in \mathcal{E}_R^- \cup \mathcal{E}_U^+$ and $k+1 \notin \mathcal{E}_R^- \cup \mathcal{E}_U^+$, the profile bisects the pairs $\boxed{k}\boxed{k{-}1}$ and $\boxed{k{+}1}\boxed{k}$ in rows j and h respectively, with either pair reversed or unreversed. We claim that if $\lambda_h \ge 0$ then the reversed pair $\boxed{k}\boxed{k{+}1}$ is bisected by the profile in the hth row, and if $\lambda_h \le 0$ then the unreversed pair $\boxed{k{+}1}\boxed{k}$ is bisected by the profile in the hth row. For $|\lambda_h| = p$, this claim follows immediately because $k+1 \notin \mathcal{E}_R^- \cup \mathcal{E}_U^+$. For $\lambda_h = p-1$, if the unreversed pair $\boxed{k{+}1}\boxed{k}$ is bisected by the profile in the hth row then (4.16) gives $h \equiv p+k \,(\mathrm{mod}\, \tilde{h}^\vee)$. For $\lambda_h = -(p-1)$, if the reversed pair $\boxed{k}\boxed{k{+}1}$ is bisected by the profile in the hth row then (4.17) gives $h \equiv -p-k-\Delta+1 \,(\mathrm{mod}\, \tilde{h}^\vee)$. Now if $k \in \mathcal{E}_U^+$ then (4.16) gives $j \equiv p+k \,(\mathrm{mod}\, \tilde{h}^\vee)$, and if $k \in \mathcal{E}_R^-$ then (4.17) gives $j \equiv -p-k-\Delta+1 \,(\mathrm{mod}\, \tilde{h}^\vee)$. Comparing these results for j and h shows that either $j \equiv h \,(\mathrm{mod}\, \tilde{h}^\vee)$ or $j+h+\Delta-1 \equiv 0 \,(\mathrm{mod}\, \tilde{h}^\vee)$. However, since $1 \le j, h \le n$ with $j \ne k$, and using the values of $\tilde{h}^\vee$ given in (2.4), we see that neither of these can hold. Thus the above claim is established. We now immediately see that $|\lambda'_h| = |\lambda_h| - 1$, implying $T' < T$ as required.

For $k \in \mathcal{E}_U^- \cup \mathcal{E}_R^+$ and $k-1 \notin \mathcal{E}_U^- \cup \mathcal{E}_R^+$, the profile bisects the pairs $\boxed{k{+}1}\boxed{\;k\;}$ and $\boxed{\;k\;}\boxed{k{-}1}$ in rows j and h respectively, with either pair reversed or unreversed. The proof then proceeds in a similar manner to the previous case.

Having obtained $T^{(1)} = T'$ from T as above, we iterate this process to produce $T^{(2)}$, $T^{(3)}$ etc.. If the corresponding partitions are denoted $\lambda^{(1)} = \lambda$, $\lambda^{(2)}$, $\lambda^{(3)}$, etc., then $\lambda^{(1)} > \lambda^{(2)} > \lambda^{(3)} > \cdots$. The nature of the ordering, together with the fact that it is bounded below by the trivial partition, implies that the process must halt after a finite number of steps, say N, having produced the trivial coloured diagram $T^{(N)} = T(1)$.

The above iteration produces a value k at each step. Moreover, if there exists w' such that $T' = T(w')$ then comparison of the above construction with that of Section 2.4 ensures that $T = T(w's_k)$. Thus, if the sequence of ks produced by the above iteration is $k_1, k_2, \ldots, k_N$, then $T = T(w)$ where $w = s_{k_N} s_{k_{N-1}} \cdots s_2 s_1$. □

5 Coloured diagrams for coset representatives

5.1 Minimal coset representatives

With W_s defined by (2.9), a mirror image of [7, Prop. 1.10(c)] proves:

Lemma 5.1.1 *For each $w \in W$, there exists a unique $u \in W_s$ and a unique $v \in \overline{W}$ such that $w = vu$. Moreover, $\ell(w) = \ell(v) + \ell(u)$.*

This result implies that W_s is a set of right coset representatives of W with respect to $\overline{W}$. It also implies that if $u \in W_s$, then u is the unique element of smallest length in the coset $\overline{W}u$.

The following result is a minor extension of [13, Lemma 4.3].

Lemma 5.1.2 *Let $w' \in W_s$ and $w = w's_k$. If $\ell(w) = \ell(w') - 1$ then $w \in W_s$. If $\ell(w) = \ell(w') + 1$ then $w \in W_s$ if and only if $w'(\alpha_k) \notin \Delta_0^+$. Moreover, if $w \notin W_s$ then there exists $j \in \overline{I}$ such that $w'(\alpha_k) = \alpha_j$ and $w = s_j w'$.*

Proof: First consider $\ell(w) = \ell(w') - 1$. For all $i \in \overline{I}$, we have $\ell(s_i w') > \ell(w') > \ell(w's_k)$. Since $\ell(s_i w' s_k) = \ell(s_i w') \pm 1$, it follows that $\ell(s_i w' s_k) > \ell(w' s_k)$. Thus, by definition, $w's_k \in W_s$.

Now consider $\ell(w) = \ell(w') + 1$ and let $\beta = w'(\alpha_k)$. Note then that $\beta \in \Delta_{re}^+$. Assume that $w \in W_s$, and let $v \in \overline{W}$. By Lemma 5.1.1, $\ell(vw) = \ell(v) + \ell(w)$ and $\ell(vw') = \ell(v) + \ell(w')$. Therefore, $\ell(vw's_k) = \ell(vw') + 1$. It follows that $vw'(\alpha_k) \in \Delta_{re}^+$ so that $v(\beta) \in \Delta_{re}^+$. Now if $\beta \in \Delta_0^+$, then on setting $v = s_\beta \in \overline{W}$, we obtain $v(\beta) \in \Delta_0^-$, so that $v(\beta) \notin \Delta_{re}^+$. Therefore, necessarily $\beta \notin \Delta_0^+$.

Now assume that $w \notin W_s$. By Lemma 5.1.1, there exists $u \in W_s$ and $v \in \overline{W}$ such that $w = vu$ with $\ell(w) = \ell(v) + \ell(u)$, from which follows $\ell(w') - \ell(v) = \ell(u) - 1$. Now

$w's_k = w = vu$ implies that $v^{-1}w' = us_k$. Since $v^{-1} \in \overline{W}$ and $\ell(v^{-1}) = \ell(v)$, we obtain $\ell(w') + \ell(v) = \ell(u) \pm 1$. Together with the above expression, this implies that $\ell(v) \in \{0, 1\}$, and thus since $v \neq 1$, we have $v = s_j$ for some $j \in \overline{I}$. We also obtain $u = s_j w' s_k$ with $\ell(u) = \ell(w')$. Then $\ell(s_j w') > \ell(w') = \ell(s_j w' s_k)$, which implies that $s_j(\beta) = s_j w'(\alpha_k) \in \Delta_{re}^-$. Since $\beta \in \Delta_{re}^+$ and α_j is the only root which changes sign under the action of s_j, it follows that $\beta = \alpha_j \in \Delta_0^+$ as required. Also $w' s_{\alpha_k} w'^{-1} = s_{w'(\alpha_k)} = s_{\alpha_j}$, which gives $w's_k = s_j w'$. The lemma then follows. □

Lemma 5.1.3 *Let $w' \in W_s$, $w = w's_k$ and $\ell(w) = \ell(w') + 1$. Set $\mu = w(\rho) - \rho$ and $\nu = w'(\rho) - \rho$. If $w \notin W_s$ then $\mu - \nu \in \Delta_0^-$. If $w \in W_s$ then $\mu - \nu = -m\delta + \gamma$ with $m > 0$ and $\gamma \in \Delta_0^+ \cup \Delta_1^+$.*

Proof: $\mu - \nu = w(\rho) - w'(\rho) = w'(s_k(\rho) - \rho) = -w'(\alpha_k)$.

In the case that $w \notin W_s$, Lemma 5.1.2 implies that $w'(\alpha_k) \in \Delta_0^+$ whereupon $\mu - \nu \in \Delta_0^-$ as required. (Lemma 5.1.2 also implies that $\mu - \nu = -\alpha_j$ for some $j \in \overline{I}$.)

Now consider $w \in W_s$. Since $\ell(w) = \ell(w') + 1$, we have $w'(\alpha_k) \in \Delta_{re}^+$. Lemma 5.1.2 implies that $w'(\alpha_k) \notin \Delta_0^+$, whereupon Theorem 3.3.1 implies that $w'(\alpha_k) = m\delta - \gamma$ with $m > 0$ and $\gamma \in \Delta_0 \cup \Delta_1$. Writing $w'^{-1}(\gamma) = m\delta - \alpha_k$ and noting that $m > 0$, Theorem 3.3.1 shows that $w'^{-1}(\gamma) \in \Delta_{re}^+$. Since $\gamma \in \Delta_0 \cup \Delta_1$, we have $\gamma = \sum_{i=1}^{\ell} r_i \alpha_i$ for $r_i \in \mathbb{Z}$ with either all r_i non-negative, or all r_i non-positive. But the definition (2.9) implies that $\ell(s_i w') > \ell(w')$ for $i \in \overline{I}$, whereupon $\ell(w'^{-1}) > \ell(w')$ and therefore $w'^{-1}(\alpha_i) \in \Delta_{re}^+$. If follows that the r_i are all non-negative and therefore $\gamma \in \Delta_0^+ \cup \Delta_1^+$. □

Corollary 5.1.4 *Let $t \geq 0$, $w' \in W_s^{(t)}$, $k \in I$, and set $w = w's_k$. Then:*

$$\sum_{i=1}^{n} (\lambda(w)_i - \lambda(w')_i)\epsilon_i \in \begin{cases} \Delta_0^+ \cup \Delta_1^+ & \text{if } w \in W_s^{(t+1)}; \\ \Delta_0^- \cup \Delta_1^- & \text{if } w \notin W_s^{(t+1)}. \end{cases} \tag{5.1}$$

Proof: Let $\mu = w(\rho) - \rho$, $\nu = w'(\rho) - \rho$ and $\mu - \nu = -m\delta + \gamma$ for some $m \in \mathbb{Z}$ and $\gamma \in \mathbf{h}_0^*$. Then (4.2) gives:

$$\sum_{i=1}^{n} (\lambda(w)_i - \lambda(w')_i)\epsilon_i = \overline{\mu - \nu} = \gamma.$$

For $w \in W_s^{(t+1)}$, Lemma 5.1.3 shows that $\gamma \in \Delta_0^+ \cup \Delta_1^+$.

Now consider $w \notin W_s^{(t+1)}$. If $\ell(w) = \ell(w') + 1$ then Lemma 5.1.3 shows that $\gamma \in \Delta_0^-$. On the other hand, if $\ell(w) = \ell(w') - 1$ then Lemma 5.1.2 shows that $w \in W_s^{(t-1)}$. Interchanging the roles of w and w' in the preceding paragraph then shows that $-\gamma = \overline{\nu - \mu} \in \Delta_0^+ \cup \Delta_1^+$, and thus $\gamma \in \Delta_0^- \cup \Delta_1^-$. The corollary then follows. □

Corollary 5.1.5 *Let $t \geq 0$, $w' \in W_s^{(t)}$, $k \in I$, and set $w = w's_k$. Then $w \in W_s^{(t+1)}$ if and only if $T(w) \succ T(w')$. Moreover, we obtain the full set $W_s^{(t+1)}$ by selecting all $w's_k$ with $w' \in W_s^{(t)}$ and $k \in I$, for which $T(w's_k) \succ T(w')$.*

Proof: Set $\gamma = \sum_{i=1}^{n}(\lambda(w)_i - \lambda(w')_i)\epsilon_i$. If $w \in W_s^{(t+1)}$ then $\gamma \in \Delta_0^+ \cup \Delta_1^+$ by Corollary 5.1.4. Theorem 3.3.1 then shows that either $\gamma = \epsilon_i - \epsilon_j$ with $i < j$, $\gamma = \epsilon_i + \epsilon_j$, $\gamma = \epsilon_i$ or $\gamma = 2\epsilon_i$, where $1 \le i, j \le n$ in each case. This shows that $T(w) \succ T(w')$. On the other hand, if $w \notin W_s^{(t+1)}$ then a similar line of reasoning shows that $T(w) \prec T(w')$.

The second part follows because if $w \in W_s^{(t+1)}$ then there exists k and w' with $\ell(w') = t$, such that $w = w's_k$. Lemma 5.1.2 then implies that $w' \in W_s^{(t)}$. □

This result enables W_s to be constructed recursively by length as described in Section 2.9.

5.2 The shape of things to come

Lemma 5.2.1 *If $w \in W$ and $\lambda \in P^+$ then $w \in W_s$ if and only if $\overline{w(\lambda+\rho)-\rho} \in \overline{P}^+$.*

Proof: Let $w \in W$, $\lambda \in P^+$ and for $i \in \overline{I}$ set $m_i = (w(\lambda+\rho) - \rho|\alpha_i^\vee)$ so that $\overline{w(\lambda+\rho)-\rho} = \sum_{i\in\overline{I}} m_i\overline{\Lambda}_i$. Note that $m_i \in \mathbb{Z}$. We now calculate:

$$\begin{aligned} m_i &= (w(\lambda+\rho) - \rho|\alpha_i^\vee) \\ &= (w(\lambda+\rho)|\alpha_i^\vee) - 1 \\ &= (2/(\alpha_i|\alpha_i))(\lambda+\rho|w^{-1}(\alpha_i)) - 1 \\ &= (2/(\alpha_i|\alpha_i))\sum_{j\in I} r_j(\lambda+\rho|\alpha_j) - 1 \end{aligned}$$

where the $r_j \in \mathbb{Z}$ are defined by $w^{-1}(\alpha_i) = \sum_{j\in I} r_j\alpha_j$. Since $\lambda \in P^+$, we have $2(\lambda+\rho|\alpha_j)/(\alpha_j|\alpha_j) \ge 1$ for all $j \in I$.

If $w \in W_s$, the definition (2.9) implies that $\ell(w^{-1}s_i) > \ell(w^{-1})$ whereupon $w^{-1}(\alpha_i) \in \Delta_{re}^+$. Thus $r_j \in \mathbb{Z}_{\ge 0}$ for each $j \in I$ and $r_k > 0$ for at least one $k \in I$. Thereupon, $m_i > -1$. Since $m_i \in \mathbb{Z}$, it now follows that $m_i \ge 0$ for all $i \in \overline{I}$ so that $\overline{w(\lambda+\rho)-\rho} \in \overline{P}^+$.

On the other hand, if $w \notin W_s$, the definition (2.9) implies that there exists at least one $i \in \overline{I}$ such that $\ell(w^{-1}s_i) < \ell(w^{-1})$ whereupon $w^{-1}(\alpha_i) \in \Delta_{re}^-$. Then $r_j \in \mathbb{Z}_{\le 0}$ for each $j \in I$ and $r_k < 0$ for at least one $k \in I$. It now follows that $m_i < -1$ and therefore $\overline{w(\lambda+\rho)-\rho} \notin \overline{P}^+$. □

Corollary 5.2.2 *Let $w \in W$ and $\lambda = \lambda(w)$. Then $w \in W_s$ if and only if*

$$\lambda(w)_1 \ge \lambda(w)_2 \ge \cdots \ge \lambda(w)_n,$$

and

- $\sum_{i=1}^{n}\lambda(w)_i = 0$ *if* $\mathbf{g} = A_\ell^{(1)}$;
- $\lambda(w)_\ell \ge 0$ *if* $\mathbf{g} = B_\ell^{(1)}, C_\ell^{(1)}, A_{2\ell}^{(2)}, A_{2\ell-1}^{(2)}$ *or* $D_{\ell+1}^{(2)}$;
- $\lambda(w)_{\ell-1} \ge |\lambda_\ell|$ *if* $\mathbf{g} = D_\ell^{(1)}$.

Proof: Applying Lemma 5.2.1 to the left side of (4.2) shows that $w \in W_s$ if and only if $\sum_{i=1}^n \lambda(w)_i \epsilon_i \in \overline{P}^+$. The required result then follows from Lemma 3.7.2, after noting that each $\lambda(w)_i \in \mathbb{Z}$. □

This result implies that if $w \in W_s$ then $\lambda(w)$ is a genuine partition in the cases for which $\mathbf{g} = B_\ell^{(1)}, C_\ell^{(1)}, A_{2\ell}^{(2)}, A_{2\ell-1}^{(2)}$ or $D_{\ell+1}^{(2)}$. For the $\mathbf{g} = D_\ell^{(1)}$ case, it also implies that $(\lambda(w)_1, \lambda(w)_2, \ldots, \lambda(w)_{\ell-1}, |\lambda(w)_\ell|)$ is a genuine partition, and for the $\mathbf{g} = A_\ell^{(1)}$ case, it implies that $\lambda(w) = (\mu; \nu)$ for two genuine partitions μ and ν with $|\mu| = |\nu|$.

5.3 Core characterisation

In this section, we prove the characterisation of $\{\lambda(w) | w \in W_s\}$ stated in Section 2.10.

The following result, which is obtained by repeated application of [10, Lemma 2.7.13], will be pivotal in the proofs below.

Lemma 5.3.1 *Let $\lambda = (\lambda_1, \lambda_2, \ldots, \lambda_\ell)$ be a partition, $\eta = (\ell-1, \ell-2, \ldots, 0)$ and let $m > 0$.*

Let $\{r_j\}_{j=1}^\ell$ be non-negative integers such that if we define $\beta_j = \lambda_j + \eta_j - r_j m$ then $\{\beta_j\}_{j=1}^\ell$ are non-negative and distinct. If $\zeta = (\zeta_1, \zeta_2, \ldots, \zeta_\ell)$ is the partition defined by $\zeta_j = \beta_{\pi(j)} - \eta_j$ where $\pi \in \mathfrak{S}_\ell$ is such that $\beta_{\pi(1)} > \beta_{\pi(2)} > \cdots > \beta_{\pi(\ell)}$, then ζ may be obtained from λ by removing certain rim m-hooks.

Conversely, if ζ is obtained from λ by removing certain rim m-hooks, then there exist $\{r_j\}_{j=1}^\ell$ and $\pi \in \mathfrak{S}_\ell$ such that $\zeta_{\pi(j)} + \eta_{\pi(j)} = \lambda_j + \eta_j - r_j m$ for $1 \le j \le \ell$.

We will also make use of the following result which may be found in [19, p3]. Here, and below, ζ' denotes the conjugate of the partition ζ.

Lemma 5.3.2 *Let ζ be a partition and let $q \ge \zeta_1$, $p \ge \zeta_1'$. Then the $p+q$ numbers*

$$\zeta_i + p - i \quad (1 \le i \le p), \qquad p - 1 + j - \zeta_j' \quad (1 \le j \le q)$$

are a permutation of $\{0, 1, 2, \ldots, p+q-1\}$.

Theorem 5.3.3 *For $w \in W_s$, let $\lambda(w) = (\lambda_1, \lambda_2, \ldots, \lambda_\ell)$. If $\mathbf{g} = B_\ell^{(1)}$, $C_\ell^{(1)}$, $A_{2\ell}^{(2)}$, $A_{2\ell-1}^{(2)}$ or $D_{\ell+1}^{(2)}$, then $\lambda(w)$ is a partition whose $\tilde{h}^\vee$-core ζ satisfies:*

$$\begin{array}{ll} \zeta \in \mathcal{A} & \textit{if } \mathbf{g} = B_\ell^{(1)}, A_{2\ell-1}^{(2)}; \\ \zeta \in \mathcal{C} & \textit{if } \mathbf{g} = C_\ell^{(1)}, A_{2\ell}^{(2)}; \\ \zeta \in \mathcal{E} & \textit{if } \mathbf{g} = D_{\ell+1}^{(2)}, \end{array} \tag{5.2}$$

with $l(\zeta) \le \ell$. If $\mathbf{g} = D_\ell^{(1)}$ then $(\lambda_1, \lambda_2, \ldots, \lambda_{\ell-1}, |\lambda_\ell|)$ is a partition whose $\tilde{h}^\vee$-core ζ satisfies $\zeta \in \mathcal{A}$ and $l(\zeta) < \ell$.

On the other hand, if $\mathbf{g} = B_\ell^{(1)}$, $C_\ell^{(1)}$, $A_{2\ell}^{(2)}$, $A_{2\ell-1}^{(2)}$ or $D_{\ell+1}^{(2)}$, and $\lambda = (\lambda_1, \ldots, \lambda_\ell)$ is a partition whose $\tilde{h}^\vee$-core ζ satisfies (5.2) then there exists a unique $w \in W$ such that $\lambda = \lambda(w)$: moreover $w \in W_s$. If $\mathbf{g} = D_\ell^{(1)}$, and $\lambda = (\lambda_1, \lambda_2, \ldots, \lambda_{\ell-1}, \lambda_\ell)$ is a generalised partition for which $(\lambda_1, \lambda_2, \ldots, \lambda_{\ell-1}, |\lambda_\ell|)$ is a partition whose $\tilde{h}^\vee$-core ζ satisfies $\zeta \in \mathcal{A}$ and $l(\zeta) < \ell$, then there exists a unique $w \in W$ such that $\lambda = \lambda(w)$: moreover $w \in W_s$.

Proof: For $\mathbf{g} = B_\ell^{(1)}$, $C_\ell^{(1)}$, $D_\ell^{(1)}$, $A_{2\ell}^{(2)}$, $A_{2\ell-1}^{(2)}$ or $D_{\ell+1}^{(2)}$, let $w \in W_s$, $\lambda(w) = (\lambda_1, \lambda_2, \ldots, \lambda_\ell)$ and $\hat{\lambda} = (\lambda_1, \lambda_2, \ldots, |\lambda_\ell|)$. Corollary 5.2.2 shows that $\hat{\lambda}$ is a genuine partition in each case, and if $\mathbf{g} \neq D_\ell^{(1)}$ then $\hat{\lambda} = \lambda(w)$.

Corollary 4.2.2 states that λ is edge-balanced. Therefore, using the extended interpretations described in Lemma 4.5.1, each pair $\boxed{k{+}1 \mid k}$ for which $0 \leq k < \ell$, straddles the profile of λ, either reversed or unreversed. If the pair $\boxed{k{+}1 \mid k}$ straddles the profile in row i then in the unreversed case, (4.16) shows that $\lambda_i - i \equiv -(k+1) \,(\mathrm{mod}\, \tilde{h}^\vee)$, and in the reversed case, (4.17) shows that $\lambda_i - i \equiv k + \Delta \,(\mathrm{mod}\, \tilde{h}^\vee)$.

It is only in the case for which $\mathbf{g} = D_\ell^{(1)}$ that we can have $\hat{\lambda} \neq \lambda$. Here, however, the symmetry of the ℓth row of the $D_\ell^{(1)}$ grid about the vertical axis then guarantees that $\hat{\lambda}$ is edge-balanced.

Now let $\mathcal{S} = \{k_1 > k_2 > \cdots > k_t\}$ be such that $k \in \mathcal{S}$ if and only if the reversed pair $\boxed{k \mid k{+}1}$ straddles the profile of $\hat{\lambda}$ and k and $k+1$ are not associated values. Thus $k_1 < \ell - 1$ when $\mathbf{g} = D_\ell^{(1)}$ and $k_t > 0$ when $\Delta = -1$ (i.e. when $\mathbf{g} = \{B_\ell^{(1)}, D_\ell^{(1)}, A_{2\ell-1}^{(2)}\}$) Let $\overline{\mathcal{S}} = \{0, 1, \ldots, l-1\} \backslash \mathcal{S}$ with $\overline{\mathcal{S}} = \{k_1' > k_2' > \cdots > k_{\ell-t}'\}$. Then if $k \in \overline{\mathcal{S}}$, either the unreversed pair $\boxed{k{+}1 \mid k}$ straddles the profile, or k and $k+1$ are associated values.

We will now apply Lemma 5.3.1 to remove $\tilde{h}^\vee$-rim hooks from the partition $\hat{\lambda}$. So define $\beta_i = (\hat{\lambda}_i + \eta_i) \,\mathrm{mod}\, \tilde{h}^\vee$ for $1 \leq i \leq \ell$, where $\eta_i = \ell - i$. Now, for $1 \leq i \leq \ell$, let k be such that the pair $\boxed{k{+}1 \mid k}$, either reversed, unreversed or associated, is bisected by the edge in the ith row of $\hat{\lambda}$. If $k \in \overline{\mathcal{S}}$, it is unreversed or associated, so that $\beta_i = (\hat{\lambda}_i + \ell - i) \,\mathrm{mod}\, \tilde{h}^\vee = \ell - (k+1)$. If $k \in \mathcal{S}$, it is reversed, so that $\beta_i = (\hat{\lambda}_i + \ell - i) \,\mathrm{mod}\, \tilde{h}^\vee = \ell + \Delta + k$. Note that $0 \leq \beta_i < \tilde{h}^\vee$ for $1 \leq i \leq \ell$ and that the values $\beta_1, \beta_2, \ldots, \beta_\ell$ are distinct. Thus on defining $\zeta_i = \beta_{\pi(i)} - \eta_i$, with $\pi \in \mathfrak{S}_\ell$ such that $\beta_{\pi(1)} > \beta_{\pi(2)} > \cdots > \beta_{\pi(\ell)}$, we obtain:

$$\zeta_i - i = \begin{cases} k_i + \Delta + \ell - (\ell - i) - i = k_i + \Delta & \text{if } 1 \leq i \leq t; \\ \ell - (k_{\ell+1-i}' + 1) - (\ell - i) - i = -1 - k_{\ell+1-i}' & \text{if } t < i \leq \ell. \end{cases} \tag{5.3}$$

Lemma 5.3.1 shows that the partition ζ can be obtained from $\hat{\lambda}$ by the removal of rim $\tilde{h}^\vee$-hooks. The partition ζ has Frobenius rank t because $\zeta_t - t = \Delta + k_t \geq 0$ (noting that $k_t > 0$ whenever $\Delta = -1$) and $\zeta_{t+1} - (t+1) = -1 - k_{\ell-t}' < 0$. To determine the Frobenius representation of ζ, we now apply Lemma 5.3.2 with $p = \ell$ and $q = \ell + \Delta$. Note that if $j \geq \ell$ then $l - 1 + i - \zeta_i' = j$ implies that $\zeta_i' - i < 0$. Since we require only those ζ_i' for which $\zeta_i' - i \geq 0$, we consider just the numbers $0, 1, \ldots, \ell - 1$ in Lemma 5.3.2, and find that:

$$\begin{aligned} \{\ell - 1 + i - \zeta_i' | 1 \leq i \leq t\} &= \{0, 1, \ldots, \ell - 1\} \backslash \{\ell - 1 - k' | k' \in \overline{\mathcal{S}}\} \\ &= \{\ell - 1 - k | k \in \mathcal{S}\}. \end{aligned}$$

This implies that $\zeta_i' - i = k_i$ for $1 \leq i \leq t$. Therefore the partition ζ has Frobenius representation:

$$\begin{pmatrix} k_1 + \Delta & k_2 + \Delta & k_3 + \Delta & \cdots & k_t + \Delta \\ k_1 & k_2 & k_3 & \cdots & k_t \end{pmatrix}. \tag{5.4}$$

From this, its membership of the required set is immediate.

Furthermore, because $\zeta_1 + \zeta_1' + 1 = 2k_1 + \Delta + 1 < \tilde{h}^\vee$ (noting that $k_1 < \ell - 1$ when $\mathbf{g} = D_\ell^{(1)}$), it follows that ζ is a $\tilde{h}^\vee$-core, thereby proving the first part of the Theorem.

For the second part, assume that $\hat{\lambda}$ is a partition for which the $\tilde{h}^\vee$-core ζ lies in the particular specified set. So, in Frobenius notation, ζ takes the form (5.4), with $0 \le t \le \ell$ and $\ell > k_1 > k_2 > \cdots > k_t \ge 0$, and additionally $k_1 < \ell - 1$ if $\mathbf{g} = D_\ell^{(1)}$, and $k_t > 0$ if $\Delta = -1$. Let $\mathcal{S} = \{k_1, k_2, \ldots, k_t\}$ and let $\overline{\mathcal{S}} = \{0, 1, \ldots, l-1\} \backslash \mathcal{S}$ with $\overline{\mathcal{S}} = \{k_1' > k_2' > \cdots > k_{\ell-t}'\}$. For $1 \le i \le \ell$, we then obtain ζ_i using (5.3). Lemma 5.3.1 states that there exist integers $\{r_i\}_{i=1}^{\ell}$ and $\pi \in \mathfrak{S}_\ell$ for which $\hat{\lambda}_i + \eta_i = \zeta_{\pi(i)} + \eta_{\pi(i)} + r_i \tilde{h}^\vee$ for $1 \le i \le \ell$. Thereupon, $\hat{\lambda}_i - i \equiv \zeta_{\pi(i)} - \pi(i) \pmod{\tilde{h}^\vee}$ for $1 \le i \le \ell$, whereby on using (5.3),

$$\hat{\lambda}_i - i \equiv \begin{cases} k_{\pi(i)} + \Delta & \text{if } \pi(i) \le t; \\ -1 - k'_{\ell+1-\pi(i)} & \text{if } \pi(i) > t, \end{cases}$$

where the congruences are taken modulo $\tilde{h}^\vee$. Lemma 4.5.1 then shows that the profile of $\hat{\lambda}$ bisects the unreversed or associated pairs $\boxed{k{+}1 \,|\, k}$ when $k \in \overline{\mathcal{S}}$ and bisects the reversed pairs $\boxed{k \,|\, k{+}1}$ when $k \in \mathcal{S}$. It follows that $\hat{\lambda}$ is edge-balanced. Theorem 4.5.2 then implies that $\hat{\lambda} = \lambda(w)$ for a unique $w \in W$. Corollary 5.2.2 shows that $w \in W_s$. In the case in which $\mathbf{g} = D_\ell^{(1)}$ and $\hat{\lambda}_\ell > 0$, the symmetry of the ℓth row of the grid about the vertical axis implies that the generalised partition $\lambda = (\hat{\lambda}_1, \hat{\lambda}_2, \ldots, \hat{\lambda}_{\ell-1}, -\hat{\lambda}_\ell)$ is also edge-balanced. So in this case also, Theorem 4.5.2 implies that $\lambda = \lambda(w)$ for a unique $w \in W$, and Corollary 5.2.2 shows that $w \in W_s$. $\square$

Theorem 5.3.4 *Let* $\mathbf{g} = A_{n-1}^{(1)}$.

For $w \in W_s$, *let the partitions* μ *and* ν *be such that* $(\mu;\nu) = \lambda(w)$. *If* ζ *is the* n*-core of* μ, *then* ζ' *is the* n*-core of* ν. *In addition,* $|\mu| = |\nu|$.

Conversely, let $\zeta \in \mathcal{F}$ *and let partitions* μ *and* ν *be such that* $|\mu| = |\nu|$, $\ell(\mu) + \ell(\nu) \le n$, ζ *is the* n*-core of* μ, *and* ζ' *is the* n*-core of* ν. *Then there exists a unique* $w \in W$ *such that* $\lambda(w) = (\mu;\nu)$*: moreover* $w \in W_s$.

Proof: Let $p = \ell(\mu)$, $q = \ell(\nu)$ and $\lambda = (\mu;\nu)$ $(= \lambda(w))$. Then $\mu_i = \lambda_i$ for $1 \le i \le p$, $\nu_i = -\lambda_{n+1-i}$ for $1 \le i \le q$ and $\lambda_i = 0$ for $p < i \le n-q$. Since $\sum_{i=0}^n \lambda_i = 0$ by Corollary 5.2.2, it follows immediately that $|\mu| = |\nu|$.

Let $0 \le k < n$. If the pair $\boxed{k{+}1 \,|\, k}$ is bisected by the profile in the ith row of λ, then (4.16) shows that $\lambda_i - i \equiv -(k+1) \pmod{n}$. Here and below, we identify $\boxed{n \,|\, n{-}1}$ with $\boxed{0 \,|\, n{-}1}$.

Let $\mathcal{S}_+ = \{k_1^+ > k_2^+ > \cdots > k_p^+\}$ be such that if $k \in \mathcal{S}_+$ then the pair $\boxed{k{+}1 \,|\, k}$ is bisected by the profile of λ in one of the uppermost p rows. Similarly, let $\mathcal{S}_- = \{k_1^- < k_2^- < \cdots < k_q^-\}$ be such that if $k \in \mathcal{S}_-$ then the pair $\boxed{k{+}1 \,|\, k}$ is bisected by the profile of λ in one of the lowermost q rows. Note that $\lambda_{k+1} = 0$ for $p \le k < n-q$. Thus, for these values of k, the pair $\boxed{k{+}1 \,|\, k}$ is bisected by the profile in the $(k+1)$th row. Corollary 4.2.2 shows that λ is edge-balanced, whereupon these values do not occur in $\mathcal{S}_+$ or $\mathcal{S}_-$. Moreover, we also have $\mathcal{S}_+ \cap \mathcal{S}_- = \emptyset$ and $\mathcal{S}_+ \cup \mathcal{S}_- = \{0, \ldots, p-1\} \cup \{n-q, \ldots, n-1\}$. Set $t = \#\{k | k \in \mathcal{S}_+, k \ge p\}$. Note that then $\#\{k | k \in \mathcal{S}_-, k < n-q\} = t$.

We will now apply Lemma 5.3.1 to remove n-rim hooks from the partition $\mu = (\mu_1, \ldots, \mu_p)$. For $1 \le i \le p$, let $k \in \mathcal{S}_+$ be such that the pair $\boxed{k{+}1 \mid k}$ is bisected by the profile in the ith row of λ, and set $\beta_i = (\mu_i + p - i) \bmod n = (\lambda_i - i + p) \bmod n = (p - k - 1) \bmod n$. Thereupon,

$$\beta_i = \begin{cases} p - (k+1) & \text{if } k < p; \\ n + p - (k+1) & \text{if } k \ge p. \end{cases}$$

Note that the values $\beta_1, \beta_2, \ldots, \beta_p$ are distinct. With $\pi \in \mathfrak{S}_p$ such that $\beta_{\pi(1)} > \beta_{\pi(2)} > \cdots > \beta_{\pi(p)}$, and $\zeta_i = \beta_{\pi(i)} - p + i$ for $1 \le i \le p$, we obtain:

$$\zeta_i - i = \begin{cases} n - (k^+_{t+1-i} + 1) & \text{if } 1 \le i \le t; \\ -(k^+_{p+t+1-i} + 1) & \text{if } t < i \le p. \end{cases} \tag{5.5}$$

Since $\zeta_t - t \ge 0$ and $\zeta_{t+1} - (t+1) < 0$, the partition ζ has Frobenius rank t. Now note that (5.5) implies that $\{\zeta_i + p - i | 1 \le i \le p\} = \{n + p - 1 - k^+_K | 1 \le K \le t\} \cup \{p - 1 - k^+_K | t < K \le p\}$. Lemma 5.3.2 now gives $\{p - 1 + j - \zeta'_i | 1 \le j \le q\} = \{n + p - 1 - k^-_K | t < K \le q\} \cup \{p - 1 - k^-_K | 1 \le K \le t\}$. This yields:

$$\zeta'_j - j = \begin{cases} k^-_{t+1-j} & \text{if } 1 \le j \le t; \\ k^-_{q+t+1-j} - n & \text{if } t < j \le q. \end{cases} \tag{5.6}$$

In particular, we have found that ζ has Frobenius representation:

$$\begin{pmatrix} n-1-k^+_t & n-1-k^+_{t-1} & \cdots & n-1-k^+_2 & n-1-k^+_1 \\ k^-_t & k^-_{t-1} & \cdots & k^-_2 & k^-_1 \end{pmatrix}. \tag{5.7}$$

Since $k^+_t \ge n - q$ and $k^-_t \le p - 1$, we have $\zeta_1 + \zeta'_1 - 1 = n - k^+_t + k^-_t \le q + p - 1 < n$, which implies that ζ is an n-core. By Lemma 5.3.1, it is obtained from μ by removing n-rim hooks, and is therefore the n-core of μ.

We now apply a similar procedure to the partition ν. For $1 \le i \le q$, let $k \in \mathcal{S}_-$ be such that the pair $\boxed{k{+}1 \mid k}$ is bisected by the profile in the $(n-1-i)$th row of λ, and set $\overline{\beta}_i = (\nu_i + q - i) \bmod n = (-\lambda_{n+1-i} - i + q) \bmod n = (q + k) \bmod n$. Thereupon,

$$\overline{\beta}_i = \begin{cases} q + k & \text{if } k < n - q; \\ q + k - n & \text{if } k \ge n - q. \end{cases}$$

Note that the values $\overline{\beta}_1, \overline{\beta}_2, \ldots, \overline{\beta}_q$ are distinct. With $\sigma \in \mathfrak{S}_q$ such that $\overline{\beta}_{\sigma(1)} > \overline{\beta}_{\sigma(2)} > \cdots > \overline{\beta}_{\sigma(q)}$, and $\overline{\zeta}_i = \overline{\beta}_{\sigma(i)} - q + i$ for $1 \le i \le q$, we obtain $\overline{\zeta}_i - i = k^-_{t+1-i}$ for $1 \le i \le t$, and $\overline{\zeta}_i - i = k^-_{q+t+1-i} - n$ for $t < i \le q$. Lemma 5.3.1 shows that the partition $\overline{\zeta} = (\overline{\zeta}_1, \overline{\zeta}_2, \ldots, \overline{\zeta}_q)$ is obtained by removing n-rim hooks from ν. On comparing the above values of $\overline{\zeta}_i - i$ with the values of $\zeta'_i - i$ given by (5.6), we see that $\overline{\zeta} = \zeta'$. The first part of the theorem then follows.

For the second part, let μ, ν and ζ be as stated, and let $p = \ell(\mu)$ and $q = \ell(\nu)$, so that $p + q \le n$. Then if we set $\lambda_i = \mu_i$ for $1 \le i \le p$, $\lambda_i = -\nu_{n+1-i}$ for $n - q < i \le n$ and $\lambda_i = 0$ for $p < i \le n - q$, we have $\lambda = (\mu; \nu)$. Note that $\sum_{i=0}^n \lambda_i = 0$.

The Frobenius representation of ζ takes the form (5.7) where $0 \le t \le \min\{p,q\}$, $k_t^+ < k_{t-1}^+ < \cdots < k_1^+ \le n-1$, and $k_t^- > k_{t-1}^- > \cdots > k_1^- \ge 0$. Since ζ is obtained from μ by removing rim hooks, we have $k_t^- < p$. Similarly, $k_t^+ \ge n-q$. Therefore, $k_t^+ - k_t^- > n-q-p \ge 0$ so that $k_t^+ > k_t^-$.

Now define $\mathcal{S}_+ = \{k_1^+ > k_2^+ > \cdots > k_p^+\}$ and $\mathcal{S}_- = \{k_1^- < k_2^- < \cdots < k_q^-\}$ such that $\mathcal{S}_+ \cap \mathcal{S}_- = \emptyset$, $k_{t+1}^- \ge n-q$ and $k_{t+1}^+ < p$. This specifies $\mathcal{S}_+$ and $\mathcal{S}_-$ uniquely, with neither set containing any element k with $p \le k < n-q$. The reasoning in the first part of the proof then shows that ζ_i satisfies (5.5) for $1 \le i \le p$, and ζ_i' satisfies (5.6) for $1 \le i \le q$.

Lemma 5.3.1 states that there exist integers $\{r_i\}_{i=1}^p$ and $\pi \in \mathfrak{S}_p$ for which $\mu_i + \eta_i = \zeta_{\pi(i)} + \eta_{\pi(i)} + r_i n$ for $1 \le i \le p$, where $\eta_i = p - i$. Thereupon, $\mu_i - i \equiv \zeta_{\pi(i)} - \pi(i) \pmod n$ for $1 \le i \le p$, whereby on using (5.5),

$$\lambda_i - i = \mu_i - i \equiv \begin{cases} -(k_{t+1-\pi(i)}^+ + 1) & \text{if } \pi(i) \le t; \\ -(k_{p+t+1-\pi(i)}^+ + 1) & \text{if } \pi(i) > t, \end{cases}$$

where the congruences are taken modulo n. Therefore, using (4.16), the profile in the uppermost p rows of λ bisects precisely those $\boxed{k{+}1 \mid k}$ for which $k \in \mathcal{S}_+$.

Similarly, Lemma 5.3.1 states that there exist integers $\{r_i'\}_{i=1}^q$ and $\sigma \in \mathfrak{S}_q$ for which $\nu_i + \eta_i = \zeta_{\sigma(i)}' + \eta_{\sigma(i)} + r_i' n$ for $1 \le i \le q$, where $\eta_i = q - i$. Thereupon, $\nu_i - i \equiv \zeta_{\sigma(i)}' - \sigma(i) \pmod n$ for $1 \le i \le q$, whereby on using (5.6),

$$\lambda_{n+1-i} - (n+1-i) = -(n+1) - (\nu_i - i) \equiv \begin{cases} -(k_{t+1-\sigma(i)}^- + 1) & \text{if } \sigma(i) \le t; \\ -(k_{q+t+1-\sigma(i)}^+ + 1) & \text{if } \sigma(i) > t, \end{cases}$$

where the congruences are taken modulo n. Therefore, using (4.16), the profile in the lowermost q rows of λ bisects precisely those $\boxed{k{+}1 \mid k}$ for which $k \in \mathcal{S}_-$. Since $\lambda_{k+1} = 0$ for $p \le k < n-q$, the profile in the $(k+1)$th row of λ bisects $\boxed{k{+}1 \mid k}$, and so λ is edge-balanced. Theorem 4.5.2 now applies to show that there exists a unique $w \in W$ such that $\lambda(w) = \lambda = (\mu;\nu)$. Since $\sum_{i=0}^n \lambda_i = 0$, Corollary 5.2.2 then shows that $w \in W_s$. $\square$

In the following corollary, we summarise the above results using the sets $\mathcal{P}^+(\mathbf{g})$ defined in Section 2.10.

Corollary 5.3.5 *If $\mathbf{g} = B_\ell^{(1)}$, $C_\ell^{(1)}$, $D_\ell^{(1)}$, $A_{2\ell}^{(2)}$, $A_{2\ell-1}^{(2)}$, or $D_{\ell+1}^{(2)}$, then there is a bijection between W_s and the set $\mathcal{P}^+(\mathbf{g})$ of generalised partitions. The bijection is such that if $\lambda \in \mathcal{P}^+(\mathbf{g})$ is the bijective image of $w \in W_s$ then:*

$$\overline{w(\rho) - \rho} = \sum_{i=1}^{\ell} \lambda_i \epsilon_i. \tag{5.8}$$

If $\mathbf{g} = A_{n-1}^{(1)}$, then there is a bijection between W_s and the set $\mathcal{P}^+(\mathbf{g})$ of pairs $(\mu;\nu)$ of partitions. This bijection is such that if $(\mu;\nu) \in \mathcal{P}^+(\mathbf{g})$ is the bijective image of $w \in W_s$ then:

$$\overline{w(\rho) - \rho} = \sum_{i=1}^{\ell(\mu)} \mu_i \epsilon_i - \sum_{i=1}^{\ell(\nu)} \nu_i \epsilon_{n+1-i}. \tag{5.9}$$

Proof: The stated bijections follow immediately from Theorems 5.3.3 and 5.3.4. The expressions for $\overline{w(\rho) - \rho}$ immediately follow from (4.2). $\square$

Acknowledgement

One of us (RCK) is grateful for the award of a Leverhulme Emeritus Fellowship which enabled him to partially support the other (TAW). Further partial support for TAW was provided by the Australian Research Council.

References

[1] N. Bourbaki, *Groups et algèbras de Lie*, Éléments de mathématique, chapitre 6, Hermann, Paris 1968.

[2] E. Cartan, Sur la structure des groupes de transformations finis et continus, Thesis, Paris, 1894.

[3] J.F. Cornwell, *Group theory in physics Vol III: supersymmetries and infinite-dimensional algebras*, Academic Press, London, 1989.

[4] E. Date, M. Jimbo, A. Kuniba, T. Miwa and M. Okada, Paths, Maya diagrams, and representations of $\widehat{\mathfrak{sl}}(n, \mathbb{C})$, *Adv. Stud. Pure Math.* **19** (1989) 149–191.

[5] H. Eriksson and K. Eriksson, Affine Weyl groups as infinite permutations, *Electronic J. Combin.* **5** (1998) #18.

[6] J. Hong, S.-J. Kang and H. Lee, Young wall realization of crystal graphs for $U_q(C_n^{(1)})$. *Commun. Math. Phys.* **244** (2004) 111–131.

[7] J.E. Humphreys, *Reflection groups and Coxeter groups*, Cambridge University Press, Cambridge, 1990.

[8] A. Hussin, Characters of affine Kac-Moody algebras, PhD Thesis, University of Southampton, Southampton, 1995.

[9] A. Hussin and R.C. King, Affine Kac-Moody algebras and their representations, in *Symmetries and structural properties of condensed matter V*, Eds. T. Lulek, W. Florek and B. Lulek, World Scientific Press, Singapore, 1997, 296–309.

[10] G. James and A. Kerber, *The representation theory of the symmetric group*, Encyclopedia of mathematics and its applications **16**, Addison-Wesley, Reading, 1981.

[11] M. Jimbo, K. Misra, T. Miwa and M. Okada, Combinatorics and representations of $U_q(\widehat{\mathfrak{sl}}(n))$ at $q = 0$, *Commun. Math. Phys.* **136** (1991) 543–566.

[12] V.G. Kac, *Infinite-dimensional Lie algebras*, 3rd edn., Cambridge University Press, Cambridge, 1990.

[13] S.-J. Kang, Kac-Moody Lie algebras, spectral sequences, and the Witt formula, *Trans. Amer. Math. Soc.* **339** (1993) 463–495.

[14] S.-J. Kang, Crystal bases for quantum affine algebras and combinatorics of Young walls, *Proc. London Math. Soc.* **86** (2003) 29–69.

[15] W. Killing, Die Zusammensetzung der stetigen endlichen Transformationsgruppen I-IV, *Math. Ann.* **31** (1888) 252–290; **33** (1889) 1–48; **34** (1889) 57–122; **36** (1890) 161–189.

[16] R.C. King, Progress on numerator formulae expansions for affine Kac-Moody algebras, *Annals of Comb.* **5** (2001) 381–395.

[17] D.E. Littlewood, *The theory of group characters and matrix representations of groups*, 2nd edn., Clarendon Press, Oxford, 1950.

[18] G. Lusztig, Some examples of square integrable representations of semisimple p-adic groups, *Trans. Amer. Math. Soc.* **277** (1983) 623–653.

[19] I.G. Macdonald, *Symmetric functions and Hall polynomials*, 2nd edn., Oxford University Press, 1995.

[20] R.V. Moody, Euclidean Lie algebras, *Canad. J. Math.* **21** (1969) 1432–1454.

[21] K. Misra and T. Miwa, Crystal base of the basic representation of $U_q(\widehat{\mathfrak{sl}}(n))$, *Commun. Math. Phys.* **134** (1990) 79–88.